Prospect for New Guidance in the Design of FRP Structures

EuCIA
European Composites Industry Association

CONTENTS

PROSPECT FOR NEW GUIDANCE IN THE DESIGN OF FRP STRUCTURES

PART I: POLICY FRAMEWORK

1. PURPOSE, JUSTIFICATION AND BENEFITS

1.1 Introduction

CEN Technical Committee 250 (CEN/TC250) has taken the initiative to prepare a document addressing the purpose and justification for new European technical rules and associated standards for the design and verification of composite structures made of FRPs (Fibre Reinforced Polymer or Plastic). CEN/TC250 formed a CEN Working Group WG4 to further develop the work item. The convenor is prof. Luigi Ascione of the University of Salerno (Italy). The Working Group, after about three years of activity and many meetings, drew up a first proposal of Scientific Technical Report. The successive update drafts have been presented and discussed on the occasion of the meetings of CEN/TC250. In January 2016 the Report has been published by the Joint Research Centre (JRC): Report EUR 27666 EN. The Report has been subjected to public inquiry until July 2016. During this period the National Standardization Bodies (NSB) of the Member States have sent comments which have been examined by WG4. This activity have been performed from September 2016 to April 2017. The present document represents the revised and updated version of the report after the public inquiry.

The CEN/TC250 initiative was motivated by the expanding and extensive construction of new structures entirely made with FRPs. The corresponding market has become more and more important in Europe during the last two decades.

The analysis of the present situation in the construction sector and the identification of the design concepts provided by the current structural design codes and trends in the construction market are the bases

1.2 Trends in the construction sector

Over the past twenty years, several innovative solutions have confirmed the usefulness of composite structures made of FRPs (Fibre Reinforced Polymer or Plastics), both within and outside Europe. The main types of FRP in consideration here are GFRP (Glass Fibre Reinforced Polymer) and CFRP (Carbon Fibre Reinforced Polymer). These solutions are often imposed by specific needs such as the requirement for speed of assembly on site or the necessity for an enhanced resistance to aggressive environments, which in turn reduces overall and maintenance costs. In addition, the lightweight of the FRP composite makes the assembly and the launch of the structure easier, besides offering a geotechnical advantage for all structures that have to rest on deformable soils. The superior strength to weight ratio of FRP thus allows for a greater load bearing capacity, when compared to conventional building materials.

Within this context, the use of FRP profiles, shell structures and sandwich structures is particularly advantageous for applications in the Civil Engineering field. FRP bearing structures are therefore widely used for the construction of buildings for industrial or residential purposes. FRP usage is also increasingly widespread for civil engineering works. Applications range from lock gates, to entire bridges or bridge decks both for pedestrian and vehicular traffic.
In addition to the advantages listed above, other main benefits associated with the use of FRP in buildings and civil engineering works are:

- Better opportunities for prefabrication;
- Reduced traffic downtime during assembly and launch of the structure;
- Reduced risks for accidents associated with onsite work;
- Reduced manpower costs associated with onsite work;
- Competitive prices over the structure's life cycle;
- High quality of the finished structure;
- Great freedom in architectural shape;
- Superior suitability for the enlargement of existing bridges;
- Great adaptability for a wide range of accessory solutions such as railing systems, walkways, inspection parapets, roof panels, balconies, façade cladding, viaduct and bridge edge elements;
- Easier transportation of structural components to areas of difficult access, e.g. those hit by natural disasters.

The most frequently used FRP manufacturing techniques for buildings and civil engineering works are pultrusion and vacuum assisted resin infusion also called Vacuum Assisted Resin Transfer Moulding (VARTM). Other common manufacturing processes are prepregging, hand lay-up, filament winding and compression moulding.
An idea of the market volume that revolves around the FRPs in Europe can be deduced from the following data relative to the latest five-year period: the total annual production for GFRP (Glass Fibre Reinforced Polymer) only was about 1 Million tons, of which 35% was for the civil construction field.

1.3 Need for European guidelines

Because of their steadily increasing market volume and given the complexity of selection from available materials for FRP structures, it became obvious that it is necessary to develop a standardization document for both the production of FRP structural elements and practical rules for the design and verification of structures to be used for buildings and civil engineering works.
Several countries have contributed to the development of currently available guidelines, among which it may be appropriate to mention the following ones:

EUROCOMP	Structural Design of Polymer Composites (Design Code and Handbook, Finland, France, Sweden, UK, 1996);
CUR 96	Fibre Reinforced Polymers in Civil Load Bearing Structures (Dutch Recommendation, 2003);
BD90/05	Design of FRP Bridges and Highway Structures (The Highways Agency, Scottish Executive, Welsh Assembly Government, the Department for Regional Development Northern Ireland, May 2005);
DIBt	Medienliste 40 für Behälter, Auffangvorrichtungen und Rohre aus Kunststoff, Berlin (Germany, May 2005);
CNR-DT 205/2007	Guide for the Design and Construction of Structures made of Pultruded FRP elements (Italian National Research Council, October 2008);
ACMA	Pre–Standard for Load and Resistance Factor Design of Pultruded Fiber Polymer Structures (American Composites Manufacturer Association, November 2010);
DIN 13121	Structural Polymer Components for Building and Construction (Germany, August 2010);
BÜV	Tragende Kunststoff Bauteile im Bauwesen [TKB] – Richtlinie für Entwurf, Bemessung und Konstruktion (Germany, 2010).

The increasing number of structural FRP applications has led to a growing interest from researchers around the world, with a profusion of international conferences and scientific contributions as a result. These activities address both mechanical modelling and testing of numerical models, as well as studies on laboratory samples and real scale prototypes. In addition, numerous international journals are now specifically dedicated to work discussing FRP composite materials and structures used in building and civil engineering works.
The experience so far gained through the realization of FRP composite structures in many European and non-European countries, as well as the theoretical and experimental understanding gained in this field makes it possible today to develop a single set of guidelines aimed for the EC countries. These guidelines may compile a body of rules based on the considerable scientific and technological progress achieved by member countries in this field, to be applied to the design and execution of FRP composite structures.

2 Examples of composite structures in Europe

Some relevant examples of civil engineering structures, realized (or under realization) in Europe with the use of FRPs, are given below as an illustration of the widespread use of this kind of structures and of the growing interest for them.

Realizations in Denmark

Kolding, Denmark. Pedestrian and cycle bridge from 100% pultruded GFRP profiles. The bridge is 40 m long and 3.2 m wide. Its total weight is 120 kN The load capacity is 5 kN/m^2. The bridge was inspected after 15 years' service life and no damage was found. Contractor: Fiberline Composites A/S, Middelfart, Denmark, 1997.

Nørre Aaby, Denmark. Construction of a pedestrian and cycle bridge with 100% pultruded Glass FRP (GFRP) profiles. The bridge is 23 m long and was built to replace an existing Reinforced Concrete (RC) bridge, damaged from usage and corrosion. It weighs only 60 kN compared to around 1200 kN for a RC bridge. Consequently, it was possible to reuse the existing foundation. The bridge was installed in just two hours, thus avoiding disruption to traffic. Contractor: Fiberline Composites A/S, Middelfart, Denmark. 2007.

Copenhagen, Denmark. Renovation of a sewage plant with 1200 m^2 pultruded GFRP coverings. The sewage plant is one of the biggest in Northern Europe and chose GFRP due to high durability requirements. Contractor: Fiberline Composites A/S, Middelfart, Denmark. 2008.

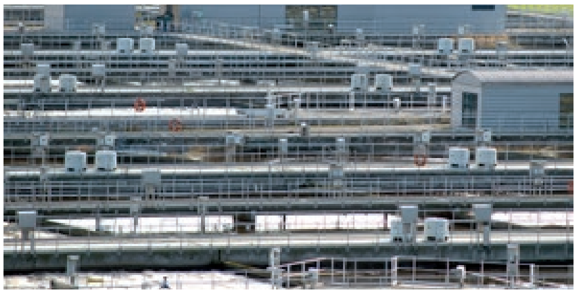

Svendborg, Denmark. Construction of a pedestrian and cycle bridge with pultruded GFRP Deck. The bridge is 40 m long and 3.2 m wide. The bridge was installed in just two hours, thus avoiding disruption to traffic. Contractor: Fiberline Composites A/S, Middelfart, Denmark, 2009.

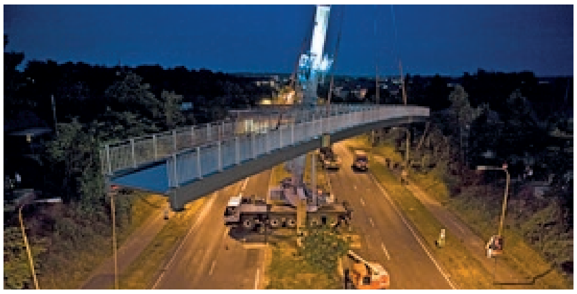

Karrebæksminde, Denmark. Renovation of a bascule road bridge where a pultruded GFRP deck was installed on the old steel structure, and a pedestrian and cycle bridge from 100% pultruded GFRP profile was hung on the side to increase capacity. It is the first Danish road bridge made with a composite deck. It replaces a wooden deck that had to be replaced/renovated about every 5 years. The installation of the bridge was performed at night to minimize the interruption of the traffic, and it was completed within a few hours. Contractor: Fiberline Composites A/S, Middelfart, Denmark, 2011.

Copenhagen, Denmark. Renovation of a metro tunnel with pultruded phenolic GFRP gratings. The gratings were part of an upgrade of the emergency exits, and were made using phenolic resin in order to achieve the specified fire rating "B". Contractor: Fiberline Composites A/S, Middelfart, Denmark, 2012.

Esbjerg, Denmark. Pedestrian and cycle bridge with pultruded GFRP deck. The bridge is constructed with steel beams adhesively bonded to the GFRP deck. It is 18 m long and 3 m wide. Contractor: Fiberline Composites A/S, Middelfart, Denmark, 2012.

Realizations in France

Joué les Tours, France. Solar charging station (SUDI™). Structure made to more than 80 % of its weight in composite (GFRP specific pultruded profiles and low pressure moulding parts). It supports 40 m^2 of solar panel. Contractor: SOLUTIONS COMPOSITES, Mettray
(37), France.

Plessis Robinson (92) France. Helipad made with pultruded GFRP profiles. A very efficient solution in terms of fire protection, weight and quick installation. Contractor: TH Composites, France.

Ephemeral cathedral of Creteil, France. Realization of a GFRP gridshell, made with pultruded tubes. Gridshells offer an important freedom of shape for the designer. The covered surface is 350 m^2. 1775 m of pultruded tubes were used. The weight of the structure is 5 kg/m^2. Design: Navier laboratory. Contractor: Structural engineering company T.E.S.S., 2014.

Realizations in Germany

Klipphausen (Dresden), Germany. It is the first road bridge built from 100 % GFRP pultruded beams and deck in Germany. Contractor: Fiberline Composites A/S, Middelfart, Denmark, 2002.

Hamm Uentrop, Germany. Construction of a 100% GFRP cooling tower as a beam-column system made from more than 100t of pultruded structural profiles. Contractor: Fiberline Composites A/S, Middelfart, Denmark, 2005.

Neumünster, Germany. 100% GFRP cooling tower as a beam-column system made from more than 40t of pultruded structural profiles. Contractor: Fiberline Composites A/S, Middelfart, Denmark, 2008.

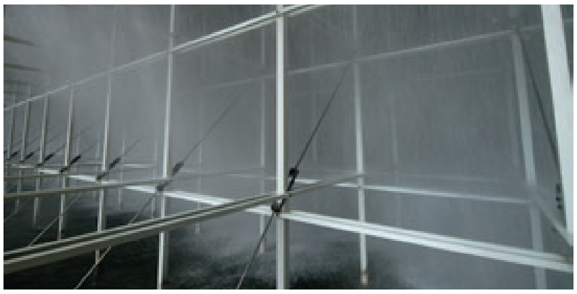

Friedberg Bridge, Germany. Motorway bridge under construction. The bridge, along 27.0 m and width 5.0 m, consists of two steel beams covered by an innovative multi-cell platform made of Fiberline's "FBD 600" GFRP profiles. The precast composite structural profiles were glued in-situ on the two steel beams. Contractor: Fiberline Composites A/S, Middelfart, Denmark, 2008.

Reinbek, Hamburg, Germany. Construction of a pedestrian bridge (Holländerbrücke). The bridge was made of steel beams and a GFRP pultruded deck. 100 m long and 3.5 m wide, it crosses the busy Hamburgerstraße. The modules of the bridge were built in a factory and then transported by road to Reinbek where they were placed in position on the foundations. Contractor: Fiberline Composites A/S, Middelfart,
Denmark. 2009.

Mittelsburen, Germany. 100% GFRP cooling tower as a beam-column system made from more than 120t of pultruded structural profiles. Contractor: Fiberline Composites A/S, Middelfart, Denmark, 2013.

Realizations in Greenland

Kujalleq, Greenland. The ASSET-bridge was prefabricated by the staff of Hee Entreprise A/S at Fiberline Composites' factory. The weight of the GFRP was just 12 tonnes, in sharp contrast to classic building materials such as steel and concrete, which for the same bridge solution would have weighed between 25 and 65 tonnes. Contractor: Fiberline Composites A/S, Middelfart, Denmark, 2016.

Realizations in Iceland

Hellisheidi, Iceland. 100% GFRP cooling tower as a beam-column system made from more than 100t of pultruded structural profiles. Contractor: Fiberline Composites A/S, Middelfart, Denmark, 2008.

Realizations in Italy

Archaeological area of Pitigliano, Grosseto (Italy). Construction of a pedestrian bridge. Span 27.0 m. GFRP pultruded profiles. Contractor: ECT System, Castelfidardo, Ancona, 2004.

S. Maria Paganica Church, L'Aquila (Italy). Replacing the roof of the church damaged by the earthquake of April 2009. GFRP pultruded members. Designers: prof. Salvatore Russo, ing. Alessandro Adilardi. Contractor: Top Glass S.p.A, Osnago (LC), 2010.

Salerno (Italy). Pedestrian bridge at the University of Salerno. Length: 148 m; main span: 37 m. GFRP pultruded I-beam. The deck is made of GFRP sandwich panels. Designer: prof. Luciano Feo, 2014 (In construction).

Realizations in Netherlands

'Bronlibelle' Bridge in Harderwijk, the Netherlands. A 6.3 m wide, 22 m long GFRP bicycle / footbridge connecting two new districts of Harderwijk. At the same time unlocking an efficient route for heavy emergency vehicles (e.g. firetrucks). The bridge deck is made by applying the vacuum infusion technology, thus providing excellent properties with desired freedom for design. The bridge is designed according to CUR96, EN 1990 and EN 1991. Architectural and preliminary design by Royal HaskoningDHV. Engineering, production and installation by Delft Infra Composites B.V.

Spieringsluis, Werkendam, the Netherlands. First FRP lock-gate in the Netherlands, installed in Werkendam. Total width of the lock is 6 m. Dimensions of each panel: width 3.5 m, height 6.5 m. Has been developed on request from Rijkswaterstaat through the SMOZcommittee. Produced by Polymarin in cooperation with DSM (resins), PPG (glass fibre reinforcement) and Bekaert (pultruded profiles), 2000.

Lock gates, ETA Lock KW28, canal Erica – Ter Apel, Emmen, (The Netherlands) Four doors, per gate: height 5.0 m, length 3.5 m, thickness 122 mm, specific weight of the doors 1000 kg/m^3. Produced by VARTM. Designed and produced as flexible, thin flat doors, slightly curved to resist creep deformations. These doors support 2.6 m water height difference. Engineered according the CUR96 and the Eurocodes EN 1990 and EN 1991. Engineered, produced and installed by FiberCore Europe, 2012.

Floriadebrug, Venlo (The Netherlands). Bicycle/pedestrian bridge with steel beams covered with a GFRP pultruded deck (BIJL plank 500 mm x 55 mm). The bridge is 127.5 m long and 6 m wide and has been designed to carry vehicles up to 12t weight. Contractor: Aa-Dee, Schijndel, the Netherlands and manufacturer of composite deck materials Bijl Profielen B.V., Heijningen, The Netherlands, 2012.

Slender canopy with dimensions 43 m x 12 m (column every 10 m). Installed at the DSM Chemelot Campus in Geleen (The Netherlands). Calculated according the CUR96 and Eurocodes EN 1990 and EN 1991. Construction made in Fibre Reinforced Polymer sandwich and steel HE-M profiles. Produced and installed by Poly Products, 2009.

Hybrid GFRP-steel bridge across highway A27, Utrecht (The Netherlands). Traffic bridge. Length 142 m (2 spans of 71 m), width 6.5 m. Made with VARTM injections, (11 tons of resin in one shot). Composite deck spans the width of the bridge, carrying Eurocode traffic loads and all horizontal loads of the bridge, including collision loads (Calculated according the CUR96 and Eurocodes EN 1990 and EN 1991) The GRP-steel joints are both bolted and glued. Ducts for rainwater and electric cables are integrated. Engineered, produced and installed by FiberCore Europe, 2013.

Sint Sebastiaansbridge, Delft (The Netherlands). Bridge designed according to CUR96, EN 1990 and EN 1991. Main girders in steel. Vacuum infused GFRP sandwich structure with adhesive and bolted connections to steel members. Table lift bridge for vehicle loads (LM1) and tram. Moveable deck: span 34 m, width 12 m. Engineered by Royal HaskoningDHV. Design and tender stage, not yet in production, 2013-2014.

62 park bridges, Rotterdam, (The Netherlands). A family of park bridges, Eurocode pedestrian/bicycle loading, with lengths ranging from 6.6 to 17.3 m and widths ranging from 1.5 to 4.5 m. GRP sandwich structure InfraCore Inside deck made with VARTM. Facetted undersides. Engineered according the CUR96 and the Eurocodes EN 1990 and EN 1991. Engineered, produced and installed by FiberCore Europe 2013 (32 bridges), 2014-2015 (34 bridges).

Bridge Oosterwolde. First full FRP movable 60-ton truck load bridge in the world, build 2010, Oosterwolde, the Netherlands. The bridge is made using vacuum infusion technology by Fibercore, designed by Witteveen+Bos according to the CUR96.

Realizations in Portugal

S. Mateus Bridge, Viseu. Pedestrian hybrid footbridge with a span of 13.3 m and 2 m of width. Made of two steel girders bonded to a multi-cellular GFRP pultruded deck with panel-to-panel snap-fit connections. Designer: Mário Sá, Portugal, 2013.

Realizations in Russia

Train station Kosino, Chertanovo in Moscow. The pedestrian bridge is 41.4 m long by 3 m wide and it is made with FRP structural profiles jointed by bolting. It consists of three spans - two of 15 m and one of 13 m length – prefabricated and assembled on site. The bridge was installed in just 49 minutes. The job lasted a total of about three hours and was carried out on Sunday morning to avoid rail traffic interruption. Contractor: Fiberline Composites A/S, Middelfart, Denmark, 2004.

P. Vernadskogo subway station, Moscow, Russia. Arched walkway realized with FRP profiles moulded by infusion. The bridge is the first one made of composite moulded by vacuum infusion. This technology offers the possibility of eliminating the processes of assembly and decreases the manpower costs. Length: 22.6 m; width: 2.8 m; weight: 55 kN. Contractor: Lightweight Structures BV, Delft, The Netherlands, 2008.

Salavat, Russia. 100% GFRP cooling tower as a beamcolumn system made from more than 100t of pultruded structural profiles. Contractor: Fiberline Composites A/S, Middelfart, Denmark, 2007.

Moscow, Russia. Deck of a pedestrian bridge with GFRP pultruded profiles. Length: 79.5 m; width: 3.7 m. Contractor: APATECH, Russia, 2010.

Realizations in Spain

Railway crossing over the high speed line Madrid-Barcelona, near Lleida city (Spain). Pedestrian walkway with GFRP profiles. The footbridge is 3 m wide and 38 m long. Contractor: Fiberline Composites A/S, Middelfart, Denmark, 2004.

Cueva de-Arrikrutz Oñati, Spain. A pedestrian walkway with GFRP profiles and grids was been built inside the cave. The bridge, 400 m long, takes visitors to a depth of 55 m. This solution is ideal to prevent degradation due to strongly corrosive moisture in the atmosphere. At the same time, the resistance of the profiles provides a sturdy non-slip decking, while preserving the beauty of the cave. Contractor: Fiberline Composites A/S, Middelfart, Denmark, 2007.

Fuente El Saz, Madrid (Spain). These two vehicular bridges, erected in 2007, are located on the outskirts of Madrid along the M111 freeway. These two bridges are identical, made up of three simple supported spans (10, 14 and 10 m) with 4 hybrid glass and carbon FRP girders each. To accelerate the deck construction process, glass fibre stay-in-place formworks were used, installed by hand. Contractor: ACCIONA Infraestructuras, S.A. Client: Comunidad de Madrid.

Madrid (Spain). Almuñécar footbridge was built in 2010 crossing the Manzanares River. It has a span of 44 m, a width of 3.5 m and it is formed by a single FRP girder of 230 kN weight with a linear piece-wise axis and an inverted "Ω" cross section 1.20 m high. The girder, completely made of carbon fibre, presents a series of longitudinal and transversal stiffeners. The girder, together with its longitudinal stiffeners, was manufactured by resin infusion in one shot. Contractor: ACCIONA Infraestructuras, S.A. Client: Excelentísimo Ayuntamiento de Madrid.

Cuenca (Spain). This stressed ribbon footbridge, built in 2011, has a total length of approximately 216 m and is formed by three spans of 72 m. Its cross section is compounded by 0.25 m thick 48 reinforced concrete slabs resting on 16 carbon fibre cables with a diameter of 42 mm. Each cable has a length of 44 m with fish-eye terminations, so five cables had to be joined to cover the distance between the two abutments. Contractor: ACCIONA Infraestructuras, S.A. Client: Excelentísimo Ayuntamiento de Cuenca.

Valencia (Spain). An FRP lighthouse was installed in only two hours in the north extension of Valencia Port. This five-storey structure, which weighs 19 tons, is formed by eight carbon FRP tubular columns made by pultrusion, and the 5 storeys are glass FRP and polyurethane octagonal sandwich panels made by resin infusion. An FRP spiral staircase is placed in the centre of the structure, going from its base to its top. To increase the lateral stiffness of the structure, between each couple of consecutive storeys, its carbon FRP columns are connected along the structure perimeter by horizontal glass FRP pipes which form in this way four octagonal rings. Contractor: ACCIONA Infraestructuras, S.A. Client: Autoridad Portuaria de Valencia.

Realizations in United Kingdom

Golf Club in Aberfeldy (Scozia). The length of the cablestayed pedestrian bridge is 113 m long and has a main span of 63 m. The two piers and the deck are made of GFRP, while the stays are made of aramid fibre cables. The only parts that are not in composite are the foundations that are made of reinforced concrete, and the steel connection between the stays and the pedestrian walkway, 1992.

Oxfordshire, UK. First road bridge for a public highway made from 100% GFRP and CFRP pultruded profiles. The bridge was inspected after 12 years' service life and no damage to the GFRP and CFRP was found. Contractor: Fiberline Composites A/S, Middelfart, Danmark, 2002.

Motorway M6, Lancashire, UK. Road bridge over a motorway. The bridge is 52 m long and has been designed to carry vehicles up to 400 kN weight. GFRP pultruded profiles "FBD 600 ASSET". Contractor: Fiberline Composites A/S, Middelfart, Danmark, 2006.

Greater Manchester, UK. The 13 m wide, 9 m long Moss Canal traffic bridge comprises pultruded GFRP doubleweb beams (DWBs) laid on their sides to act as both a cellular deck and the main longitudinal beams. The fibre type was changed from carbon in the standard DWB to glass for this specific application. This deck was prooftested under 10 million cycles of local wheel load fatigue at the University of Bristol, supervised by Dr Wendel Sebastian. The DWB deck arrangement weighs 40% of the original deteriorated concrete deck, so the original bridge abutments and foundations were re-used. Designer - SKM Ltd. Main contractor - Askam Construction Ltd. Supplier - Pipex Ltd / Strongwell, 2012.

Realizations in Sweden

The first FRP pedestrian bridge in Sweden (2017). It is a 17.6 m long, 3.5 m wide. The bridge consists 7 longitudinal sandwich beams with CFRP skin laminates and light weight concrete as core material. The bridge weights about 17 tons and located in south of Sweden in a city called Malmö. There is 1.5 tons of carbon fibres and epoxy in the structure and it was manufactured using prepreg system.

Realizations in Switzerland

Ponteresina, Switzerland. Footbridge in 2 spans of 12.5 m for temporary use in the winter (designer: prof. T. Keller). GFRP profiles. Contractor: Fiberline Composites A/S, Middelfart, Denmark, 1997.

Münchensteinerstrasse, Basilea. Eyecatcher building made of GFRP pultruded beam. The building consists of 5 floors with a total of 15 m of height; the surface amounts to 120 m^2. Contractor: Fiberline Composites A/S, Middelfart, Denmark, 1999.

Novartis Campus Entrance Building, Switzerland. Lightweight GFRP cell-core sandwich roof on loadbearing glass envelop. Dimensions 21.6 m x 18.5 m. Designer: prof. T. Keller, 2006.

3 STEP-BY-STEP PROCEDURE

The present scientific and technical proposals intended to serve as a starting point for further work in order to achieve a harmonized European view on the design and verification of composite structures made of FRPs. Its fundamental purpose is to stimulate debate. To enable this objective to be fulfilled, it contains preliminary proposals for technical provisions and identifies key issues requiring further discussion. It is emphasised, however, that it is not intended for use in practice at this stage.

It is proposed that new European technical rules for such structures are related to the principles and fundamental requirements of the EN Eurocodes. Thus, technical rules for FRP structures would not be self- standing rules but rather they will complement rules of the relevant EN Eurocodes.

New European technical rules for the design and verification of composite structures made of FRPs are planned for all types of buildings, bridges, and construction works exposed to all kind of actions.

CEN/TC250 policy, as set out in resolutions 254 and 255, is that the work for all new Parts of the Eurocodes, including the new European technical rules for FRP new structures follows a step-by-step approach, as follows:

1. Step: Preparation and publication of a JRC "Science and Policy Report" (S&P report), subject to agreement of CEN/TC250.
2. Step: After agreement of CEN/TC250, preparation and publication of CEN Technical Specifications (previously known as ENV).
3. Step: After a period for trial use and commenting, CEN/TC250 will decide whether the CEN Technical Specifications should be converted into Eurocode Parts.

The stepwise procedure allows for a progressive development in order to consider observations from national experts and users and to take into account comments received by CEN members. It should be noted that the initial purpose of the "Science and Policy Report" was widened complying with CEN/TC250 decision 340 by adding an overview of the state of the art and a collation of existing national regulations and standards for the design and verification of composite structures made of FRPs.

The revised and updated version of the document has been submitted to a balloting between the Member States, ended on July 7, 2017. The outcome of the balloting has been favourable to the transition from step 1 to step 2. The related activities are about to start when this version is released.

4 COMPOSITION OF WG4

The composition of WG4 is as follows:

	Name	E-Mail	Appointed by
		Committee Members	
1	Ascione, Luigi (convenor)	l.ascione@unisa.it	CEN/TC 250
2	Wilkins, Tracey	tracey.wilkins@bsigroup.com	BSI
3	Beinish, Hervé	h.beinish@cerib.com	AFNOR
4	Cailleau, Etienne	etienne.cailleau@afnor.org	AFNOR
5	Caron, Jean- François	caron@enpc.fr	AFNOR
6	Ferrier, Emmanuel	emmanuel.ferrier@univ-lyon1.fr	AFNOR
7	Haghani, Reza	reza.haghani@chalmers.se	SIS
8	Landon, François	francois.landon@afnor.org	AFNOR
9	Stefanou, Ioannis	ioannis.stefanou@enpc.fr	AFNOR
10	Chirea, Cristina	cristina.chirea@asro.ro	ASR0
11	Denton, Steve	dentons@pbworld.com	BSI
12	Gray, Helen	helen.gray@bsigroup.com	BSI
13	Mottram, Toby	toby.mottram@warwick.ac.uk	BSI
14	Wendel, Sebastian	Wendel.Sebastian@bristol.ac.uk	BSI
15	Knippers, Jan	j.knippers@itke.uni-stuttgart.de	DIN
16	Oppe, Matthias	m.oppe@knippershelbig.com	DIN
17	Waimer, Frederic	frederic.waimer@wernersobek.com	DIN
18	Thorning, Peter	pth@fiberline.com	DS
19	Moussiaux, Eric	eric.moussiaux@exelcomposites.com	EuCIA (Liaison Org.)
20	Correia, João Ramôa	joao.ramoa.correia@ist.utl.pt	IPQ

21	Cruz, José Sena	jsena@civil.uminho.pt	IPQ
22	Silvestre, Nuno Pereira	nsilvestre@tecnico.ulisboa.pt	IPQ
23	Abakanov, Mirken	kazmemst@bk.ru	KAZMEMST (Partner Standardization Body)
24	Bespayev, Aliy	aliy40@mail.ru	KAZMEMST (Partner Standardization Body)
25	Tuleyev, Tursymbay	tursun.1958@mail.ru	KAZMEMST (Partner Standardization Body)
26	Kukule, Aiva	Aiva.Kukule@lvs.lv	LVS
27	akrastinš, Leonids	leonids.pakrastins@rtu.lv	LVS
28	De Corte, Wouter	wouter.decorte@ugent.be	NBN
29	Tromp, L.	liesbeth.tromp@rhdhv.com	NEN
30	Triantafillou, Thanasis	ttriant@upatras.gr	NQIS ELOT
31	Karwowski, Wojciech	w.karwowski@il.pw.edu.pl	PNK
32	Godonou, Patrice patrice	godonou@angstrom.uu.se	SIS
33	Zarnic, Roko	roko.zarnic@fgg.uni-lj.si	SIST
34	Taby, Jon	jon.taby@fireco.no	SN
35	Caner, Alp	acaner@metu.edu.tr	TSE
36	Paulotto, Carlo	carlo.paulotto@acciona.es	UNE
37	Cerny, Miroslav	cerny@klok.cvut.cz	UNMZ
Document Monitors			
38	Belkebir, Malika	malika.belkebir@afnor.org	AFNOR
39	Wilkins, Tracey	tracey.wilkins@bsigroup.com	BSI
40	Kempa, Susan	susan.kempa@din.de	DIN

41	Farrugia, Francis P.	francis.p.farrugia@mccaa.org.mt	MCCAA
42	Holthuijsen, Rolph	rolph.holthuijsen@nen.nl	NEN
43	Lurvink, Mark	mark.lurvink@nen.nl	NEN
44	Peters, Suzanne	suzanne.peters@nen.nl	NEN
45	Sirks, Jeanne	jeanne.sirks@nen.nl	NEN

PROSPECT FOR NEW GUIDANCE IN THE DESIGN OF FRP STRUCTURES

PART II: PROSPECT FOR CEN GUIDANCE

1. GENERAL

1.1 SUBJECT AND SCOPE

(1) The goal of this scientific and technical report is to stimulate the debate about future guidelines and rules for the structural analysis and design of Fibre Reinforced Polymer (FRP) used in load-bearing structures, for buildings and civil engineering works.

(2) The topics taken into account address to the FRP parts with a fibre volume fraction of at least 15%, i.e. the ratio of fibre volume to total volume. The FRP composite has to be made up of glass fibres (E- glass fibres, R-glass fibres), carbon fibres of type HS, HT, IM or HM and aramid fibres with a thermoset matrix of unsaturated polyester, viny lester and epoxy resins.

(3) The report applies to FRP structures made of (i) beams, (ii) laminated plates and shells or (iii) sandwich structures.

(4) Structures in which micro-cracks are not permissible fall outside the scope of this report.

(5) The report does not include reinforcing rods, cables or external reinforcement to existing structures using FRP.

(6) The structural elements taken into account are realized by means of the main manufacturing processes. Possible manufacturing processes are: prepregging, pultrusion, compression moulding, resin transfer moulding, filament winding and hand lay-up.

1.2 NORMATIVE REFERENCES

ASTM C 271/C 271 M:2016	Standard Test Method for Density of Sandwich Core Materials
ASTM C 272/C 272 M:2016	Standard Test Method for Water Absorption of Core Materials for Sandwich Constructions
ASTM C 273/C 273 M:2016	Standard Test Method for Shear Properties of Sandwich Core Materials
ASTM C 297/C 297 M:2016	Standard Test Method for Flatwise Tensile Strength of Sandwich Constructions
ASTM C 363/C 363 M:2016	Standard Test Method for Node Tensile Strength of Honeycomb Core Materials
ASTM C 364/C 364M:2016	Standard Test Method for Edgewise Compressive Strength of Sandwich Constructions
ASTM C 365/C 365 MA:2016	Standard Test Method for Flatwise Compressive Properties of Sandwich Cores
ASTM C 366/C 366 M:2016	Standard Test Methods for Measurement of Thickness of Sandwich Cores
ASTM C 393/C 393 M:2016	Standard Test Method for Core Shear Properties of Sandwich Constructions by Beam Flexure
ASTM C 394/C 394 M:2016	Standard Test Method for Shear Fatigue of Sandwich Core Materials
ASTM C 480/C 480 M:2016	Standard Test Method for Flexure Creep of Sandwich Constructions
ASTM C 481:2016	Standard Test Method for Laboratory Aging of Sandwich Constructions
ASTM C 581:2015	Determining Chemical Resistance of Thermosetting Resins Used in Glass-Fiber-Reinforced Structures Intended for Liquid Service
ASTM D 695:2015	Standard Test Method for Compressive Properties of Rigid Plastics
ASTM D 790:2017	Standard Test Method for Flexural Properties of Unreinforced and Reinforced Plastics and Electrical insulating Materials

ASTM D 792:2013	Standard Test Method for Density and Specific Gravity (Relative Density) of Plastics by Displacement
ASTM D 903:2010	Standard Test Method for Peel or Stripping Strength of Adhesive Bonds
ASTM D 1151:2013	Effect of Moisture and Temperature on Adhesive Bonds
ASTM F 1645/F 1645M:2016	Standard Test Method for Water Migration in Honeycomb Core Materials
ASTM D 1828:2013	Atmospheric Exposure of Adhesive-Bonded Joints and Structures
ASTM D 2247:2015	Testing Water Resistance of Coatings in 100% Relative Humidity
ASTM D 2344/D 2344M:2016	Standard Test Method for Short Beam Strength of Polymer Matrix Composite Materials and their Laminates
ASTM D 2918:2012	Determining Durability of Adhesive Joints Stressed in Peel
ASTM D 2919:2014	Determining Durability of Adhesive Joints Stressed in Shear by Tension Loading
ASTM D 2990:2017	Standard Test Methods for Tensile, Compressive, and Flexural Creep and Creep-Rupture of Plastics
ASTM D 3039/D 3039M:2017	Standard Test Method for Tensile Properties of Polymer Matrix Composite Materials
ASTM D 3410/D 3410M: 2016	Standard Test Method for Compressive Properties of Polymer Matrix Composite Materials with Unsupported Gage Section by Shear Loading
ASTM D 3518/D 3518M:2013	Standard Test Method for in-Plane Shear Response of Polymer Matrix Composite Materials by Tensile Test of a ±45° Laminate
ASTM D 3762:2010	Adhesive-Bonded Surface Durability of Aluminium (Wedge Test)
ASTM D 4255/D 4255 M:2015	Standard Test Method for in-Plane Shear Properties of Polymer Matrix Composite Materials by the Rail Shear Method
EN 1990:2003/A1:2006	Eurocode 0: Basis of structural design, including national annexes
EN 1991-1-5:2004	Eurocode 1: Actions on structures – Part 1-5: General actions – Thermal actions

EN 1991-1-6:2005	Eurocode 1: Actions on structures – Part 1-6: General actions – Actions during execution
EN 1997-1:2005	Geotechnical design - Part 1: General rules
EN 13121-1:2003	GRP tanks and vessels for use above ground - Part 1: Raw materials - Specification conditions and acceptance conditions
EN 13121-2:2004	GRP tanks and vessels for use above ground - Part 2: Composite materials - Chemical resistance
EN 13121-3:2008/A1:2010	GRP tanks and vessels for use above ground - Part 3: Design and workmanship
EN 13121-4:2005	GRP tanks and vessels for use above ground - Part 4: Delivery, installation and maintenance
EN 13706-1:2002	Reinforced plastic composites- Specification for pultruded profiles - Part 1: Designation
EN 13706-2:2002	Reinforced plastic composites - Specification for pultruded profiles - Part 2: Methods of Test and General Requirements
EN 13706-3:2002	Reinforced plastic composites- specification for pultruded profiles - Part 3: Specification requirements
EN 16245: 2013	Fibre-reinforced plastic composites – Part 1-5: Declaration of raw material characteristics
ISO 175:2010	Plastics — Methods of test for the determination of the effects of immersion in liquid chemicals
ISO 846:1997	Plastics — Evaluation of the action of microorganisms
ISO 877-1-3:2009	Plastics — Methods of exposure to solar radiation
ISO 4582:2017	Plastics — Determination of changes in colour and variations in properties after exposure to daylight under glass, natural weathering or laboratory light sources
ISO 4611:2010	Plastics — Determination of the effects of exposure to damp heat, water spray and salt mist
EN ISO 4892-1/2/3	Plastics — Methods of exposure to laboratory light sources. Part 1: General guidance (2016); Part 2: Xenon-arc lamps (2013); Part 3: Fluorescent UV lamps (2016)

ISO 6601:2002	Plastics — Friction and wear by sliding — Identification of test parameters
ISO 6721-11:2012	Plastics – Determination of dynamic mechanical properties – Part 11: Glass transition temperature
ISO 9352:2012	Plastics— Determination of resistance to wear by abrasive wheels
EN ISO 12215-1/2	Small craft - Hull construction and scantlings. Part 1: Materials: thermosetting resins, glass-fibre reinforcement, reference laminate (2000); Part 2: Materials: Core materials for sandwich construction, embedded materials (2002)
ISO 15024:2001	Fibre-reinforced plastic composites - Determination of mode I interlaminar fracture toughness, GIC, for unidirectionally reinforced materials
ISO 15114:2014	Fibre-reinforced plastic composites - Determination of the mode II fracture resistance for unidirectionally reinforced materials using the calibrated end-loaded split (C-ELS) test and an effective crack length approach
ISO 15314:2004	Plastics — Methods for marine exposure
EN ISO 62:2008	Plastics — Determination of water absorption
EN ISO 75-1/2/3	Plastics - Determination of temperature of deflection under load - Part 1: General test method (2013); Part 2: Plastics and ebonite (2013); Part 3: High-strength thermosetting laminates and long fibre reinforced plastics (2004)
EN-ISO 178:2010	Plastics - Determination of flexural properties
EN-ISO 527-1/4/5	Plastics - Determination of tensile properties - Part 1: General principles (2012); Part 4: Test conditions for isotropic and orthotropic fibre-reinforced plastic composites (1997); Part 5: Test conditions for unidirectional fibre-reinforced plastic composites (2009)
EN ISO 604:2003	Plastics - Determination of compressive properties
EN ISO 899-1/2	Plastics – Determination of creep behaviour – Part 1: Tensile creep (2017); Part 2: Flexural creep by three-point loading (2003/Amd 2015)
EN ISO 1172:1998	Textile glass reinforced plastics. Prepregs, moulding compounds and laminates - Determination of the textile-glass and mineral-filler content - Calcination methods
EN ISO 6270-1/2	Paints and varnishes — Determination of resistance to humidity – Part 1: Continuous condensation (2001); Part 2: Procedure for exposing test specimens in condensation-water atmospheres (2005);
EN ISO 14125:1998/A1:2011	Fibre-reinforced plastic composites. Determination of flexural properties
EN ISO 14126:1999	Fibre-reinforced plastics. Determination of compressive properties in the in-plane direction

EN ISO 14129:1997	Fibre-reinforced plastic composites. Determination of the in-plane shear stress/shear strain response, including the in-plane shear modulus and strength, by the ± 45° tension test method
EN ISO 14130:1997	Fibre-reinforced plastic composites. Determination of apparent interlaminar shear strength by short-beam method
EN ISO 16474-1/2/3:2013	Paints and varnishes - Methods of exposure to laboratory light sources - Part 1: General guidance; Part 2: Xenon-arc lamps, Part 3: Fluorescent UV lamps
EN ISO 22088-1/2/3/4/5/6	Plastics — Determination of resistance to environmental stress cracking (ESC)- Part 1: General guidance (2006); Part 2: Constant tensile load method (2006); Part 3: Bent strip method (2006); Part 4: Ball or pin impression method (2006); Part 5: Constant tensile deformation method (2009); Part 6: Slow strain rate method (2009)

Specific standards relative to the sandwich panels are reported in §3.1.3, while specific standards relative to durability tests are reported in §3.2.

1.3 GUIDELINES

CUR 96	Fibre Reinforced Polymers in Civil Load Bearing Structures (Dutch Recommendation, 2003);
EUROCOMP	Structural Design of Polymer Composites (Design Code and Handbook, 1996);
BD90/05	Design of FRP Bridges and Highway Structures (The Highways Agency, Scottish Executive, Welsh Assembly Government, the Department for Regional Development Northern Ireland, May 2005);
DIBt	DIBt – Medienliste 40 für Behälter, Auffangvorrichtungen und Rohre aus Kunststoff, Berlin (In German, May 2005);
CNR-DT 205/2007	Guide for the Design and Construction of Structures made of Pultruded FRP elements (Italian National Research Council, October 2008);
ACMA	Pre–Standard for Load and Resistance Factor Design of Pultruded Fiber Polymer Structures (American Composites Manufacturer Association, November 2010) under review by ASCE;
DIN 13121	Structural Polymer Components for Building and Construction (August 2010);
BÜV	Tragende Kunststoffbauteile im Bauwesen [TKB] – Richtlinie für Entwurf, Bemessung und Konstruktion (in German, 2014).

1.4 ASSUMPTIONS

(1) Verifications and designs are considered to fulfil the requirements stated in this scientific and technical report on condition that:

- the selection of the structural system, the analysis and design of the structure is carried out by suitably qualified and experienced personnel;
- the production of material and structural parts, and construction on site are undertaken by personnel with the right professional skills and experience;
- proper supervision and quality control take place while the work is carried out, for example at the design and engineering firm, during the production of materials and parts, when assembling the materials and parts in factory or workshop, on construction site, etc.;
- the materials are used as described in this report or else equivalent relevant product or processing standards, normative requirements, and/or product specifications are followed;
- the manufacturing process for materials and parts fulfils the appropriate European product and process standards, to the extent not otherwise specified in this report. If no product and process standard is available, the designer, manufacturer and contractor should guarantee the required reliability of materials and structural properties through quality assurance measures. It should be shown that material and structural properties and geometrical tolerances satisfy at least the values specified in the design;
- the structure is properly maintained in accordance with maintenance instructions;
- the structure will be used in accordance with the design assumptions.

(2) FRP materials have a temperature-dependent behaviour due to the polymeric nature of their matrix. The following temperature ranges are considered for service conditions:

- ambient temperature: from -40 °C to +40 °C;
- elevated temperature: up to the maximum service temperature (dependent on the T_g, see §3.1(14));
- service temperature: Temperature range indicating minimum and maximum temperatures for short-term and long-term usage in dry as well as wet conditions, under which a given material or FRP system can be used without altering structural and durability properties more than for the effects taken into account by the applied conversion factors. It shall be defined by the designer, based on environmental data and local conditions.

1.5 TERMS AND DEFINITION

Anisotropic: non-isotropic; non-uniform mechanical and/or physical properties in different directions.

Characteristic value: value having a prescribed probability of not being attained in a hypothetical unlimited test series. This value generally corresponds to a specified fractile of the assumed statistical distribution of the particular property under examination.

Conversion factor η: a conversion factor shall be applied where it is necessary to convert the test results into values which can be assumed to represent the behaviour of the material or product in the structure or the ground.

Design working life: assumed period for which a structure or part of it is to be used for its intended purpose with anticipated maintenance but without major repair being necessary.

Fatigue: phenomenon that consists in the reduction of the material strength or product resistance resulting from the effects of repeated actions.

Isotropic: having uniform properties in all directions.

Limit states: states beyond which the structure no longer fulfils the relevant design criteria.

Load: any cause of stresses or deformations in a structure.

Partial load factors: numerical values for partial load factors are recommended as basic values that provide an acceptable level of reliability about the loads.

Partial material factors: numerical values for partial material factors are recommended as basic values that provide an acceptable level of reliability about the properties of materials and products.

Nominal value: value fixed on non-statistical bases, for instance on acquired experience or on physical conditions.

Orthotropic: a situation involving two or three axes of symmetry.

Serviceability limit states: states that correspond to conditions beyond which specified service requirements for a structure or structural member are no longer met.

Ultimate limit states: states associated with collapse or with other similar forms of structural failure.

1.5.1 TERMS RELATING TO FIBRE-REINFORCED POLYMER

Aramid fibres: synthetic fibres made from aromatic polyamide polymers, such as p-phenylene terephthalamide (PPTA), produced by spinning.

Carbon fibres: fibres consisting of very long, thin chains of carbon molecules, produced by pyrolysis of synthetic fibres such as rayon, polyacrylonitrile (PAN) or pitch in an inert atmosphere.

Continuous fibre mat: fibre mat of continuous fibre bundles that are laid criss-cross and joined together by a binding agent (or stitching). Sometimes called a continuous swirl mat. Often called CFM (Continuous Filament Mat)

Discontinuous fibre mat: fibre mat of short (30-50 mm) fibre bundles that are laid criss-cross and joined together by a binding agent (or stitching). Often called CSM (chopped strand mat).

Epoxy resin: thermoset resin system based on epoxy groups. Cure is achieved by cross-linking of the epoxy groups through the addition of a hardener system.

Fibre spraying: method of producing FRP whereby resin and short fibres are applied in layers with a spray gun, followed by manual rolling. It is an open mould technique with one hard mould side.

Filament winding: method of producing FRP whereby resin-coated fibre bundles are wound around a mould. It is an open mould technique with one hard mould side.

First ply failure: FRP failure criterion whereby it is assumed that the maximum bearing capacity of the laminate is reached when the maximum bearing capacity of the weakest ply is reached. This usually concerns matrix failure in plies loaded transverse to the fibre.

Glass fibre: fibre made from silica (SiO2). Distinctions are made between E-glass, S-glass, R-glass and others, each with their own characteristics as to stiffness, strength, electrical resistance, etc. E-glass is the most common type of glass. R-glass has higher stiffness and strength than E-glass.

Glass transition temperature (*T*g): The temperature at which the polymer changes from the glassy state to the rubbery state.

Hand lay-up: method of producing FRP whereby the resin is applied to the fibre reinforcement in layers by manual rolling. It is an open mould technique with one hard mould side.

Heat distortion temperature: The temperature at which a standard beam under controlled heating conditions reaches a prescribed deflection (EN-ISO 75).

Laminate: FRP built up from plies in layers, in principle with varying fibre orientation(s) and thickness(es).

Non-crimp fabric: uni-, bi- or multi-directional fibre reinforcement whereby one, two or more layers of continuous fibre glass bundles are laid in different directions on top of one another and stitched. Known as NCF (= non-crimp fabric) or stitched fabric. NCF is non-woven.

Panel: flat laminate (plate) with specific parameters.

Ply: elementary layer of FRP with essentially orthotropic material properties from which a laminate is built up.

Polyester resin: thermoset resin system made from unsaturated polyester dissolved in styrene. Cure is achieved by cross-linking of the unsaturated polyesters and styrene monomers initiated by a free radical donor (peroxide).

Prepregging: method of producing FRP whereby prepregs are placed on a mould and then consolidated using a vacuum (with or without overpressure) and heat. It is a closed mould technique with one hard and one soft mould side.

Prepregs: fibre reinforcements that are pre-impregnated with epoxy resin and then partially hardened (B- stage).

Pultrusion: method of producing FRP whereby resin-coated fibre bundles and reinforced fibres are pulled through a heated mould (die) and at the same time hardened. It is a partly open and partly closed mould technique. Only suitable for profiles.

Resin Transfer Moulding (RTM): method of producing FRP whereby the resin is forced into the fibre reinforcement under pressure. It is a closed mould technique with two hard mould sides.

Roving: coarse, continuous (glass) fibre bundle.

Sandwich element: a laminar construction comprising a combination or alternating dissimilar simple or composite materials assembled and intimately fixed in relation to each other so as to use the properties of each to attain specific structural advantages for the whole assembly.

Sizing: surface layer around the fibre to protect the fibre and improve resin bonding.

Spray roving: short fibres (25 – 50 mm), mixed with resin, that are applied with a spray gun. The short glass fibres are obtained by cutting up glass roving.

Vacuum injection: also called Vacuum Assisted Resin Transfer Moulding (VA-RTM). Method of producing FRP whereby the resin is forced into the fibre reinforcement under vacuum (under pressure). It is a closed mould technique with one hard and one soft mould side or two hard mould sides.

Vinyl ester resin: thermoset resin system made from unsaturated vinyl ester dissolved in styrene. Cure is achieved by cross-linking of the unsaturated vinyl esters and styrene monomers initiated by a free radical donor (peroxide).

Woven fabric: bi-directional fibre reinforcement with continuous fibre bundles in two directions at right angles to one another, crossing each other at the binding points. In the case of coarse fibre bundles (rovings), it is known as WR (= woven roving). In the case of fine fibre bundles it is known as woven cloth or woven fabric.

1.5.2 ABBREVIATIONS

CFRP	Carbon fibre reinforced polymer
CFM	Continuous filament mat
CSM	Chopped strand mat (usually) or continuous swirl mat (occasionally)
FRP	Fibre reinforced polymer
GFRP	Glass fibre reinforced polymer
PFRP	Pultruded fibre reinforced polymer
HDT	Heat distortion temperature
HM	High modulus carbon fibres
HS	High strength carbon fibres
HT	High tensile strength carbon fibres
IM	Intermediate modulus carbon fibres
IL	Interlaminar
ILSS	Interlaminar shear strength
NCF	Non crimp fabric
RTM	Resin transfer moulding (pressure injection)
SLS	Serviceability limit state
UD	Unidirectional fibre reinforcement. Common designations: UD roving, UD tape (prepreg), UD non-crimp fabric and UD woven fabric.
ULS	Ultimate limit state
VARTM	Vacuum injection (vacuum assisted resin transfer moulding)
WR	Woven roving

1.6 SYMBOLS

Uppercase Roman letters

A	Area of the cross-section without holes
A_{NET}	Area of the cross-section with holes
E	Elastic modulus
E_d	Design values of the generic action
$\mathcal{G}_I$	Fracture energy for mode I
$\mathcal{G}_{II}$	Fracture energy for mode II
L_0	Buckling length of inflection
L^*	Length of bonding
M_{ED}	Design value of bending moment
M_{Rd1}	Design value of the flexural resistance
M_{Rd2}	Design value of the flexural resistance related to instability
$N_{Ed,b}$	Design value of axial force per bolt
$N_{Ed,t}$	Design value of axial tensile load
$N_{Rd,t}$	Design value of axial tensile resistance
$N_{Ed,c}$	Design value of axial compressive load
$N_{Rd,c}$	Design value of axial compressive resistance
$N_{Rd1,c}$	Design value of axial compressive resistance related to material strength
$N_{Rd2,c}$	Design value of axial compressive resistance related to instability

$P_{Rd,c}$	Design value of global buckling load of a sandwich panel
$P_{Rd,cb}$	Design value of global buckling load of a sandwich panel due to bending
$P_{Rd,cs}$	Design value of global buckling load of a sandwich panel due to shear
R_d	Design value of capacity within a generic limit state
$R_{k\ 0.05}$	Characteristic value of a generic quantity
T_g	glass transition temperature
T_S	Service temperature
T_{Rd}	Design value of cross section resistance to torsion
$T_{Sd}^{(sv)}$	Design value for internal Saint-Venant's torsion
$T_{Ed}^{(w)}$	Design value of internal torsion with constrained warping
$T_{Rd}^{(tight)}$	Maximum tightening torque
V_{Ed}	Design value of shear load
V_{Rd}	Design value of shear strength
$V_{Ed,b}$	Design value of the force per bolt
V_X	Standard deviation of generic quantity
X_d	Design value of generic material property
X_k	Characteristic value of generic material property
W	Cross-section modulus without holes
W_{net}	Cross-section modulus with holes

Lowercase Roman letters

a_d	Nominal value of a generic geometrical property
b_F	Flange width
b_w	Web depth
c_r	Row load distribution coefficient
d	Bolt diameter
d_0	Hole diameter in bolted joints
d_r	Dasher diameter
$f_{d,t}$	Esign value of tensile strength of the material
$f_{d,c}$	Design value of compressive strength of the material
$f_{d,V}$	Design value of shear strength of the material
$f_{k,V,loc}$	Characteristic value of stress which determines the local instability
$f_{d,Tc}$	Design value of compressive strength in y or z direction
$f^{(core)}_{d,hV}$	Design value of the shear strength of the core orthogonal to the facings
$f^{(core)}_{d,pV}$	Design value of shear strength of the core parallel to the facings
$f^{(core)}_{d,c}$	Design value of compressive strength of the core
$f_{d,0,br}$	Design value of strengths for pin-bearing failure in the 0° direction
$f_{d,90,br}$	Design value of strengths for pin-bearing failure in the 90° direction
$f_{d,0,t}$	Design value of tensile strength of the material in the direction of the element axis

$f_{d,90,t}$	Design value of tensile strength of the material in the direction orthogonal to the element axis
$f_{d,I}$	Design value of strength of the adhesive for mode I
$f_{d,II}$	Design value strength of the adhesive for mode II
k_s	Factor for an unknown variation coefficient according to EN 1990
k_{tc}	Stress concentration factor in net tension failure
k_{cc}	Stress concentration factor in pin-bearing failure
$s_{d,II}$	Design value of sliding of the adhesive for mode II
t_a	Adhesive thickness
t_f	Flange thickness
t_w	Web thickness

Greek letters

γ_M	Material partial factor
γ_{M1}	Material partial factor linked to uncertainties in obtaining the correct material properties
γ_{M2}	Material partial factor linked to uncertainties due to the nature of the constituent parts and production method
$\delta_{d,I}$	Design value of opening of the adhesive for mode I
η_c	Conversion factor
η_{ct}	Conversion factor for temperature effects
η_{cm}	Conversion factor for humidity effects
η_{cv}	Conversion factor for creep effects

η_{cv20}	Value of η_{cv} for 20 years
η_{cf}	Conversion factor for fatigue effects
μ_R	Average value of a generic quantity
$\sigma_{Ed,Tc}$	Design value of compressive stress in y or z direction
$\sigma_{Ed}^{(W)}$	Normal stress due to bi-moment
$\sigma_{\mathrm{Rd,wr}}^{(\mathrm{I})}$	Factored compressive stress for face wrinkling verification
$\sigma_{\mathrm{Rd,D}}^{(\mathrm{I})}$	Factored critical dimpling stress for sandwich panel
$\tau_{Ed}^{(SV)}$	Shear stress due to the Saint Venant's torsion
$\tau_{Ed}^{(W)}$	Shear stress due to torsion with constrained warping
$\tau_{d,c}$	Design value of shear stress of the core

1.7 AGREEMENTS ON REFERENCE AXES

The figures below shown the reference axes utilized in this document for plies, laminates and structural members (Figures 1.1, 1.2, 1.3, 1.4).
Frequently, the material principal axes of symmetry of an orthotropic material, like a FRP material, which are related to the directions of the fibres, do not coincide with the axes of the reference coordinate system, chosen as the most useful for studying a structural problem

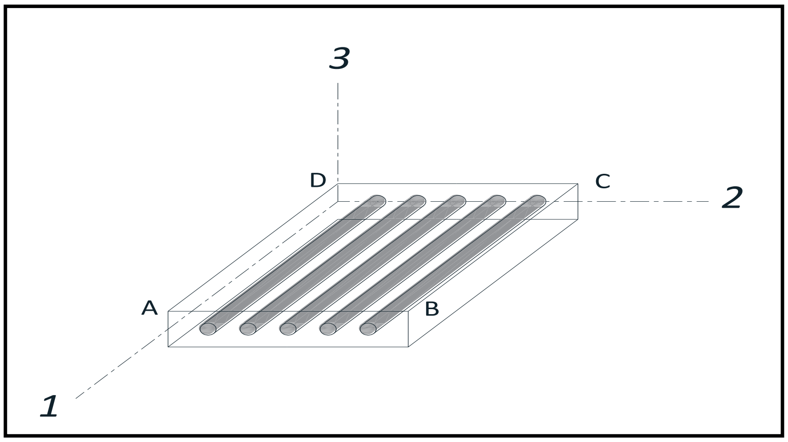

Figure 1.1 - Material principal axes for a ply with fibre lying along a unique direction.

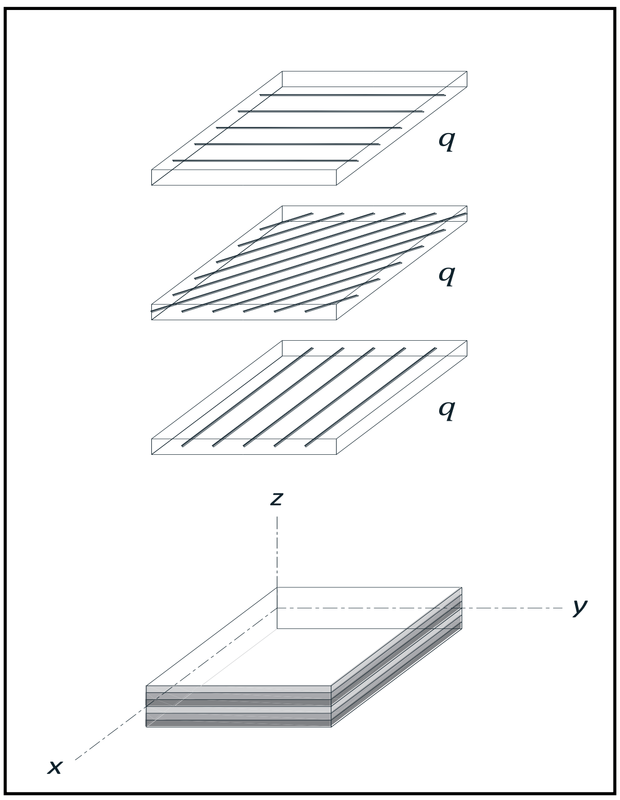

Figure 1.2a – A laminate made up of laminae with different fibre orientations.

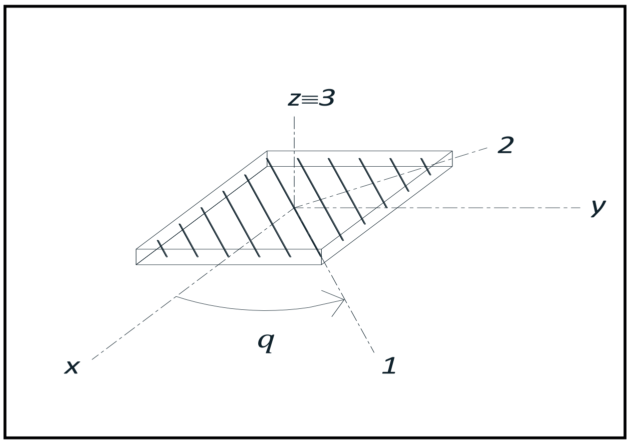

Figure 1.2b – A fibre-reinforced lamina with natural and structural reference system.

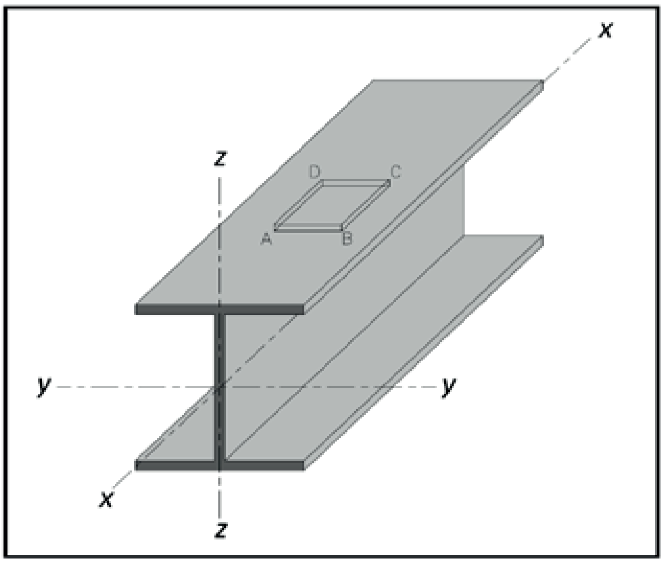

Figure 1.3 - Coordinate system for a composite beam, with ABCD reference to laminate and ply level (see Figure 1.2).

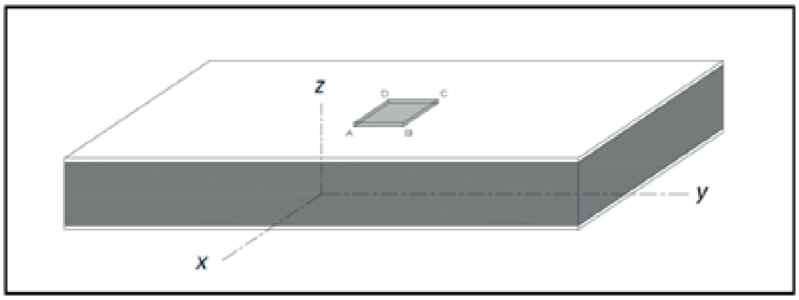

Figure 1.4 – Reference coordinate system for a sandwich panel, with ABCD reference to laminate and ply level (see Figure 1.2).

2. BASIS OF DESIGN

2.1 Basic requirements

(1) Fibre-reinforced polymer structures should be designed and calculated in accordance with the general rules given in EN 1990, EN 1991 and the associated National Annexes. The additional provisions detailed in this report also apply.

(2) The fundamental requirements in statement 2 of EN 1990 are applicable. These are considered to have been fulfilled if:

- the design is based on limit states with the loads and load combinations specified in EN 1990 and EN 1991;
- the rules and procedures for resistance, serviceability and durability specified in this scientific and technical report have been applied;
- it has been demonstrated that the mechanical properties and geometrical tolerances applied in the calculation have been achieved, that as a minimum this has been evaluated in the least favourable locations in the structure and that the potential influence of additives and the production process has been taken into account.

(3) It should be taken care of that:

- the supplier shall have a quality system that is certified by an independent external body that ensures a sufficient level of quality and reproducibility; for example ISO 9001 or equivalent;
- adequate supervision and quality control of the production process as well as of the final products should be implemented and assessed by a qualified body;
- the choice of the structural elements and joints, as well as the design of the structure, should be carried out by qualified technicians and experts;
- the structure should be realized by operators with an adequate level of knowledge and experience;
- the fabrication should follow detailed specifications (see Section 9);
- the selected materials and products should be used as specified in Section 3; in particular, materials should be selected taking into account the maximum service temperature the structure will be subjected to.

(4) The design of the structure should satisfy the static equilibrium, resistance, service and durability requisites. In the case of fire, the resistance of the structural elements as well as the joints should be adequate for the exposure time that is required. To this end, fire protection systems might be used. Fire reaction requirements set in building codes should also be met.

(5) The design of the structure should take into account all the possible actions that could affect its service life. The risks to which it could be subjected to should be identified and, if present, either reduced or eliminated.

(6) The basic requisites are considered satisfied when the following is guaranteed:

- an appropriate choice of materials and products;
- a careful execution of structural details;
- appropriate procedures of design control, production, realization and use.

2.2 Durability

(1) The design of the structure should guarantee a constant performance over time in terms of serviceability, strength and stability taking into account both the environmental conditions as well as the maintenance programme.

(2) The environmental conditions should be identified during the design phase in order to evaluate their influence on the durability of the structure, with any eventual measures being included to protect the material or the structural parts.

(3) In order to evaluate the performance of the structure in terms of its durability, theoretical models as well as tests results and studies on the behaviour of similar structures reported in the literature can be referred to.

(4) Components that are susceptible to corrosion, mechanical wear or fatigue should be designed in such a way that inspection, maintenance and repair can be carried out adequately. Furthermore these components should be accessible for inspection during use and maintenance.

(5) In order to guarantee the durability of the structure, the following should be taken into account:

- the function;
- the environmental conditions;
- the composition, properties and performance of the materials;
- suitability of the verification methods;
- the choice of the type of joints;
- the quality and level of realization control;
- the planned maintenance during the service life;
- the application of protective measures that prevent or limit deterioration in a property, based on an assessment of use, design working life, loads and required maintenance;
- the allowance in the analysis or design for a certain level of deterioration in a material property over time or changes in load or deformation due to long-term effects that may occur, such as creep, relaxation, and fatigue.

(6) Depending on the type of the load which affects the durability and design life (according to EN 1990), FRP structures should be designed so as to take into account:

- the chemical-physical conditions in which the structure is used including:
  - ultraviolet (UV) radiation,
  - temperature influences,
  - humidity, water and chemicals;
- time-dependent influences including:
  - creep,
  - relaxation,
  - wear;
- fatigue;
- accidental loads (according to EN 1991-1-7) including:
  - fire,
  - lightning strike,
  - impact,
  - explosion;
- the transportation phase;
- the installation phase;
- the inspection and maintenance phases.

7) In lack of more precise approaches, the effects of material degradation could be taken into account by using appropriate conversion factors (see § 2.3.5 and § 2.3.6).

2.3 Verification by the partial factors method

(1) Verification of both elements and joints should be carried out in relation to both the serviceability limit states (SLS) and ultimate limit states (ULS), as defined by the currently adopted regulations.

(2) The partial factors method should be used to verify that none of the limit states are violated during all the design phases, adopting the calculated values of actions and resistances. The following condition should be satisfied:

$$E_d \leq R_d, \qquad (2.1)$$

where E_d and R_d are the design values, in the considered direction, of the generic action and corresponding capacity (in terms of resistance or deformation) respectively, within a generic limit state.

(3) The design values, in the considered direction, can be obtained from the characteristic values with appropriate partial factors for the various limit states. Load combination factors can be set out with reference to the EN 1991 document.

(4) Statement 6 of EN 1990 applies when working with partial factors.

(5) The partial factors (material and conversion) referred to in this report exclusively apply to fibre-reinforced polymers with a fibre volume fraction of at least 15 %. The composite should be made up of glass fibres (E-glass fibres, R-glass fibres), carbon fibres of type HS, HT, IM or HM and aramid fibres with a thermoset matrix of unsaturated polyester, viny lester and epoxy resins.

2.3.1 Action effects calculation

(1) The computed actions are set out in the currently adopted regulations, with reference to the service life of the structure.

2.3.1.1 Action effects due to erection or installation

(1) Consideration should be given to load situations during erection or installation. EN 1991-1-6 applies to the loads to be applied in the erection phase.

(2) Allowance should be made for subsidence as well as imposed deformation. Creep and relaxation should also be taken into account in this respect.

2.3.1.2 Thermal action effects

(1) The calculations should take into account the effects of thermal actions. The effects of thermal actions should be considered as well as variable loads using a partial load factor and a partial factor for load combinations.

2.3.1.3 Prestresses

(1) Where prestress is applied, it is necessary to take into consideration the response of the FRP under long-term static load, such as the occurrence of creep, relaxation and creep rupture.

(2) If prestresses are applied, the material properties used in the calculation should be substantiated by test data.

(3) In the case of pre-stressed structures relaxation should be taken into account.
In the absence of more detailed information and accepted models, the design must be done by tests.

2.3.2 Design values of the properties of materials, elements and products

(1) The values of the properties of materials, of structural elements and of products used for the joints should be determined by laboratory tests and elaborated from a statistical point of view to give characteristic values in accordance with EN 1990.

(2) In the case of preliminary designs, the ply or laminate properties could be determined from theoretical models or values available in technical literature.

(3) Unless stated otherwise the characteristic value must be defined as:
- 5 % fractile if a low value for a material or product property is unfavourable;
- 95 % fractile if a high value for a material or product property is unfavourable.

(4) In verifying the deformability, the average (arithmetic mean) values of moduli of elasticity should be used. In some cases, a lower or higher value than the mean for the moduli of elasticity may have to be taken into account (e.g. in case of instability).

(5) To determine the characteristic values, 5% fractile ($R_{k\,0.05}$) and 95 % fractile ($R_{k\,0.95}$), of a generic quantity the following relationships (2.2a,b) can be used. Representative samples from the actual production should be used to allow the assumption of normal distribution. The size of the test bodies should be adapted to the actual structural dimensions in order to avoid strong variations of the results.

$$R_{k\,0.05} \leq \mu_R - k_s \cdot V_x \quad (2.2a)$$

$$R_{k\,0.95} \leq \mu_R - k_s \cdot V_x \quad (2.2b)$$

where:
- μ_R is the average value of the quantity,
- V_X is the standard deviation of the quantity,
- k_s is the factor for an unknown variation coefficient according to EN 1990.

(6) The design value, X_d, of the generic property of resistance or deformation of a material can be expressed, in a general form, through the following relation:

$$X_d = \eta_c \cdot \frac{X_k}{\gamma_M}, \quad (2.3)$$

where η_c is a conversion factor which takes into account, in a multiplicative manner, the special problems related with the environmental degradation or load duration (§2.3.5), X_k is the characteristic value of the property and γ_M is a partial factor covering uncertainty in obtaining the correct material properties.

(7) In Eq. (2.3), the conversion factor η_c is obtained by multiplying the specific conversion factors relevant for all the environmental actions and long-term effects affecting the behaviour of the material. The values attributed to these factors are indicated in §2.3.6. As an alternative, values resulting from an adequate series of laboratory tests on prototypes could also be attributed to these coefficients.

2.3.3 Design capacity

(1) The design capacity, R_d , can be expressed as the following:

$$R_d = R\{X_{d,i}, a_{d,1}\}, \quad (2.4)$$

where the arguments of the function $R\{\cdot\}$ are design values (Eq. (2.3)) of mechanical properties $X_{d,i}$, and nominal values of geometric properties $a_{d,i}$.

2.3.4 Material partial factors

2.3.4.1 FRP laminates and structures

(1) For ULS verifications, the material partial factor γ_M for a FRP laminate or structure should be calculated from:

$$\gamma_M = \gamma_{M1} \cdot \gamma_{M2}, \qquad (2.5)$$

where:

- γ_{M1} is the material partial factor linked to uncertainties in obtaining the correct material properties; γ_{M1} is 1.0 if production process and quality system are certified by an EOTA-member and material properties are derived by tests; γ_{M1} is 1.15 in the case of material properties derived from tests, or 1.35 in the case of material properties derived from theoretical models or values available in technical literature; in the case of laminates having several layers with various orientations, if their properties are derived from classical laminate theory using the properties of the layers obtained from tests, the value γ_{M1} equal to 1.15 is adopted.

- γ_{M2} is the material partial factor owing to uncertainties in material properties due to the nature of the constituent parts and depends on the production method. In the case of fully cured laminates the corresponding values are given in Table 2.1, where V_x is the variation coefficient to be determined from tests (EN1990, Annex D). The test to demonstrate V_x must be done as part of the design or before construction.

Table 2.1 – Values of γ_{M2}.

Conditions	ULS (strength)	Local stability	Global stability
Production processes and properties of FRP with $V_x \leq 0.10$	1.35	1.5	1.35
Production processes and properties of FRP with $0.10 < V_x \leq 0.17$	1.6	2.0	1.5

Fully cured means that the T_g and resin properties specified in the design have, as a minimum, been realized before the supporting structure is put into use (e.g. post-curing can be achieved by controlled heat treatment). A laminate is considered fully cured when an alpha factor > 0.95 has been achieved, to be determined in accordance with ISO 11357-5 2013, DSC-method. The level of cure should be at least the same level as for which the design properties have been derived for.

(2) In preliminary design, if the material properties are derived from theoretical models (γ_{M1} = 1.35) for prepregging, pultrusion, vacuum infusion and filament winding, the expected quality corresponds to V_x<0.1. For hand lamination and equivalent technologies the expected quality corresponds to V_x< 0.17.

(3) For SLS verifications, the material partial factor γ_M should be put equal to 1.0.

(4) In the case of sandwich structures with foam core, the following values (Table 2.2) of the material partial factors γ_{M2} for foam could be utilized:

Table 2.2 – Partial factors γ_{M2} for core materials.

Core material	Kind of verification		
	ULS (Strength)	Local stability	Global Stability
Foam under shear $V_x \leq 0.10$	1.5	1.7	1.2
Foam under shear $0.10 < V_x \leq 0.17$	2.0	2.2	1.5
Foam under compression $V_x \leq 0.10$	1.2	1.4	1.2
Foam under compression $0.10 < V_x \leq 0.17$	1.5	2.0	1.5

(5) For other core materials, the partial factors γ_{M2} should be derived by test according to EN1990, Annex D.

2.3.4.2 Joints

(1) For bonded joints with structural adhesives, the material partial factors γ_{M1} and γ_{M2} at ULS could be those given in Table 2.3, where V_X is the variation coefficient to be determined from tests (EN1990, Annex D).

Table 2.3 – Values of the partial materiel factors γ_{M1} and γ_{M2} for adhesives joints.

	γ_{M1}
Manual application of the adhesive with limited controls of the thickness and surface pre-treatment	1.75
Manual application of the adhesive with systematic control of the thickness and surface pre-treatment	1.5
Identified application of the adhesive with defined and repeatable controlled parameters including surface pre-treatment	1.2
	γ_{M2}
Adhesive characteristic strength values in accordance with EN1990 annex D for $V_X \leq 0.10$	1.2
Adhesive characteristic strength values in accordance with EN1990 annex D for $0.10 < V_X \leq 0.17$	1.5

(2) For bolted joints, the value of the material partial factor of the joined FRP elements, γ_M, for ULS, should be determined according to Table 2.1.

(3) In order to verify the single parts of the joints made with materials other than FRP, the partial factor γ_M of those parts should be determined in accordance with the currently adopted regulations or any other certified set of regulations.

2.3.5 Approach to special problems by using conversion factors

(1) Several reference values which could be attributed to the conversion factor η_c, introduced in §2.3.2, are reported in the next section. They could be used in order to determine the reduced values of the design parameters. They follow from either environmental degradation effects or load duration effects.

(2) Protective coverings already tested as able to mitigate the environmental degradation and to allow the service life of the structure to remain unaltered, should be used in aggressive environments. In the presence of an adequate protective system able to counteract a specific environmental effect, the value of the corresponding conversion factor can be assumed to be equal to 1.0.

2.3.6 Relevant conversion factors

1) The total conversion factor, η_c, for the limit states analysis should be determined from:

$$\eta_c = \eta_{ct} \cdot \eta_{cm} \cdot \eta_{cv} \cdot \eta_{cf}, \qquad (2.6)$$

where:

- η_{ct} *is the conversion factor for temperature effects;*
- η_{cm} *is the conversion factor for humidity effects;*
- η_{cv} *is the conversion factor for creep effects;*
- η_{cf} *is the conversion factor for fatigue effects.*

If appropriate, other conversion factors can be added in the product above, for example in the case of alkaline attack, freezing-thawing cycles, etc.

(2) The values mentioned in this chapter only concern glass and carbon fibres (see Section 2.3(5)), as well as a thermoset matrix of unsaturated polyester, viny lester and epoxy resins.

(3) In case of other fibres the conversion factors must be derived from tests. Different values might be used provided that they are supported by tests.

(4) For every given situation it is necessary to determine which conversion factors are possible. Table 2.4 indicates the main conversion factors that could be taken into account in different limit states. For ULS and SLS more details are provided in Sections 6 and 7.

Table 2.4 – Conversion factors to be taken into account.

	Aspect being verified						
Influencing factor	Strength (ULS)	Stability (ULS)	Fatigue (ULS)	Creep (SLS)	Momentary deformation (SLS)	Comfort (vibrations) (SLS)	Damage (SLS)
η_{ct}	√	√	√	√	√	√	√
η_{cm}	√	√	√	√	√	√	√
η_{cv}	√			√			√
η_{cf}	√	√		√	√	√	√

2.3.6.1 Temperature

(1) For normal temperature service conditions (See § 1.4(2)), the conversion factor for temperature effects could be as follows:

- for verification of strength and stability: $\eta_{ct} = 0.9$;
- for verification of deformability:
  - at a service temperature of $T_s \leq T_g - 40$ °C: $\eta_{ct} = 1.0$,
  - at a service temperature of $T_g - 40°C < T_s < T_g - 20°C$: $\eta_{ct} = 0.9$;
- instead of the momentary T_g, the momentary HDT of the resin can be also used for the calculation;
- the T_g should be taken as the onset of the storage modulus curve obtained from dynamic mechanical analysis.

(2) For elevated temperature service conditions (See § 1.4 (2)), the conversion factor for temperature effects should be determined based on testing.

2.3.6.2 Humidity

(1) The values of the conversion factor for humidity effects, η_{cm}, could be those given in Table 2.5.

Table 2.5 – Values of η_{cm}

Exposure classes	Conversion factor	Influence of humidity
	Fully Cured	
I	1.0	e.g. dry goods, indoor climate
II	0.9	outdoor climate, T_S< 30°C
III	0.7	continuously exposed to water, strong UV exposure, 30-40°C

Fully cured means that the T_g and resin properties specified in the design have, as a minimum, been realized before the supporting structure is put into use (e.g. post-curing can be achieved by controlled heat treatment). A laminate is considered fully cured when an alpha factor greater than 0.95 has been achieved, to be determined in accordance with ISO 11357-5, DSC-method. The level of cure should be at least the same level as for which the design properties have been derived for.

2.3.6.3 Creep

(1) Creep should be verified for permanent and quasi permanent loading conditions.

(2) Depending on the load duration class (Tables 2.6 and 2.7) various design verifications have to be carried out. For each level of requested proof, all load effects having longer load durations also need to be taken into account.

Table 2.6 – Load-duration classes.

Load-duration class	Accumulated duration of characteristic load
Permanent	more than 10 years
Long-term	6 months – 10 years
Medium-term	1 week – 6 months
Short-term	less than 1 week
Instantaneous	less than 1 minute

Table 2.7 – Classification of loads.

Action	Class
Dead load	permanent
Prestress	permanent
Vertical live loads for building constructions	
Living and comfort space, office space, work space, corridors	medium
Rooms, assembly rooms and spaces planned to be used by groups	short
Salesrooms	medium
Factories and workshops, stables, stockrooms and entrances, spaces for significant number of persons	long
Traffic and parking area for light-weight vehicles	medium
Access ramp to traffic and parking area	short
Area for the use of counterbalance forklift trucks	medium
Non accessible roofs, staircases or landings, accessions, balconies or the like	short
Horizontal loads for building constructions	
Live loads due to persons on parapets, balustrades and other retaining devices	short
Horizontal loads of crane and machine operation	short
Vertical live loads on bridges	
Highways and streets with high or medium truck occurrence, main roads with low truck occurrence	long
Local streets with low truck occurrence	medium
Agricultural roads	short
Wind load	short
Snow load	medium

(3) The value of the conversion factor η_{cv} (t_v) to account for creep effects (t_v being the accumulated load duration) depends on fibre and resin type, fibre lay-up and content, temperature, type of loading (normal and/or shear stress), load duration and aspect of verification (strength $\eta^{f}_{cv}(t_v)$ or stiffness $\eta^{E}_{cv}(t_v)$).

(4) The conversion factors $\eta^{f}_{cv}(t_v)$ and $\eta^{E}_{cv}(t_v)$ can also be determined by the following relationship in case $\eta_{cv,20}$ is known:

$$\eta_{cv}(t_v) = (\eta_{cv,20})^{T},\ T = 0.253 + 0.141 \cdot \mathrm{Log}\ t_v; \qquad (2.7)$$

where:
- $\eta_{cv,20}$ is the basic value of η_{cv} for 20 years (e.g. according to Annex A - Tables 10.2 or 10.3) or derived through testing (e.g. EN ISO 899-1, EN ISO 899-2 and ASTM D2990),
- Log t_v is the decimal logarithm of the accumulated duration of load t_v in hours [*h*].

Figure 2.1 and Annex A (Table 10.1) list different sets of values for η_{cv} (t_v) for different types of FRP materials and various load durations. The values for $\eta_{cv,20}$ are given in Annex A. Table 10.2 provides values $\eta^{f}_{cv,20}$ for strength and Table 10.3 $\eta^{E}_{cv,20}$ for strain/deflection verifications.

(5) In the double logarithmic scaling, the conversion factor results in straight lines (Figure 2.1).

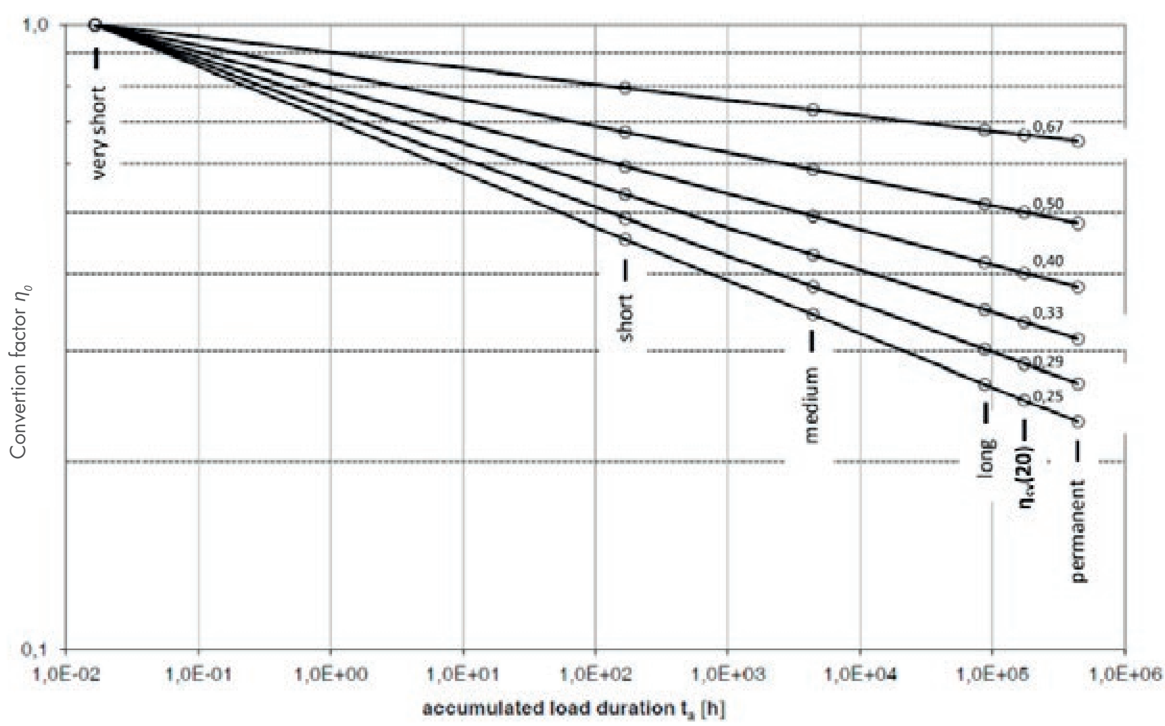

Figure 2.1 - Dependency of the conversion factors η_{cv} (see equation 2.7) from the value $\eta_{cv,20}$ and the accumulated load duration t_v (for instance as for various values as given in Table 10.2 and 10.3).

2.3.6.4 Fatigue

(1)For structures subjected to cyclic variations in the size of the load fatigue should be considered, and where the number of expected fatigue load cycles is expected to exceed 5000, or where the absolute maximum value of the cyclic load is greater than 40 % of the characteristic failure load.

(2) Fatigue has an effect on both stiffness and strength. In the Serviceability Limit State verification allowance should be made for loss of stiffness in the material due to fatigue using a conversion factor for fatigue effects of $\eta_{cf} = 0.9$.

(3) For ULS a verification of fatigue resistance should be performed according to Section 6.5.

(4) For a detailed consideration, stiffness reduction in the case of fatigue in undisturbed material might be directly determined from tests instead of calculation using the conversion factor. The stated values do not apply to connections or details.

(5) If the influence of fatigue is a significant design load case, the conversion factors should be determined by experiments.

2.3.6.5 Adhesive joints

(1) The presence of water or damp atmosphere or aggressive environment can drastically lower the long-term performance of the adhesive joint (especially in the case of poor surface pre-treatments).

(2) The degradation effects on stiffness and strength of adhesive joints should be determined by laboratory tests for the specific adhesive type and adherent combination, surface pre-treatment and cure conditions.

(3) In the case of preliminary design, the degradation effects (ageing, temperature, moisture, chemicals) for the adhesive could be taken into account by using the values of the conversion factor η_c given above.

2.4 Requirements for fasteners

(1) Metal fasteners with a protective coating may be used in the open air if they can be inspected and replaced. Otherwise, fasteners in the open air should be made of a corrosion-resistant material, according to EN1993-1-8 and EN 1090.

(2) When using metal fasteners in carbon fibre reinforced structures, insulation should be used to prevent galvanic corrosion.

2.5 References

Borowicz, D.T., Bank, L.C., Behavior of pultruded fiber-reinforced polymer beams subjected to concentrated loads in the plane of the web (2011). Journal of Composites for Construction, Vol. 15 (2), pp. 229-238.

Bakis, C., Bank, L., Brown, V., Cosenza, E., Davalos, J., Lesko, J., Machida, A., Rizkalla, S., Triantafillou, T., Fiber-Reinforced Polymer Composites for Construction—State-of-the-Art Review (2002). J. Composites for Construction, Vol. 6(2), pp. 73–87.

Commissie C124, CUR Aanbeveling 96 Vezelversterkte Kunststoffen in Civiele Draagconstructies, (2003), pp. 10- 16.

Commissie C124, Rapport 2003-6 Vezelversterkte Kunststoffen in Civiele Draagconstructies - Achtergrond rapport bij CUR Aanbeveling 96, (2003), pp. 20- 46.

Ellingwood, B., MacGregor, J.G., Galambos, T.V, Cornell, C.A., Probability Based Load Criteria: Load Factors and Load Combinations (1982). J. Struct. Div. ASCE, Vol. 108 (5), pp. 978-997.

Ellingwood, B.R., Toward load and resistance factor design for fiber-reinforced polymer (FRP) composite structures (2003). J. Struct. Engineering. ASCE, Vol. 129 (4), pp. 449-458.

Engindinez, M., Zureick, A.H., Deflection response of glass fiber-reinforced pultruded components in hot weather climates (2008). J. Composites for Const. ASCE, Vol. 12 (3), pp. 355-363.

Feo, L., Mancusi, G., The influence of the shear deformations on the local stress state of pultruded composite profiles (2013). Mechanics Research Communications, Vol. 47, pp. 44-49.

King, L., Toutanji, H., Vuddandam, R., Load and resistance factor design of fiber reinforced polymer composite bridge deck (2012). Composites Part B: Engineering, Vol. 43 (2), pp. 673-680.

Minghini, F., Tullini, N., Laudiero, F., Identification of the short-term full-section moduli of pultruded FRP profiles using bending tests (2014). Journal of Composites for Construction, Vol. 18 (1), 04013030-1-9.

Thumrongvut, J., Seangatith, S., An experimental study on the performance of fixed-end supported PFRP channel beams under flexure (2013). Advanced Materials Research, Vol. 702, pp. 31-36.

Wang, Y., and Zureick, A.H. Characterization of the Longitudinal Tensile Behavior of Pultruded I-shape Structural Members Using Coupon Specimens (1994). Composite Structures, Vol. 29, pp. 463-472.

Zureick, A. H., Polymer composites for infrastructure (1997). Durability Analysis of Composite Systems Proc. 3rd Int.Conf. (Edited by Reifsnider, Dillardand Cardon), A.A. Balkema, Rotterdam, the Netherlands, pp. 181-184.

Zureick, A., Scott D., Short-Term Behavior and Design of Fiber-Reinforced Polymeric Slender Members under Axial Compression (1997). J. Composites for Const., ASCE, Vol. 1 (4), pp.140-149.

3 MATERIALS

3.1 General

(1) The materials used should be suitable for the intended application.

(2) FRP materials should be:
• unambiguously identified by the manufacturer;
• certified under the responsibility of the same manufacturer;
• accepted on site through the acquisition and verification of all documents given by the manufacturer, as well as by any experimental tests for acceptance.

(3) This document relates to the analysis and design of FRP structures manufactured from the fibre types and thermoset resin types within the application area, as stated in Section 1, i.e.:
• fibres: E-glass fibre, R-glass fibre, HS, HT and HM carbon fibre, aramid fibre;
• fibre volume fraction of at least 15%;
• thermoset resins: unsaturated polyester, vinyl ester, phenolic and epoxy resins.

(4) Other resin and fibre types might be used providing that suitability for the application has been demonstrated.

(5) Properties of raw materials should be specified according to EN 16245.

(6) The reliability of material properties should be according to EN 1990.

(7) For pultrusion, EN 13706 should be used as a product classification standard.

(8) Characteristic values used in a design should be determined by laboratory tests according to EN1990. For unidirectional laminates at least the following properties, listed in Table 3.1, should be determined as a minimum.
The properties listed in Table 3.1 could be used to characterize the unidirectional plies used to form multidirectional laminates. When laminates are built by stacking up multidirectional fabrics and mat, woven or stitched, the same tests listed in Table 3.1 could be used to characterize the plies formed by this type of fabrics along two orthogonal directions of interest. Pultruded profiles could be treated as laminated elements. The properties of the laminates forming the different parts of a generic profile could be evaluated cutting off flat coupons from the same profiles and testing them according to the test procedures listed in Table 3.1. The properties of the laminates should be evaluated in two directions of interest at least. The failure criteria selected to assess the strength of the laminates in the different directions should be clearly stated in the test report. When, due to the profile geometry, it is not possible cutting off valid specimens from it, it is possible to manufacture pultruded laminates for testing, according to what is described in Section 6 of EN13706-2.

Table 3.1 – Mechanical properties.

Property	Test method
Tensile moduli along the directions 1 and 2 (Fig. 1.2)	EN ISO 527-4
Tensile strengths along the directions 1 and 2	EN ISO 527-4
Compressive moduli along the directions 1 and 2 (Fig. 1.2)	EN ISO 14126
Compressive strengths along the directions 1 and 2 (Fig. 1.2)	EN ISO 14126
Pin-bearing strengths along the directions 1 and 2 (Fig. 1.2)	EN 13706-2
Interlaminar shear strengths along the directions 1 and 2 (Fig. 1.2)	EN ISO 14130
Poisson's ratios along the directions 1 and 2 (Fig. 1.2)	EN ISO 527-4
In-plane shear modulus	EN ISO 15310
In-plane shear strength	EN ISO 14129
Fibre content by weight	EN ISO 1172
Thermal expansions along the directions 1 and 2 (Fig. 1.2)	EN ISO 11359-2
Glass transition temperature	EN ISO 11357-2
Heat deflection temperature	EN ISO 75

(9) Other mechanical and physical properties might be required by agreement between customer and supplier.

(10) Creep effects on the laminate stiffness and laminate strength are normally taken into account multiplying their short term properties, determined according to the tests listed in Table 3.1, by the proper conversion factors, η_{cv}, as described in Section 2.3.6.3. When required, conversion factors can be experimentally determined according to e.g. ISO 899-1, ISO 899-2 and ASTM D2990.

(11) A common case is that of balanced symmetric laminates. In all the following the report will mostly refer to such kind of laminates. As a reminder, it should be noted that a laminate is symmetric if layers of the same material, thickness, and orientation are symmetrically located with respect to the middle surface of the laminate. Furthermore, in the case considered here (the laminates are also balanced) for each at layer oriented at +√ there is another oriented at -√ with same thickness and material; and for each 0°-layer there is a complementary 90°-layer, also of the same thickness and material. In this case a set of equivalent laminate moduli (E_1, E_2, G_{12}, V_{12}) can be defined. These moduli represent the stiffness of a fictitious, equivalent, orthotropic plate that behaves like the actual laminate under in-plane loads. For such a laminate the directions 1 and 2 play the role of principal directions of orthotropy. In this case the properties in Table 3.1 should be determined with respect to such two directions.

(12) In case of other kinds of laminates the mechanical and physical properties to be determined should be required by agreement between customer and supplier. In any case the reliability of material properties should be according to EN 1990.

(13) The resin used should be appropriate to the surface treatment ('sizing') of the fibre. The choice of resin should be appropriate to the required properties, such as glass transition temperature, chemical resistance, fire reaction properties and electrical conductivity. Additives and fillers may be added to the resin to provide its specific properties. The effect of additives and fillers on the mechanical properties should be taken into account. The resin used should also be compatible with the sizing material used in the reinforcement.

(14) The glass transition temperature of cured unreinforced resin (T_g), as per EN ISO 11357-2, should be at least 20^{0}C above the maximum service temperature (Section 1.4: Assumptions) and at least 60^{0}C.

(15) Areas with holes or exposed core material, and joint areas with bolts etc. should be properly sealed in order to avoid premature ageing and water migration, except for exposure classes I and II (see 2.3.6.2).

(16) The characteristic values of FRPs mechanical parameters should be sufficiently stable with respect to the degradation induced by environmental actions (see §3.2).

3.1.1 Fibres, resins, adhesive, ply and laminate properties

(1) When using values available in the technical literature (see § 2.3.2 (2)), allowance should be made in the analysis and design for the influence of fibre sizing and possible differences between different products suppliers. Annex B gives indicative values for fibre, resin, ply and laminate properties, to be used in preliminary design. This annex also provides analytical models useful for predicting such properties.

(2) The mechanical characterization of the adhesives to be utilized for adhesive joints (Section 8.4) has to be performed in agreement of the following standards: ASTM D903, ISO 15114 and ISO 15024.

3.1.2 FRP beam elements

(1) With reference to pultruded FRP beam elements (Section 6.2), in addition to the properties relative to the material, the evaluation of section properties should be done according to EN 13706. The reliability of properties should be according to EN 1990.

3.1.3 Sandwich structures

(1) The following physical and mechanical properties should be required in order to qualify and certify sandwich structures (Section 6.4):

- Flatwise tensile strength of sandwich constructions (ASTM C297/C297M:2015);
- Edgewise compressive strength of sandwich constructions (ASTM C364/C364M:2007);
- Flexural properties of sandwich constructions (ASTM C393/C393M:2011);
- Flexure creep of sandwich constructions (ASTM C480/C480M:2008);
- Laboratory aging of sandwich constructions (ASTM C481:1999);
- Water migration in honeycomb core material (ASTM F1645/F1645M);
- Materials for sandwich construction (ISO 12215-5:2008).

(2) Further laboratory tests on sandwich structures may be required from the supplier in order to certify the strength and buckling performance of the delivered products.

3.2 Durability tests

(1) When required, the durability tests on FRP materials could consist of the following tests regarding long-term environmental and biological actions and abrasion:

- Plastics — Evaluation of the action of microorganisms (ISO 846)
- Plastics — Methods of exposure to solar radiation (ISO 877 all parts)
- Plastics — Determination of changes in colour and variations in properties after exposure to daylight under glass, natural weathering or laboratory light sources (ISO 4582)
- Plastics — Methods of exposure to laboratory light sources (ISO 4892 all parts)
- Plastics — Determination of the effects of exposure to damp heat, water spray and salt mist (ISO 4611)
- Plastics — Determination of water absorption (EN ISO 62)
- Plastics — Methods of test for the determination of the effects of immersion in liquid chemicals (ISO 175)
- Determining Chemical Resistance of Thermosetting Resins Used in Glass-Fiber-Reinforced Structures Intended for Liquid Service (ASTM C 581:2015)
- Plastics — Methods for marine exposure (ISO 15314)
- Plastics — Determination of resistance to environmental stress cracking (ESC) (EN ISO 22088 all parts)
- Plastics — Friction and wear by sliding — Identification of test parameters (ISO 6601)
- Plastics—Determination of resistance to wear by abrasive wheels (ISO 9352)
- Adhesive-bonded surface durability of aluminium (wedge test) (ASTM D 3762)

(2) When required, freeze-thaw tests might be performed in the direction of interest. Freeze-thaw tests could be limited to the tensile behaviour and executed with the following procedure:

i. The specimens are stabilized in a climatic chamber for a week under a RH=100% and temperature of 38°C. Then, the specimens are submitted to 100 cycles of at least 4 hours at -18°C followed by 12 hours in the climatic chamber. A minimum of ten specimens are required: five are to be conditioned and five are to be used as control specimens.

ii. At the end of the test the specimens are inspected in order to identify superficial alteration, scaling and cracking. Finally the specimens should be tested for strengths and elastic moduli.
The test is positive if the specimens retain at least 85% of the strength and elastic modulus of control specimens, and no visible defect is identified on their surface.

(3) When required, aging tests might be performed in the direction of interest. Aging tests could be limited to the tensile behaviour and executed with the following procedure:

i. Both wet and dry composite specimens are aged according to Table 3.2. Both exposed and control specimens are then tested for strengths and elastic moduli. A minimum of sixty specimens is required: thirty for the duration of 1000 hours and thirty for the duration of 3000 hours. Within each duration, five specimens are to be conditioned in a moist environment and five are to be used as control specimens; further ten specimens are used for the saline environment and the last ten specimens for the alkaline one.

ii. Acceptance is positive if under examination with 5X magnification no erosion, cracking and crazing is present. The conditioned specimens should retain the percentage of tensile strength and elastic modulus given in Table 3.2, with respect to the unconditioned ones.

Table 3.2 – Moisture/procedure.

<table>
<tr><th>Durability test</th><th>Reference Standard</th><th>Test parameters</th><th>Test duration (hours)</th><th>Retained values (%)</th></tr>
<tr><td>Moisture resistance</td><td>ASTM D 2247
ASTM E 104</td><td>Relative humidity: ≥90%
temperature: 38 ± 2 °C</td><td rowspan="3">1000

3000</td><td rowspan="3">85

80</td></tr>
<tr><td>Salt water resistance</td><td>ASTM D 1141
ASTM C 581</td><td>immersion in salt water at 23 ± 2 °C</td></tr>
<tr><td>Alkali resistance</td><td>ASTM D7705-7705M</td><td>immersion in a dilution with pH= 9,5 or larger;
temperature: 23 ± 2 °C</td></tr>
</table>

(4) When required, weathering resistance might be evaluated. Changes in polymeric materials exposed to weathering arise mainly from the combined effect of UV radiation from the sun, effects of temperature and humidity cycles (see § 4.2.1). Natural and accelerated weathering tests (Table 3.3) might be used to evaluate materials performance and predict their behaviour under natural exposure during the expected service life. The methodology and approach for accelerating tests is based on the application of increasing levels of weathering variables (temperature, irradiance and moisture), which fasten the degradation mechanisms of materials. It should be noted, however, that no accelerated weathering test can be specified as a total simulation of natural field exposure

Table 3.3 – Test procedures for weathering resistance assessment.

Weathering test		Principle	Reference Standard
Natural ageing	Outdoor (real time)	Outdoor exposition of materials, during long periods of time (years)	EN ISO 877
Accelerated ageing	Laboratory test	Laboratory light source, with cycles of temperature and humidity or water spray (typical duration of 1000 h)	EN ISO 4892 (plastics) EN ISO 16474 (coatings)
	Outdoor test	Concentrated natural sunlight, with or without water spray	EN ISO 877 (plastics)

During accelerated weathering tests, aesthetic properties (such as visual inspection of the surface, gloss and colour measurements) are usually monitored. After predefined ageing periods, mechanical properties might also be determined.

3.3 References

Ascione L., Feo L., Mechanical behaviour of composites for construction (2012). Encyclopaedia of Composites, p. 1–25. John Wiley and Sons, New York, NY.

Bank, L. C. Composites for Construction (2006). John Wiley and Sons, New York, NY.

Barbero, E. Introduction to composite materials design (1998). Taylor & Francis.

Bitzer, Tom. Honeycomb Technology: Materials, design, manufacturing, applications and testing (1997). Chapman & Hall.

Christensen, R. M., Mechanics of Composite Materials (2005). Dover Publications NY.

Ferry, J.D. Viscoelastic properties of polymers (1980). John Wiley and Sons, New York, NY.

Pritchard, G (Ed.). Reinforced Plastics Durability (1999). Woodhead Publishing Limited, Cambridge, UK.

4 DURABILITY

(1) This section describes the effects and related measures that have an impact on the material properties of fibre-reinforced polymers. Based on the correct selection and processing of materials and protective measures, conversion factors are specified to account for the effects of temperature, humidity, creep and changing load, as in § 2.3.6. This chapter deals with measures to protect the structure's function from aging and weathering. The main exposure environments as available in established literature should be taken into consideration.

4.1 General

(1) Durability means that all requirements on reliability are to be met throughout the design working life.
(2) Components of structures should be designed such that:
- They will fulfil the requirements throughout their design working life, in principle without repair or replacement. For this purpose the risk of failure at the beginning of the design working life will remain unchanged such that, when allowing for normal increase in the risk of failure due to aging of the structure, the risk of failure at the end of the design working life will remain below the required limit value.
- They, or the complete structure of which they are part of, can be inspected once or repeatedly and where necessary repaired throughout the entire design working life such that, the risk of failure of that component always remains below the required limit value.

(3) The second of the methods above is recommended for FRP structures where experience of using the material in structures is limited. With the correct choice of materials and production, FRP structures generally need low maintenance. Conversion factors allow then for the anticipated effects of aging, climate, etc., throughout the service life.

(4) When designing the required protection for the structure, it is necessary to take into account the use, the design service life (see EN 1990), the maintenance programme and the applied loads.

(5) The effects of long-term as well as varying loads and the environment in which the structure is located should be taken into account (see § 4.2).

(6) Laminate characteristics having a major impact on the durability of an FRP component are:
- void content (number of air bubbles);
- cure process – correct cure (e.g. post curing contributes to a longer service life);
- chemical resistance of the resin – the resin and protective substances used should be resistant to the climate of use. It is advisable to assess the suitability of the resin in consultation with the resin supplier;
- fibre-resin interface. This is determined by factors including the fibre type, resin, sizing and process conditions, including humidity and pressure during cross-linking;
- mixing quality, ratio of components and resin systems;
- fibre and/or fabric wrinkles (fibre misalignment).

(7) The ILSS provides a measure of the fibre-resin bond. The achieved glass transition temperature T_g or the HDT (for entire system) provides a measure for the degree of cure. As part of the inspection of properties, this report specifies that the ILSS and T_g are verified by tests. ILSS and T_g should be determined according to EN ISO 14130 and EN ISO 11357-2, respectively. See § 9.2 for more information on inspection of properties.

(8) When a resin suitable for the ambient climate is correctly processed, in combination with protection against UV by means of a coating, a durable material is generally obtained and the factors stated in § 2.3.5 are sufficient for indoor and outdoor application. Practical experience and accelerated aging tests have shown that a service life for FRP structures of 50 years or more can be achieved without any problem.

(9) The influence of additives and fillers on durability should be taken into account in the design. In particular, consideration should be given to the influence of fire-retardant additives on durability.

(10) Too high a concentration of fillers can adversely affect durability. Its influence depends on whether a gel coat has been used or whether another coating has been applied afterwards. Every combination of fillers and resin behaves in a unique way. These factors should be taken into account.

4.2 Measures for specific environmental conditions

4.2.1 UV radiation

(1) Glass and carbon fibres exhibit good resistance to UV radiation. Aramid fibres are susceptible to UV radiation and thus should be prevented from being directly exposed to sun.

(2) The polymeric matrix of FRP materials is susceptible to photodegradation initiated by the UV component of solar radiation. However, the most deleterious effects of UV radiation on FRP materials are not due to direct photolytic effects, which are limited to the surface regions, but to the increased propensity for moisture and aqueous solutions to ingress into the material structure. Superficial crazing and cracking can potentially serve as sites for moisture sorption and fracture initiation. After prolonged periods of exposure, as damage progresses into the bulk, fibre-matrix interphase could be reached, and both physical and mechanical properties could exhibit significant changes. Therefore, FRP structures may have to be protected against UV radiation through the use of appropriate additives (UV blockers/absorbers) and/or by means of surface protections (gel coats or paints).

(3) Polymeric protective coatings are themselves susceptible to UV radiation, serving as “sacrificial layers” in delaying the effects of UV exposure. Therefore, such coatings need to be maintained or replaced and be object of periodic inspection during service life.

4.2.2 Thermal material effects

(1) The effects of any degradation in material properties under the influence of raised temperature should be included in the calculation by:

- the use of a conversion factor for temperature effects as detailed in § 2.3.6,

or

- directly deriving this effect through tests on materials at this raised temperature.

(2) As an alternative to the glass transition temperature, assumptions may also be based on the HDT when FRP system is considered, as determined by EN-ISO 75. The HDT should be at least 20 °C above the maximum service temperature of the structure. For aramid fibres the maximum permitted service temperature and the material behaviour at temperatures higher than 60 °C should be determined in consultation with the material supplier.

(3) Aramid fibres have a more limited thermal range than glass fibres and carbon fibres. The properties of aramid fibres are liable to change at around 100 °C.

(4) The colour of the composite material may have a great importance on the temperature reached inside the material. Dark colours may increase the temperature above the required limit. Tests results performed according to EN 16245-2 to be provided by the manufacturer are required to assess these effects.

(5) For sandwich structures with insulating cores (foam, woods, balsa…), the temperature can be very different between the top and bottom faces, when exposed to a source of heating (e.g. the sun). This can lead to an undesired curvature, to fatigue phenomenon and even to damage. These effects should be taken into account. For hollow cores, this problem does not really exist.

4.2.3 Humidity, water and chemicals

(1) FRP materials can be potentially degraded when subjected to humidity, water and chemicals. A variety of degradation mechanisms may affect their physical and mechanical properties, both stiffness- and strength-related. These mechanisms depend on several factors, namely the type of polymeric matrix, fibre reinforcement (type, content, architecture) and manufacturing process.

(2) In general, loss of stiffness and strength due to humidity, water and chemicals is a slow and in some cases irreversible process. The resistance of FRP to humidity, water and other chemicals is governed in the first instance by the polymeric resin and its level of cure. Resins and fibres considered in this document are generally well resistant to chemicals. A proper embedment in the resin isolates and protects the fibre reinforcement and will reduce the degree of penetration of moisture/chemicals. Isophthalic polyester, epoxy and viny lester resins generally show good resistance to (salt) water. Carbon fibre is resistant to both acidic and basic environments. Glass fibre is resistant to acids but may (except for especially resistant types) degrade in a basic environment.

(3) The effects of any degradation in material properties under the influence of humidity, water and chemicals should be included in the calculation by:

- the use of a partial conversion factor for humidity and water as detailed in § 2.3.6;

or

- directly deriving this effect through tests on materials that are exposed to the actual actions.

(4) No conversion factors have been defined for the influence of chemicals. This effect should be determined by tests.

(5) The partial factors in § 2.3.6 apply where there is no continuous exposure to service temperatures above 40 °C. If the structure is continuously exposed to high concentrations of moisture or chemicals combined with a long-term service temperature above 40 °C, the effect of this should be determined by means of tests.

(6) In order to decrease the permeability of FRP to moisture and chemicals in solution, it is of paramount importance to guarantee a resin-rich layer at the surface, with appropriate thickness. For further protection, gel coats or a protective surface coating may be used in addition.

(7) In case of long-term exposure to water or high concentrations of chemicals, the laminate should be completely cured before being subject to any loads and a coating or chemical barrier layer should be applied.

(8) Exposure to water can lead to the growth of algae (marine fouling), which might damage the coating. Measures such as regular cleaning and/or the use of an anti-fouling coating can be applied if necessary.

(9) The case of sandwich structures is very sensitive. Humidity can lead to debonding between core and facings. Humidity diffusion inside the core should be avoided (by adequate protection/covering of open/free edges, protection of holes, surface veils, etc.).

4.2.4 Static charge

(1) If required by the application, provisions should be put in place to divert electrical charges. For example, through external measures such as a lightning conductor or the use of a conducting mat on the surface of the FRP.

(2) Fibre-reinforced polymers are non-conductive, unless they are filled with conductive particles or fibres, such as carbon fibres.

4.2.5 Fire

(1) The fire safety of FRP structural components and joints should comply with applicable codes, regarding both fire reaction and fire resistance requirements.

(2) In what concerns fire reaction, most resin systems used in FRP components are flammable and, under fire conditions, release heat and smoke and spread flames. Conventional thermoset resin systems do not emit toxic gases and do not drip. This issue should be taken into consideration.

(3) The fire reaction properties of FRP components can be considerably improved by using inherently flame retardant resins (e.g., phenolics), fillers, flame retardants, passive fire protection systems (e.g. coatings, boards) or bulking materials in combination with fire resistant resins.

(4) If fillers or flame retardants are used, their influence on the FRP mechanical properties should be taken into account.

(5) In what concerns fire resistance, the strength and stiffness properties of FRP components are temperature-dependent. In general, when the glass transition temperature of the resin is exceeded, the mechanical properties are notably reduced, particularly those that are more matrix-dependent. Due to their low thermal conductivity, the temperature increase in FRP components when subjected to fire is relatively slow (namely when compared to metallic materials).

(6) The fire resistance of FRP components is very much dependent on:
- the structural function of the FRP members (higher for members in bending, lower for members in compression),
- the number of sides exposed to fire,
- the cross-section geometry (higher for sections with thicker walls and closed geometry, particularly if multi-cellular).

(7) The fire resistance of FRP components can be significantly improved by using:
- passive (e.g., coatings, boards),

or
- active (e.g., sprinklers, water cooling) fire protection systems.

(8) Depending on the fire resistance requirements of the FRP structure, specific fire protection systems may need to be considered for the joints between FRP components.

(9) Fire protection systems developed for other materials (e.g., steel), cannot be applied straightforwardly to FRP structures.

(10) Refer to Section 5.4 for more specifications on fire related issues.

4.2.6 Joints

(1) For mechanical joints, no separate durability analysis other than that of the overall system is required.

(2) For adhesive or hybrid joints specific attention should be given to prestress, relaxation, creep, and moisture at interfaces. Analysis can be performed according to established textbooks.

4.3 References

Department of Defense Handbook, US. MIL-HDBK-17-2F, Composite Materials Handbook Volume 2. Polymer Matrix Composites Materials Properties (2002). AMSC N/A Area CMPS

Editor, Vistasp M. Karbhari. Durability of composites for civil structural applications (2007). Woodhead Publishing Limited

5 BASIS OF STRUCTURAL DESIGN

5.1 Analysis criteria

(1) The analysis of the structural response should be carried out taking into account the linear elastic behaviour up to failure and, if necessary, the orthotropic nature of the materials. No redistribution of stresses due to plasticity can be assumed. The stress state on the structural elements and joints should be determined through a global analysis of the structure, considering, when relevant, the deformability of the joints.

(2) The second order effects should also be taken into account in the analysis, if they are significant. The second order effects due to vertical loads should also be taken into account in the analysis if the condition is satisfied:

$$\alpha_{cr} = \frac{F_{cr}}{F_{Ed}} < 10, \tag{5.1}$$

where α_{cr} a is the factor by which the design loading would have to be increased to cause elastic global instability of the structure, F_{Ed} is the design loading on the structure, F_{cr} is the critical buckling load for global instability mode (determined from elastic buckling analysis).

(3) The second order effects are taken into account by performing either a geometrically nonlinear analysis (for any value of α_{cr}) or a linear analysis with amplification of internal forces and moments due to applied horizontal loads by means of the factor:

$$\frac{\alpha_{cr}}{\alpha_{cr}-1}, \tag{5.2}$$

provided that $\alpha_{cr} \geq 3$.

(4) The analysis of thin-walled FRP profiles with open section subjected to torsion should be carried out taking into account both the uniform (Saint-Venant) and the non-uniform (warping) torsional stiffness.

(5) For bolted joints, the forces of every single bolt should be evaluated taking into account the elastic properties of the structural elements connected to them. The verification should be carried out considering all the possible failure modes of the joints.

(6) For adhesively bonded joints, the verification should be preferably carried out in terms of delamination by considering the interface fracture energy and the possible fracture modes. Cyclic loading of the bonded joints should be carefully considered in the verification.

(7) The method of analysis should be relevant for the actual behaviour.

(8) The anisotropic elastic moduli of composite materials, laminates or sandwich structures, as well as their strength properties, may be obtained by direct experimental testing. The use of classical theoretical models for composite materials only allows one to obtain indicative values (see Appendix B).

(9) When finite element analysis is performed, the definition and handling of failure criteria should be clearly defined and described.

(10) When sofware are used for structural analysis, a reference case should be presented for showing their suitability.

5.2 Verification criteria

(1) The verification of resistance should be carried out considering the eventual simultaneous presence of more than one stress component.

(2) The verification of stability should take into account the eventual interaction between local and global instability phenomena. A local verification of the parts under compression should be carried out when the constraint conditions prevent global instability. The verification of stability should take into account the presence of imperfections if a geometrically nonlinear analysis is performed.

(3) The verification of local and global stability should be carried out by using the most appropriate values for the elastic moduli as in §2.3.2 (4).

(4) The inclusion of all the imperfections could be scoped by modelling a single (dominant) imperfection with appropriate magnitude.

5.3 Deformability evaluation

(1) Both the flexural deformability and shear deformability should be taken into account in order to evaluate the deflection of the structural elements under bending, shear and compression. In fact, composite and anisotropic materials have a very specific behaviour in this regard, especially sandwich structures involving cores, which have low shear modulus.

5.4 Behaviour in the case of fire

(1) The fire resistance of FRP structural components and joints should conform to applicable building codes.

(2) The mechanical properties of FRP materials are highly sensitive to elevated temperatures, particularly for matrix-dependent properties. In fact, when the FRP temperature approaches or exceeds the resin glass transition temperature, T_g, the strength and moduli are notably reduced.

(3) Under conditions of exposure to fire, the mechanical properties of FRP materials could be significantly prevented from decreasing by adopting either passive fire protection systems (e.g., coatings or boards with an appropriate thickness) or active protection systems (e.g., sprinklers, water cooling).

(4) The accidental load combinations indicated in the currently adopted guidelines should be used in fire design verifications for a given established exposure time.

(5) For analysis of the capacity of the structure during fire, the part of the laminate that is heated to a temperature exceeding the T_g of the resin must be considered as non-load bearing.

(6) For analysis of the capacity of the structure after fire, the part of the laminate that has been heated to a temperature higher than the degradation temperature of the resin must be considered as non-load bearing.

5.5 Design assisted by testing

(1) The analysis and design of structures or structural elements might be supported by tests. Information concerning design supported by testing is given in the Annex D of EN 1990.

5.6 References

Vinson, J.R. The Behavior of Shells Composed of Isotropic and Composite Materials (1993). Kluver Academic Publishers.

Barbero, Ever J. Introduction to Composite Materials Design (1998). Taylor & Francis.

Gay, Daniel, HOA, Suong V., et TSAI, Stephen W. Composite materials: design and applications (2002). CRC press.

Nicolais, L., Borzacchiello, A, et Stuart, M. Lee, Encyclopaedia of Composites (2012). John Wiley and Sons, New York, NY.

Reddy, J.N. Mechanics of Laminated Composite Plates (1997). CRC press.

6 ULTIMATE LIMIT STATES

6.1 General

(1) In this section, the basic ULS verifications are presented. In particular, the following structural elements are examined:

- Profiles;
- Laminated plates and shells;
- Sandwich structures.

In this document, the term "profile" is applied to one-dimensional beam elements realized by pultrusion or different techniques. In the case of pultrusion, the fibres lie along the beam axis. In the case of other techniques, the fibres can also lie along different directions. Sometimes, in the following, sandwich structures are also referred to as sandwich panels.

6.2 Ultimate limit states of profiles

(1) The following most common cases of internal beam forces are examined:

- Normal force: axial tension (see § 6.2.1.1) and axial compression (see § 6.2.1.2);
- In-plane flexure (see § 6.2.2);
- Shear (see § 6.2.3);
- Torsion (see § 6.2.4);
- Combination of in-plane tension and flexure (see § 6.2.5);
- Combination of in-plane compression and flexure (see § 6.2.6);
- Combination of flexure and shear (see § 6.2.7).

(2) The usual presence of high resin concentration in the web-flange junctions of steel-like unidirectional pultruded profiles requires a careful investigation of their actual mechanical behaviour, since these junctions behave as deformable rather than as rigid. The actual constitutive law of this portion of the profiles is relevant, mainly with respect to ULS for stability problems and connections (Appendix E). Further, this issue may lead to the premature failure of the profiles due to interlaminar shear stresses. Information concerning both aspects should be provided by manufacturers to users.

(3) The pultruded profiles may have different properties in the web(s) and flange(s).

6.2.1 Normal force

6.2.1.1 Axial tension

(1) In the case of profiles subjected to axial tensile load, the design value of the applied tensile force, $N_{Ed,t}$, should satisfy the following condition:

$$N_{Ed,t} \leq N_{Rd,t} \, . \tag{6.1}$$

In Equation (6.1) the design value of the resistance to tensile loads, $N_{Rd,t}$, is given by,

- (section without holes)

$$N_{Rd,t} = A \cdot f_{d,t}, \tag{6.2}$$

- (section with holes)

$$N_{Rd,t} = 0.9 \cdot A_{net} \cdot f_{d,t}, \tag{6.3}$$

where $f_{d,t}$ is the design value of tensile strength of the material in the direction of the fibres, A is the gross area of the cross-section, and A_{net} is the net area of the cross-section. In the case of circular holes, A_{net} is given by,

$$A_{net} = A - \sum_{i=1}^{n} t_k d_i \tag{6.4}$$

where n is the number of holes, d_i is the diameter of i-th hole and t_k is the thickness of the element k where the hole is located.

6.2.1.2 Axial compression

(1) In the case of elements subjected to axial compressive load, the design value of the applied compressive force, $N_{Ed,c}$, should satisfy the condition:

$$N_{Ed,c} \leq N_{Rd,c}. \tag{6.5}$$

In the relationship (6.5) the design value of the resistance to compressive loads, $N_{Rd,c}$, of the profile can be obtained as follows:

$$N_{Rd,c} = \min\{N_{Rd1,c}, N_{Rd2,c}\}, \tag{6.6}$$

where $N_{Rd1,c}$ is the design value of the compressive force that causes the crushing of the material, and $N_{Rd2,c}$ is the design value of the compressive force that causes the buckling of the element.

(2) The value of $N_{Rd1,c}$ can be calculated through the following expression,

$$N_{Rd1,c} = A \cdot f_{d,c} \tag{6.7}$$

where $f_{d,c}$ is the design value of the compressive strength of the material in the direction of the fibres. The possible effects of holes in members under axial compression should be considered to account for the net cross-section reduction.

(3) The value of $N_{Rd2,c}$ can be determined either through experimental tests (see § 5.5 (1)) or numerical modelling (§ 5.2(4)). In the latter case, the characteristic value from which the value of $N_{Rd2,c}$ is obtained can be determined from an elastic buckling analysis.

(4) In the case of pultruded profiles with double symmetric section, the design value of the compressive force that causes the instability of the member, $N_{Rd2,c}$, is given by,

$$N_{Rd2,c} = \chi \cdot N_{Rd,loc}, \tag{6.8}$$

where $N_{Rd,loc}$ is the design value of compressive force that determines the local instability of the pultruded members, and χ is a reduction factor that takes into consideration the interaction between the local and global buckling of the member. In case of double symmetric profiles, Annex C provides formulas to calculate the values of $N_{Rd.loc}$ and χ.

(5) For pultruded profiles having all section walls converging into a single point (shear centre), such as angle, cruciform and T sections, the design value of the compressive force that causes the instability of the member is given by,

$$N_{Rd2,c} = \min\{N_{Rd,E}, N_{Rd,T}\}, \tag{6.9}$$

where $N_{Rd,E}$ is the design value of the global (flexural or Euler) buckling load, given by Eq. (12.15), and $N_{Rd,T}$ is the design value of the torsional buckling load. Annex C provides formulas to calculate the value of $N_{Rd,T}$ for torsional buckling.

6.2.2 IN-PLANE FLEXURE

1) Structural members subjected to in-plane flexure, usually designated as beams, should undergo both resistance and stability verifications. In each cross-section, the design value of the applied bending moment, M_{Ed} should satisfy the condition:

$$M_{Ed} \leq M_{Rd} \tag{6.10}$$

In (6.10) the design value of resistant bending moment, M_{Rd} , is obtained from the minimum between the resistant bending moment of the profile, M_{Rd1} , and the bending moment associated to the elastic buckling of the beam, M_{Rd2} :

$$M_{Rd} = \min\{M_{Rd1}; M_{Rd2}\} \tag{6.11}$$

(2) The design value of the resistant bending moment of the profile, M_{Rd1} , is obtained from:

- section with no openings:

$$M_{Rd1} = W \cdot \min\{f_{d,t}; f_{d,c}\} \tag{6.12}$$

- section with openings:

$$M_{Rd1} = 0.9 \cdot W_{net} \cdot \min\{f_{d,t}; f_{d,c}\} \tag{6.13}$$

where W is the flexural modulus of the gross cross-section, W_{net} is the flexural modulus of the net crosssection, while $f_{d,t}$ and $f_{d,c}$ are the design values of the tensile and compressive strengths of the material in the direction of the fibres, respectively.

(3) The design value of the bending moment associated to the elastic buckling of the beam, M_{Rd2} , may be obtained from either experimental tests (see § 5.5(1)) or numerical modelling (§ 5.2(4)). In the latter case, the characteristic value from which the value of M_{Rd2} is obtained can be determined from an elastic buckling analysis.

(4) In case of beams subjected to flexure in the plane of maximum inertia of the section (major- or strong-axis bending), the value of M_{Rd2} can be obtained from the relation,

$$M_{Rd2} = \chi_{FT} \cdot M_{Rd,loc} \tag{6.14}$$

where $M_{Rd,loc}$ is the design value of the bending moment associated to local buckling of the pultruded profile and χ_{FT} is the reduction coefficient that takes into consideration the interaction between the local buckling of the profile and the global buckling (flexural-torsional instability) of the beam. Annex D provides expressions to estimate $M_{Rd,loc}$ and χ_{FT} .

(5) For beams subjected to flexure in the minor-axis, the design value of the bending moment associated to local instability of the pultruded profile, $M_{Rd,loc}$, could be evaluated either through experimental tests (see § 5.5(1)) or numerical modelling (§ 5.2(4)). Alternatively, an analytical model can be used by assuming a linear distribution of normal stresses along the flange width and the flange constrained at the connection with the web. This constraint may be either modelled as a pinned support ($\tilde{k} = 0$) or, more accurately, as a rotational spring with the flexural stiffness of the web being given by,

$$\tilde{k} = \frac{E_{Tc} \cdot t_w^3}{12 \cdot b_w \cdot \left(1 - \nu_{LT} \nu_{TL}\right)} \tag{6.15}$$

6.2.3 Shear

(1) For each cross-section, the design value of the applied shear force, V_{Ed}, should satisfy the condition:

$$V_{Ed} \leq V_{Rd} \, . \qquad (6.16)$$

(2) The design value of the shear resistance force, V_{Rd}, is obtained from,

$$V_{Rd} = \min\{V_{Rd1}, V_{Rd2}\} \, . \qquad (6.17)$$

where V_{Rd1} is the design value of the shear force that causes material failure (in shear) and V_{Rd2} is the design value of the shear force that causes the local buckling of the cross-section (in shear).

(3) The value V_{Rd1} can be obtained using the relation,

$$V_{Rd1} = A_V \cdot f_{d,V} \, , \qquad (6.18)$$

where $f_{d,V}$ is the design value of shear resistance of the material in the plane of the cross-section and A_V is the shear area of the cross-section, given in Table 6.1 for the most widely used profiles.

Table 6.1 – Area resistant to shear A_v for several thin pultruded profiles.

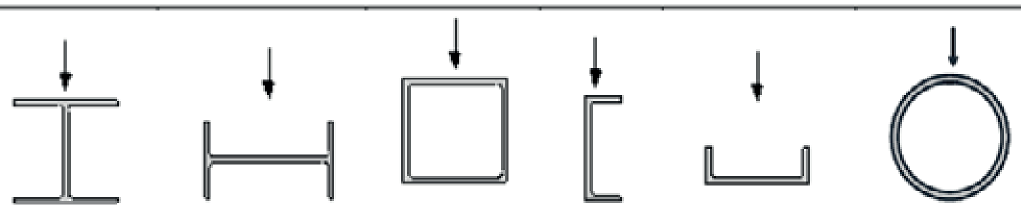

(a)	(b)	(c)	(d)	(e)	(f)
$b_w \cdot t_w$	$(2b_f \cdot t_f)/1{,}2$	$2b_w \cdot t_w$	$b_w \cdot t_w$	$(2b_f \cdot t_f)/1{,}2$	$\pi R \cdot t$

In Table 6.1, the symbols *b* and *t* denote the width and the thickness of the web (w) or the flange (f), respectively, and *R* is the radius of the circular section mid-surface.

(4) The value of V_{Rd2} can be determined through the following expression,

$$V_{Rd2} = V_{Rd,loc} = A_V \cdot \left(f_{d,loc}^{shear}\right)_w = A_V \cdot \left(f_{k,loc}^{shear}\right)_w \times \frac{\eta_c}{\gamma_M} \qquad (6.19)$$

where $\left(f_{d,loc}^{shear}\right)_w$ and $\left(f_{k,loc}^{shear}\right)_w$ are respectively the design and characteristic values of the shear stress associated to local buckling. Annex F provides closed-form analytical formulae to obtain the value of $\left(f_{k,loc}^{shear}\right)_w$.

(5) Local verification should be done on sections where concentrated loads (or reactions) are applied. In this case, in the absence of a general formula for resistance against web crippling, the design value of the resistance against concentrated loads may be obtained from experimental tests (see § 5.5(1)) or numerical modelling (§ 5.2(4)). In order to avoid premature failure at these locations, appropriate stiffening systems may be applied to the critical sections.

6.2.4 Torsion

(1) In case of members subjected to torsion, the design value of the applied torsional moment, T_{Ed}, should satisfy,

$$\frac{T_{Ed}}{T_{Rd}} \leq 1 , \tag{6.20}$$

where T_{Rd} is the design value of the resistance to torsion of the cross-section.

(2) The value of T_{Ed} should be obtained from,

$$T_{Ed} = T_{Ed}^{(SV)} + T_{Ed}^{(w)} , \tag{6.21}$$

where $T_{Ed}^{(SV)}$ is the design value of the torsional moment associated to the Saint-Venant's torsion (uniform torsion) and $T_{Ed}^{(w)}$ is the design value of the torsional moment associated to constrained warping (non-uniform torsion). These values may be determined from elastic analysis taking account of the cross-section properties of the member, the conditions of restraint at the supports and the distribution of the actions along the member.

(3) The following stresses due to torsion should be taken into account: shear stress $\tau_{Ed}^{(SV)}$ due to uniform torsion, shear stress $\tau_{Ed}^{(w)}$ due to non-uniform torsion and normal stress $\sigma_{Ed}^{(w)}$ due to non-uniform torsion (associated to warping bi-moment).

(4) For profiles with open cross-section, such as I, H, U and C shapes, shear stress due to uniform torsion is given by,

$$\tau_{Ed}^{(SV)} = \frac{T_{Ed}^{(SV)}}{I_t} t_{max} \tag{6.22}$$

where t_{max} is the thickness of the thickest wall of the cross sections. In case of two-flange sections (I and H), the shear stress due to non-uniform torsion may calculated from the following approximate formula,

$$\tau_{Ed}^{(w)} = \frac{T_{Ed}^{(w)}}{b_f \cdot t_f \cdot b_w} \qquad (6.23)$$

where b_f and t_f are respectively the width and the thickness of the flange, and b_w is the width of the web.

For profiles with open cross-section, the effects of non-uniform torsion are typically much more relevant than those caused by uniform torsion and the calculation of $\tau_{Ed}^{(w)}$ depends much on the cross-section geometry. Details about the determination of $\tau_{Ed}^{(w)}$ should be found in technical literature. In any case, the Equation (6.24) is equivalent to the following stress-based criterion,

$$\tau_{Ed}^{(SV)} + \tau_{Ed}^{(w)} \leq f_{d,V} \qquad (6.24)$$

where $f_{d,V}$ is the design value of shear resistance of the material.

(5) For profiles with closed cross-section, such as hollow, tubular, pipe and multi-cellular crosssections, for the sake of simplicity, it might be assumed that the effects of constrained warping of the crosssection are negligible in comparison with those caused by Saint-Venant's torsion, and it may be assumed that $\tau_{Ed}^{(w)} = 0$. In this case, the Equation (6.20) is approximately given by:

$$\tau_{Ed}^{(SV)} = \frac{T_{Ed}^{(SV)}}{2 \cdot A_m \cdot t} \leq f_{d,V} \qquad (6.25)$$

where A_m is the area defined by the middle line in the closed cross-section and $f_{d,V}$ has been defined above.

6.2.5 Combination of flexure and axial tensile force

(1) Cross-sections subjected to a design value of the applied axial tensile load, $N_{Ed,t}$, combined with a design value of the applied bending moment, M_{Ed}, causing flexure about the major axis of inertia (strong-axis), should satisfy the following condition,

$$\frac{N_{Ed,t}}{N_{Rd,t}} + \frac{M_{Ed}}{M_{Rd1}} \leq 1\,, \qquad (6.26)$$

where $N_{Rd,t}$ is the design value of the resistance to tensile loads defined in § 6.2.1.1 and M_{Rd1} is the design value of the resistant bending moment of the cross-section about the strong-axis, given by Equations (6.12) and (6.13).

(2) In addition to the aforementioned verification of resistance, stability should also be verified. In the absence of a more accurate evaluation of the interaction between bending and axial tensile force, it is conservative to ignore tensile loads and estimate only the bending moment about the major axis of inertia associated to the buckling of the beam.

(3) In case of members under bi-axial bending and axial tension, in the absence of a general interaction formula, the design value of the resistance may be obtained from experimental tests (see § 5.5(1)) or numerical modelling (§ 5.2(4)).

6.2.6 Combination of flexure and axial compression force

(1) Cross-sections subjected to a design value of the axial compression force, $N_{Ed,1}$, combined with a design value of bending moment, M_{Ed}, causing flexure about the major axis of inertia (strong-axis), should satisfy the following condition,

$$\frac{N_{Ed,c}}{N_{Rd1,c}} + \frac{M_{Ed}}{M_{Rd1}} \leq 1, \tag{6.27}$$

where $N_{Rd1,c}$ is the design value of the compressive force that causes the crushing of the material, defined in § 6.2.1.2, and M_{Rd1} is the design value of the resistant bending moment of the profile, provided by Equations (6.12) and (6.13).

(2) In addition to the aforementioned verification of resistance, stability should also be verified. In the absence of a more accurate evaluation of the interaction between bending and axial compressive force, this verification can be carried out through the following condition,

$$\frac{N_{Ed,c}}{N_{Rd2,c}} + \frac{M_{Ed} \Big/ \left(1 - \frac{N_{Ed,c}}{N_{Rd,E}}\right)}{M_{Rd2}} \leq 1, \tag{6.28}$$

where $N_{Rd2,c}$ is the design value of the compressive force that causes the buckling of the member, M_{Rd2} is the design value of the bending moment associated to lateral-torsional buckling of the member and $N_{Rd,E}$ is the design value of the global (flexural or Euler) buckling load of the member, given by Equation (12.15), Annex C.

(3) In the presence of a variable bending moment, the design value of the applied bending moment, M_{Ed}, should be taken as the maximum value along the length of the member.

(4) In case of members under bi-axial bending and axial compression, in the absence of a general interaction formula, the design value of the resistance may be obtained from experimental tests (see § 5.5(1)) or numerical modelling.

6.2.7 Combination of flexure and shear

(1) Members subjected to a combination between bending about the major axis of inertia and shear, should satisfy the following condition:

$$\left(\frac{M_{Ed}}{M_{Rd}}\right)^2 + \left(\frac{V_{Ed}}{V_{Rd}}\right)^2 \leq 1, \tag{6.29}$$

where M_{Ed} is the design value of the applied bending moment, V_{Ed} is the design value of the applied shear force, V_{Rd} is defined in (6.17) and M_{Rd} corresponds to the minimum between M_{Rd1} and M_{Rd2} defined in section 6.2.2.

(2) In case of members under bi-axial bending and shear, in the absence of a general interaction formula, the design value of the resistance may be obtained from experimental tests (see § 5.5(1)) or numerical modelling.

6.3 Ultimate limit states of laminated plates and shells

(1) The verifications to be achieved concern both resistance (see 6.3.1) and stability (see 6.3.2).

(2) One has to keep in mind that the layers of a laminate may present natural principal axes different from one layer to another, due to usual anisotropy.

(3) The most common case is that of balanced symmetric laminates, to which this document mostly refers (see 3.1 (11)).

6.3.1 Resistance verifications

(1) The following two levels of verifications can be considered:

- Ply level (see 6.3.1.1);

or

- Laminate level (see 6.3.1.2).

(2) Resistance must be verified for the following stress resultants conditions, including the effects of the presence of holes and imperfections:

- Tension
- Compression
- Bending
- In-plane shear
- Interlaminar shear
- Interlaminar tension and compression
- Multiaxial stress conditions

6.3.1.1 Ply level

(1) In the verification at ply level, the verification of resistance *(first ply failure)* could be carried out by using the well-known Tsai-Hill criterion. Consequently, in terms of stress components referred to the material principal axes of the orthotropic ply, the following inequality should be satisfied:

$$\left(\frac{\sigma_{Ed,1}}{\sigma_{Rd,1}}\right)^2+\left(\frac{\sigma_{Ed,2}}{\sigma_{Rd,2}}\right)^2+\left(\frac{\tau_{Ed,12}}{\tau_{Rd,12}}\right)^2-\frac{\sigma_{Ed,1}\cdot\sigma_{Ed,1}}{\sigma^2_{Rd,1}}\leq 1. \qquad (6.30)$$

Generally, the design value of normal strengths, $\sigma_{Rd,i}$ (i = 1,2) are different for tension and compression.

Relationship (6.30) applies to plies with one single fibre direction. In the case of plies with fibres lying along n different directions, the same applies to each layer, in which the ply can be decomposed with the fibres lying along each of above mentioned directions and thickness equal to that of the ply divided by *n*.

(2) More sophisticated, but widely used criteria, such as Tsai-Wu, Puck and Hashin, which take into account differences between tension and compression, could be also used.

6.3.1.2 Laminate level

(1) When carrying out analyses at laminate level, the design value of the ultimate strength of the laminate should be used. Such a value could be obtained through iterative procedures by taking into account the progressive degradation of the stiffness of the layers due to the matrix cracks or micro cracks involved by the successive failure of the layers. Within this approach the results of the classical laminates theory could be utilized.

(2) For preliminary design of the balanced symmetric laminates, made of glass fibre reinforced thermoset polymers, in case of uniaxial loading condition, and in case of a fibre volume fraction as stated in the scope (Section 1.1(2)), of which at least 12.5% in each of the directions (0°, 90°, +45°, -45°), the following design criterion could be used:

$$\varepsilon_{\mathrm{Ed,i}} \leq \eta_{\mathrm{c}} \cdot \frac{0.012}{\gamma_{\mathrm{M}}} \quad \text{or} \quad \gamma_{\mathrm{Ed,ij}} \leq \eta_{\mathrm{c}} \cdot \frac{0.016}{\gamma_{\mathrm{M}}} \quad , \tag{6.31}$$

where *i, j* denote the material principal directions of orthotropy; $\varepsilon_{\mathrm{Ed,i}}$ denotes the design linear strain along the axis *i* and $\gamma_{\mathrm{Ed,ij}}$ denotes the design shear strain between the axes *i, j*.

(3) Alternatively, a design by testing procedure could also be adopted.

(4) It is recommended that the strength of the laminate is controlled by the fibres. This goal is reached if the fibres in most part of the plies are oriented closely to the load direction.

6.3.2 Stability verifications

(1) The stability of laminated plates and shells should be determined at laminate level taking into account the long-term effect on the material and geometry.

(2) The stability of laminated plates and shells can be analysed either through numerical/analytical modelling or through experimental tests (see § 5.5 (1)).

(3) The technical literature provides the values of the critical loads in many situations of interest. Annex F provides some of these values for orthotropic laminates with a length/width ratio greater than 5.
The loading conditions taken into account are: compression, shear, and pure bending. Annex F also provides some interaction formulae useful for the stability verification of such kind of laminated plates subjected to combined loads: compression with shear, compression with bending, bending with shear.

(4) The limits of imperfections taken into account in the design must be specified and taken as allowable limits for imperfections in the realisation phase (see chapter 9.4.1), including the effects of creep.

6.4 Ultimate limit states of sandwich stuctures

(1) The information presented in this chapter is based on technical literature generally available on the design of sandwich structures. Here, only basic theoretical models are taken into account in order to estimate failure and instability modes of sandwich structures. These models are based on perfect constituents and simplified linear elastic approaches. The following aspects are not considered:

- non-linearities related to the mechanical behaviour of the sandwich constituents, especially the core;
- geometrical imperfections due to the fabrication and their influence on buckling;
- influence of pre-existing (even small) debonded regions and defects.

(2) The following sandwich structures failure modes should be considered:

- Facing Failure (6.4.1);
- Transverse Shear Failure (6.4.2);
- Flexural Crushing of Core (6.4.3);
- Local Crushing of Core (6.4.4);
- Global Buckling (6.4.5);
- Shear Crimping (6.4.6);
- Facing Wrinkling (6.4.7);
- Intracell Buckling or Dimpling (6.4.8);
- Delamination of facing and core (6.4.9).

(3) In the following the symbols x and y denote the reference coordinate axes in the plane of the facings (Figure 1.4); the third axis is denoted by *z*. If the facings consist of balanced symmetric laminates, with fibres lying along the two orthogonal directions *x* and *y*, such axes also coincide with the principal axes of orthotropy of the facings.

(4) The nomenclature used for sandwich panel in this document is given below (Figure 6.1).
- *d*: sandwich panel thickness;
- *E*: normal stiffness of facings ;
- E_C: normal stiffness of core;
- *G*: shear stiffness of facings;
- G_C: shear stiffness of core;
- *h*: distance from centre top facing to centre bottom facing;
- *t*: thickness of a Facing;
- *b*: width of the panel;
- $\lambda=1-\nu_{xy}\nu_{yx}$, where ν_{ij} is the Poisson's ratio, which give the strain in the direction *j* induced by a normal stress in the orthogonal direction *i*.

The subscript "c" denotes the core, while subscripts "1" and "2" denote top and bottom facings. If both facings are the same, then $t_1 = t_2 = t_f$, $E_1 = E_2 = E_f$,and $\lambda=1-\nu_{xy}\nu_{yx}$,

(5) In dependence of the plan dimensions, the sandwich structures can behave as beams or plates. In the first case the coefficient λ can be assumed as unitary.

(6) The given failure criteria have to be satisfied in both the directions x and y, as well as in all other directions of interest.

(7) The contribution of the core to the flexural and axial stiffness of the sandwich is considered to be sufficiently weak and can be generally neglected (e.g. soft cores such as foams, honeycombs, etc. but not solid wood or harder core).

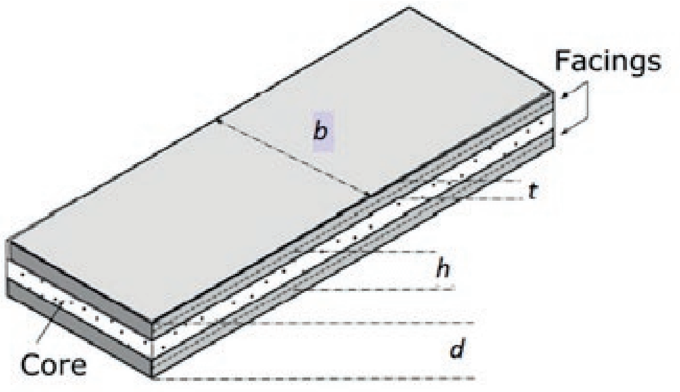

Figure 6.1 – Sandwich description.

(8) For preliminary design, a maximum allowed linear strain of 1.2% of the facings can be assumed. Furthermore a maximum allowed shear strain of 1.6% of the core can be assumed.

6.4.1 Facing failure

(1) This mode of failure (Figure 6.2) may occur in either compression or tension facing. It is caused by insufficient:

- panel thickness,
- facing thickness,
- facing strength.

In Figures 6.2 - 6.9 the core is schematically represented by a shaded area or by means of vertical lines.

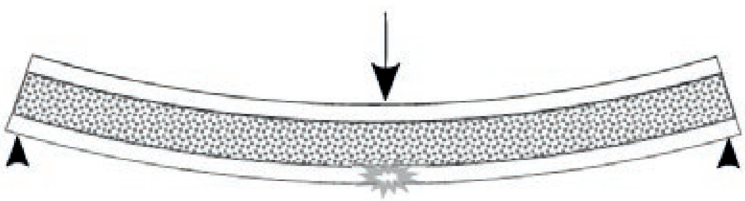

Figure 6.2 – Tensile facing failure.

(2) For balanced symmetric laminates, and if the contribution of the core to the flexural and axial stiffness of the sandwich is sufficiently weak (assumption (7) in § 6.4) , then the design value of normal stress on the facing «i» could be evaluated as follows:

$$\sigma_{\mathrm{Ed,i}} = \frac{M_{\mathrm{Ed}}}{t_{\mathrm{i}} \cdot h} + \frac{N_{\mathrm{Ed}}}{2 \cdot t_{\mathrm{i}}}, \tag{6.32}$$

where M_{Ed} is the design value of bending moment and N_{Ed} is the design value of axial load, evaluated per unit-length orthogonal to the examined direction.

(3) The signs of both M_{Ed} and N_{Ed} have to be considered.

(4) The verification is satisfied if:

$$\begin{aligned} &\sigma_{Ed,i} \leq f_{d,ti} \quad \textit{if} \quad \sigma_{Ed,i} \geq 0 \\ &\textit{or} \\ &\left|\sigma_{Ed,i}\right| \leq f_{d,ci} \quad \textit{if} \quad \sigma_{Ed,i} < 0 \end{aligned} \tag{6.33}$$

where $f_{d,ti}$ and $f_{d,ci}$ are the design value of the tensile or compressive strength of the facing «*i*» in the examined direction.

(5) The compressive strength value is often lower than the tensile strength one, and it should be taken in verifying facing failure.

(6) In a more general case (different facings, different materials or different facing thicknesses) expression (6.32) is no longer valid due to the change of the neutral axis induced by the asymmetry, and due to a new stress repartition at the facings. In particular, the neutral axis, due to the anisotropy of the plies, is often different in the x and y directions. This new stress repartition has to be estimated by using the classical laminate theory and should respect (6.33).

6.4.2 Transverse and horizontal shear failure

(1) This mode of failure (Figure 6.3) may occur for insufficient:
- core shear strength,

or
- panel thickness.

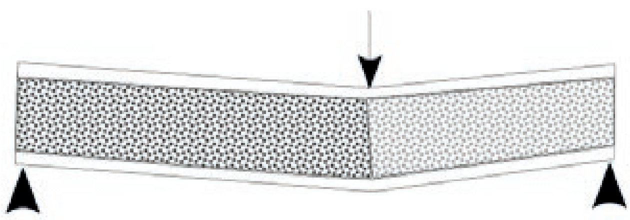

Figure 6.3 - Transverse shear failure.

(2) In order to prevent the transversal shear failure, the design value of shear per unit-length orthogonal to the examined direction, V_{Ed}, should satisfy the condition:

$$V_{Ed} \leq V_{Rd}, \tag{6.34}$$

where the design value of shear capacity V_{Rd} per unit-length in the examined direction is given by:

$$V_{Rd} = f_{d,hV}^{(core)} \cdot h, \tag{6.35}$$

with $f_{d,hV}^{(core)}$ being the design value of the shear strength of the core, orthogonal to the facings.

(3) In order to prevent the horizontal core shear failure, the design value of shear stress in the examined direction of the core, $\tau_{d,hc}$ should satisfy the following relationship:

$$\tau_{d,hc} \leq f_{d,pV}^{(core)}, \qquad (6.36)$$

with $f_{d,hV}^{(core)}$ being the design value of shear strength of the core, parallel to the facings.

6.4.3 Flexural crushing of the core

(1) This mode of failure (Figure 6.4) is caused by:

- insufficient flatwise compressive strength,

or

- excessive panel deflection.

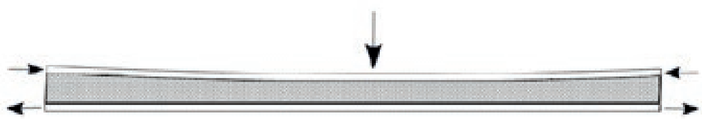

Figure 6.4 - Flexural crushing of the core.

(2) Crushing of the core is a second order effect since the curvatures of facings have to be known in order to estimate the normal load induced by the moment on the core. Finite element analysis could be used to estimate crushing.

6.4.4 Local crushing of the core

(1) This mode of failure (Figure 6.5) is caused by low core compressive strength.

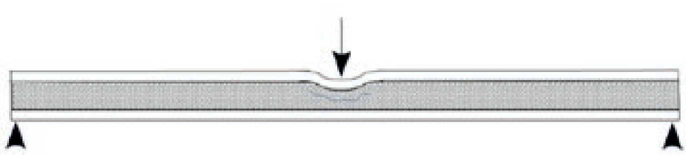

Figure 6.5 - Local crushing of the core.

(2) The compression stress in the core could be evaluated by modelling the loaded facing as a beam or a plate resting on an elastic foundation – the core – and subjected to axial and transverse forces. Local crushing can be caused, mainly, by transverse forces distributed on small areas.

(3) In practice, this failure mode it should be avoided by applying the load over a sufficiently large area A_{cr}. The quantity A_{cr} can be roughly estimated as:

$$A_{cr} = \frac{P_{Ed}^{(core)}}{f_{d,c}^{(core)}} \tag{6.37}$$

where $P_{Ed}^{(core)}$ is the design value of the concentrated load on the core and $P_{Ed}^{(core)}$ the design value of compressive strength of the core in the direction orthogonal to the facings.

(4) Another way to prevent such a local problem is the use of adapted insert between the facings. The performance of the system should be validated experimentally.

6.4.5 Global buckling

(1) This mode of failure (Figure 6.6) is caused by:

- insufficient panel thickness,

or

- insufficient core shear stiffness.

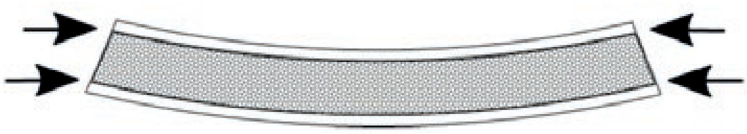

Figure 6.6 - Global buckling.

(2) As an approximate expression for the design value of global buckling load, $P_{Rd,c}$, of sandwich panels in an assigned direction, the following relation should be used:

$$P_{Rd,c} = \frac{P_{Rd,cb} \cdot P_{Rd,cs}}{P_{Rd,cb} + P_{Rd,cs}} \tag{6.38}$$

where:

- $P_{Rd,cb}$ represents the part of the critical load due to bending:

$$P_{Rd,cb} = \frac{\eta_c}{\gamma_M} \cdot \frac{\pi^2 \cdot D}{(L_0)^2}; \tag{6.39}$$

- L_0 is the buckling length in the examined direction, which depends on the boundary conditions.
- D is the equivalent flexural stiffness per unit-length and is calculated by taking into account the variation of Young's modulus along z-axis, and the position and moment of inertia of each ply, as done in the classical laminate theory. For a symmetric sandwich, D is calculated as follows:

$$D = \frac{E_f t_f^{\,3}}{6} + \frac{E_f t_f h^2}{2} + \frac{E_c t_c^{\,3}}{12} \tag{6.40}$$

where:
- E_f, t_f, E_c, t_c are respectively the equivalent Young's moduli and thickness of facings and core;
- E_f, can be measured on coupons in tension, or be estimated via the classical laminate theory;
- h is the distance from centre top facing to centre bottom facing;

For sandwich with thin facings, $t_f << t_c$, and a weak core, $E_f >> E_c$, D from Eq. (6.40) is approximated by:

$$D = \frac{E_f \cdot t_f \cdot h^2}{2}. \tag{6.41}$$

For sandwich with different facings the position of the neutral axis, d, has to be determined. Due to the potential anisotropy of facings, the neutral axis may be different in the x and y direction of the panel. The position of the neutral axis in direction z, is measured from the external facing of the bottom facing, and is deduced from:

$$d\left(E_1 t_1 + E_2 t_2 + E_c t_c\right) = E_1\left(\frac{t_1^2}{2} + t_1\left(t_2 + t_c\right)t_c\right) + E_2\left(\frac{t_2^2}{2}\right) + E_c\left(\frac{t_c^2}{2} + t_2 t_c\right). \tag{6.42}$$

Then the equivalent flexural stiffness per unit-length, D, is given by:

$$D = \frac{E_1 \cdot t_1^{\,3}}{12} + \frac{E_2 \cdot t_2^{\,3}}{12} + \frac{E_c \cdot t_c^{\,3}}{12} + E_1 \cdot t_1 \cdot \left(h + \frac{t_2}{2} - d\right)^2 + E_2 \cdot t_2 \cdot \left(d - \frac{t_2}{2}\right)^2 + E_c \cdot t_c \cdot \left(\frac{h + t_2}{2} - d\right)^2 \tag{6.43}$$

$P_{Rd,cs}$ in (6.38) is the part of the critical load due to transverse shear forces and is taken equal to the design value of the shear stiffness S_d per unit-length, defined as:

$$S_d = \frac{\eta_c}{\gamma_M} k \cdot G \cdot d \tag{6.44}$$

where:
- d is the panel thickness, as defined in Figure 6.1,
- G is an "equivalent" shear modulus of the sandwich and k a suitable shear correction factor. For homogeneous rectangular plates, k is known as equal to 5/6. For anistotropic plates and sandwiches, k-G cannot be obtained usually immediately. One can use energy balance or finite element method.
- For sandwiches and if the shear's behaviour of the core is very weak (foams), more precisely if the product of the shear stiffness by the thickness of the individual facings, $G_i.t_i$, is much higher than the product of the shear stiffness by the thickness of the core material, $G_c.t_c$ (G_i, and G_c being the shear modulus of the facings and core, respectively), (6.44) may be replaced by:

$$S_d = \frac{\eta_c}{\gamma_M} \cdot G_c \cdot \left(d - 2t\right) \tag{6.45}$$

with t the thickness of a facing.

6.4.6 Shear crimping

(1) Sometimes this mode of failure (Figure 6.7) occurs following, and as a consequence of, general buckling. It is caused by:

- too thin facings,
- low core shear modulus,
- low adhesive shear strength.

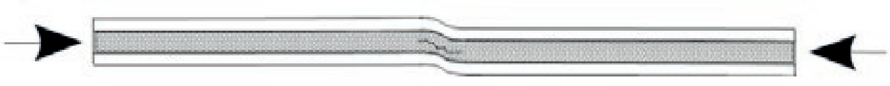

Figure 6.7 - Shear crimping.

(2) The design value of the critical compressive force that leads to shear crimping in the examined direction is deduced from Eq. 6.38 with only $P_{cs,Rd}$ (no bending, only shear stress):

$$P_{Rd,cr} = P_{Rd,cs} \qquad (6.46)$$

and consequently, shear crimping could be avoided if:

$$\sigma_{d,ci} < f_{d,ci} \qquad (6.47)$$

where $\sigma_{d,ci}$ is the design value of compression stress on the facing «i» and $f_{d,ci}$ is the design value of compression strength of the same facing.

6.4.7 Facing wrinkling

(1) If compressive stresses in a facing reach a critical value, facings may buckle as a plate on an elastic foundation. Facings may buckle inward or outward (Figures 6.8a and 6.8b).

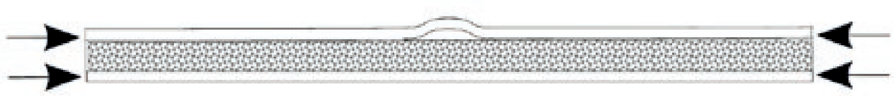

Figure 6.8 a - Facing wrinkling: outward

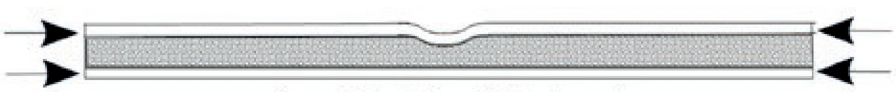

Figure 6.8b - Facing wrinkling: inward.

(2) In order to prevent this failure, the design of compressive stress, in the examined direction of the facing "*i*", should be lower than the following design value of the facing wrinkling strength:

$$\sigma_{\mathrm{Rd,wr}}^{(\mathrm{i})} = \min\left\{0.5 \cdot \frac{\eta_c}{\gamma_M} \cdot \sqrt[3]{E_i \cdot E_c \cdot G_c}\, , 0.82 \cdot \frac{\eta_c}{\gamma_M} \cdot E_i \cdot \sqrt{\frac{E_c \cdot t_i}{E_i \cdot t_c}}\right\}. \qquad (6.48)$$

where E_i is the corresponding equivalent Young's modulus of the facing "i" in the examined direction (the facings may have several different plies and orientations), E_c and G_c are the normal and shear moduli of the core in the same direction, respectively, t_c and t_f are the thicknesses of the core and facings respectively.

6.4.8 Intracell buckling

(1) This mode of failure, also known as dimpling, is applicable to cellular or corrugated cores only. It occurs with:
- very thin facing,

and
- large core cells.

It may cause failure by propagating across adjacent cells, thus inducing facing wrinkling (Figure 6.9).

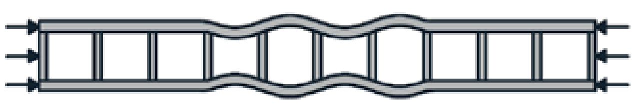

Figure 6.9 – Intracell buckling.

(2) In order to prevent this failure for cellular cores and in lack of more accurate analyses, the compressive stress in the facing should be no higher than the following one:

$$\sigma_{\mathrm{Rd,D}}^{(\mathrm{i})} = \frac{\eta_c}{\gamma_M} \cdot \bar{k} \cdot \frac{E_i}{\lambda_f} \cdot \left[\frac{t_f}{\Delta}\right]^2 \qquad (6.49)$$

where $\sigma_{\mathrm{Rd,D}}^{(\mathrm{i})}$ is design value of the critical dimpling stress in the examined direction of the facing "*i*", E_i is the equivalent compressive Young's modulus in the examined direction of the facing *i*. The quantity Δ is a characteristic cell size:
- for a square cell honeycomb, Δ is the length of the side of the cell and k ≈ 2.5;
- for hexagonal cell honeycomb, Δ is the inscribed diameter of the cell and k ≈ 2.0.

6.4.9 Delamination of facing and core

(1) In order to prevent this failure, the rules set for adhesive joints (Section 8.4) should be applied.

(2) When applying the approach shown in Section 8.4.3.2(3), the design value of normal stress, $\sigma_{Ed}^{(a)}$, and the design value of shear stress, $\tau_{Ed}^{(a)}$, on the adhesive should verify the following relationship:

$$\frac{\sigma_{Ed}^{(a)}}{f_{d,I}}+\frac{\tau_{Ed}^{(a)}}{f_{d,II}}\leq 1 \qquad (6.50)$$

where $f_{d,I}$ and fd,II are the design values of strength of the adhesive for mode I and II, respectively.

6.5 Fatigue

6.5.1 General

(1) For structures subject to cyclic variations in the magnitude of the load, and where the number of expected load cycles is expected to exceed 5000, while causing the peak stress from cyclic and permanent loads to exceed 15% of the material's design strength, or where the absolute maximum value of the cyclic load is greater than 40 % of the design load, fatigue should be taken into account.

(2) The service life of a structure subject to fatigue load is expressed by the number of load repetitions to failure.

(3) Fatigue damage occurs as a result of varying loads, regardless of the sign of the load. Fatigue damage leads to a loss of strength and stiffness and/or cracking and failure.

(4) A cyclic load might be regarded as a constant amplitude load provided that the difference between the maximum and minimum values of the load amplitude does not exceed 10 %. Above that figure, the fatigue load is regarded as a variable amplitude load, see figure 6.10.

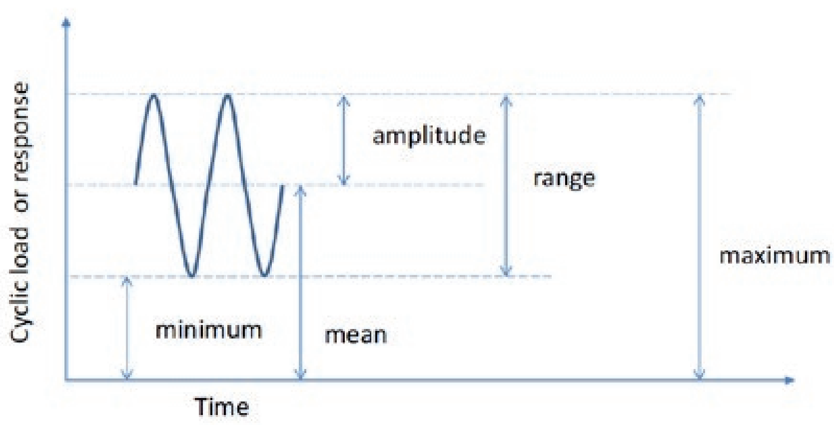

Figure 6.10 – definitions of fatigue parameters.

(5) In the case of a constant amplitude load, the fatigue life should be determined using the *S-N* (*S* = range of cycle versus *N* = number of cycles) line of the same material and of the fatigue load type under consideration, expressed as an *R* value.

(6) The stress ratio, R value, should be calculated from:

$$R=\frac{\sigma_{min}}{\sigma_{max}}, \qquad (6.51)$$

where:
- σ_{min} is the minimum stress that occurs during a cycle;
- σ_{max} is the maximum stress that occurs during a cycle.

(7) It is recommended to verify the fatigue performance for the occurring R-value.

(8) Alternatively, when determining the service life at constant amplitude the following should apply:

- if the structure is only subject to varying tensile load, an *S-N* diagram defined for R = 0.1 can be used;
- if the structure is subject to both tensile and compressive stresses, an *S-N* diagram defined for R = -1 can be used;
- if the structure is only subject to varying compressive stresses, an *S-N* diagram defined for R = 10 can be used.

(9) Values of R near 1 are susceptible to cause creep effects.

(10) Variable amplitude loads may be considered as a combination of constant amplitude loads using Rainflow counting.

(11) When determining the service life for a fatigue load with a constant or variable amplitude load with an R value for which no *S-N* line is known, the service life should be determined using a constant life diagram (CLD).

(12) The effects of variation of material properties and ageing should be accounted for in the tests, or by the use of partial factors and conversion factors in the determination of the fatigue life.

(13) Annex H describes how to derive *S-N* lines and the CLD diagram from test results.

(14) For structures that can be subjected to impact, it should be demonstrated that the service life of a structure subject to fatigue load is within limits including the effect of impact damage that could be present without detection. This should be verified by a test with representative loading and damage conditions.

6.5.2 Fatigue resistance

(1) The evaluation of fatigue with a variable amplitude load should be based on Miner's linear damage rule:

$$D = \sum_{i}^{M} \frac{n_i}{N_i} \leq 1, \qquad (6.52)$$

where:
- n_i is the number of cycles occurring in a load of a specific size and *R* value;
- N_i is the number of cycles to failure for a specific size and *R* value.

(2) A component should be considered to have failed if damage *D* is equal to or larger than 1. The effect of the combined loads from the load spectrum is calculated while disregarding sequence effects.

(3) If parts of the applied fatigue loading spectrum can cause cracking of the fibre mat-to-resin interfaces and other parts of the loading cause compression (and thus potential local buckling) of the fibre mats, then sequence effects can be important. These can be difficult to predict, so in such cases the designer might wish to consider tests such as suggested in §6.5.2.2 to determine the fatigue life of the component.

(4) To determine the characteristic number of permissible load cycles N_i, in the *S-N* diagram it is necessary to choose a service life that corresponds to a 10 % higher stress.

(5) For the relationship between load repetitions and mean number of cycles to failure, the following equivalent double logarithmic equations could be used, where the parameters *a* and *B* are determined from linear regression derived from fatigue tests:

$$\log N = a \cdot \log\left(\frac{1.10 \cdot \gamma_M \cdot \sigma_{max}}{\eta_c \cdot B}\right), \tag{6.53}$$

where:
- N is the number of cycles to failure;
- a is a regression parameter, to be determined from tests;
- σ_{max} is the maximum cyclic stress occurring;
- B is the characteristic failure stress of the laminate at 1 cycle (y-intercept value).

With this formulation it is important that the size of the fatigue stress or strain should be clearly specified. For the cyclic fatigue stress, the maximum stress, the range or the amplitude (half the range) is generally taken.

(6) Annex H describes how to derive an S-N diagram from test results.

(7) The B-value resembles but is not exactly equal to the static tensile strength (R=0.1 or tensile-tensile fatigue) or compressive strength of the laminate (for R=-10 or R=-1 or tensile-compression fatigue; compression-compression fatigue).

(8) As a conservative assumption the S-N line at R=1 could be used. In case of R= -1 the linear Goodman diagram may be used as a special case of the CLD (see Annex H).

6.5.2.1 Mixed-mode fatigue life prediction

(1) For complex geometries (for example at web-to-flange joints of cellular FRP bridge decks), mixed mode fatigue cracks might initiate and propagate at or near the fibre mat-to-resin interfaces due to coexistent local tensile stresses normal to the interface and shear stresses in the plane of the interface. This should be investigated.

(2) If the resin and mat material properties along with the local fibre mat geometries are known accurately, then the mixed mode fatigue life might be predictable using a finite element model in which the mat and resin are discretely represented.

6.5.2.2 Component fatigue testing for complex mixed mode effects

(1) If the local details are uncertain (e.g. if the fibre mat is of variable waviness), then confident prediction of local fatigue life can be difficult. In such cases, the designer might consider proof testing of the component (such as the cellular deck including the fatigue-critical joints of complex geometry) in fatigue, to produce S-N curves for the component. In order to maximize the integrity of the results from such tests, care should be taken to reproduce the actual local contact load distribution on the component as far as possible.

6.6 References

Ascione, L., Giordano, A., Spadea, S., Lateral buckling of pultruded FRP beams (2011). Composites: Part B, Vol. 42(4), pp. 819-824.

Bataineh, A. T., Ganga Rao, H. V. S., Failure Mode Analysis in Pultruded Fiber Reinforced Plastic Tension Members (2009). Report CFCWVU.

Borowicz, D.T., Bank, L.C., Behavior of Pultruded Fiber-Reinforced Polymer (FRP) Beams Subjected to Concentrated Loads in the Plane of the Web (2010). ASCE Journal of Composites for Construction, Vol. 15(2), pp. 229-238.

Clapham, P., Canning, L., Asiedu K., The reconstruction of Moss Canal bridge, Rochdale, UK (2014). Proc. ICE Bridge Engineering (http://dx.doi.org/10.1680/bren.12.00018).

Cole, T.A., Lopez, M., Ziehl P.H., Fatigue behaviour and non-destructive evaluation of full-scale FRP honeycomb bridge specimen (2006). ASCE J. Bridge Eng., Vol. 11(4), pp. 420-429.

Colombi, P., Fava, G., Fatigue of tensile steel-CFRP joints (2012). Composite Structures 94(8), pp. 2407- 2417.

Gay, D., HOA, Suong V., TSAI, Stephen W., (2002) Composite materials: design and applications. CRC press.

Hoff N. J., Mautner S.E., The Buckling of Sandwich-Type Panels, (1945). Journal of the Aeronautical Sciences (Institute of the Aeronautical Sciences), Vol. 12 (3), pp. 285-297.

Hadia, B.K., Matthews F.L., Development of Benson–Mayers theory on the wrinkling of anisotropic sandwich panels (2000). Composite Structures, Vol. 49 (4), pp. 425–434.

Karbhari, V.M., Durability of composites for civil and structural applications (2007). Woodhead Publishing Limited, pp. 126-147. ISBN 978-1-84569-035-9.

King, L., Toutanji, H., Vuddandam, R., Load and resistance factor design of fibre reinforced polymer bridge decks (2012). Composites Part B: Engineering, Vol. 43 (2), pp. 673-680.

Kinloch, A.J., Wang, Y., Williams, J.G., Yayla, P., The mixed mode delamination of fibre composite materials (1993). Composites Science and Technology, Vol. 47 (3), pp. 225-237.

Kollár, L.P., Buckling of Unidirectionally Loaded Composite Plates with One Free and One Rotationally restrained Unloaded Edge (2002). Journal of Structural Engineering, Vol. 128 (9), pp. 1202-1211.

Kollár, L.P., Local Buckling of Fiber Reinforced Plastic Composite Structural Members with Open and Closed Cross Sections (2003). Journal of Structural Engineering, Vol. 129 (11), pp. 1503-1513.

Manshadi, B.D., Vassilopoulos, A.P., De Castro, J., Keller, T., Contribution to shear wrinkling of GFRP webs in cell-core sandwiches (2011). Journal of Composites for Construction, 15 (5), pp. 833-840.

Manshadi, B.D., Vassilopoulos, A.P., De Castro, J., Keller, T., Modeling of buckling and wrinkling behavior in GFRP plate and sandwiches subjected to biaxial compression-tension loading (2011). Journal of Composites for Construction, Vol. 16 (4), pp. 477-487.

Mathieson, H., Fam, A., Static and fatigue behaviour of sandwich panels with GFRP skins and governed by soft-core shear failure (2014). ASCE J. Comp. Constr., Vol. 18(2), pp. 04013046-1-9.

McCarthy, M.J., Bank, L.C., Sensitivity Studies on Local Flange Buckling Equation for Pultruded Beams and Columns (2010). Proceedings of CICE 2010, Beijing, China.

Moon, D.Y., Zi, G., Lee, G.H., Kim, B.M., Huang, Y. K., Fatigue behaviour of a foam-filled GFRP bridge deck (2009). Composites Part B: Engineering, Vol. 40 (2), pp. 141-148.

Mosallam, A.S.,Elsadek A.A., Pul S., Semi-rigid behaviour of web-flange junctions of open-web pultruded composites. In: Proceedings of International Conference on FRP composites 2009, San Francisco, California.

Mottram, J. T., Determination of Critical Load for Flange Buckling in Concentrically Loaded Pultruded Columns (2004). Composites, Part B: Engineering, Vol. 35 (1), pp. 35-47.

Niu, K., Talreja, R., Modeling of Wrinkling in Sandwich Panels under Compression (1999). J. Eng. Mech., 125(8), pp. 875–883.

Nguyen, D. T., D'Ottavio, M., Caron, J.F., Bending analysis of laminated and sandwich plates using a layerwise stress model (2013). Composite Structures, Vol. 96, pp. 135-142.

Nguyen, D.T., Chan, T.M., Mottram, J.T., Influence of boundary conditions and geometric imperfections on lateral-torsional buckling resistance of a pultruded FRP I-beam by FEA (2013). Comp. Struct., Vol. 100, pp. 233–242.

Osei-Antwi, M., De Castro, J., Vassilopoulos, A.P., Keller, T., FRP-balsa composite sandwich bridge deck with complex core assembly (2013). Journal of Composites for Construction, Vol. 17 (6), pp. 04013011-1-9.

Qiao, P., Davalos, J.F., Barbero, E.J., Design optimization of fiber reinforced plastic composite shapes (1998). Journal of Composite Materials, Vol. 32 (2), pp. 177-196.

Qiao, P., Davalos, J. F. and Wang, J., Local Buckling of Composite FRP Shapes by Discrete Plate Analysis (2001). Journal of Structural Engineering, Vol. 127 (3), pp. 245-255.

Pagano, N.J., Stress fields in composite laminates (1978). Int. J. Solids Struct., Vol. 14, pp. 385–400.

Pascoe, J.A., Alderliesten, R.C., Benedictus, R., Methods for the prediction of fatigue delamination growth in composites and adhesive bonds – A critical review (2013). Eng Fract Mech, Vol. 112, pp. 72-96.

Razzaq, Z., Prabhakaran, R., Sirjani, M. M., Load and Resistance Factor Design (LRFD) Approach for Reinforced-Plastic Channel Beam Buckling (1996). Composites: Part B, Vol. 27B, pp. 361-369.

Roberts, T. M., Influence of Shear Deformation on Buckling of Pultruded Fiber reinforced Plastic I-profiles (2002). Journal of Composites for Construction, Vol. 6, pp. 241-248.

Russo, A., Zuccarello, B., An Accurate Method to Predict the Stress Concentration in Composite Laminates with Circular Hole under Tensile Loading (2007). Mechanics of Composite Materials, Vol 43 (4), pp. 359-376.

Sebastian, W.M., Ross, J., Keller, T., Luke, S., Load response due to local and global indeterminacies of FRP deck bridges (2012). Composites Part B: Engineering, Vol. 43(4), pp. 1727-1738.

Sebastian, W.M., Keller, T., Ross, J., Influences of polymer concrete surfacing and localised load distribution on behaviour up to failure of an orthotropic FRP deck bridge deck (2013). Composites Part B: Engineering, Vol. 45(1), pp. 1234-1250.

Sebastian, W.M., Webster, T., Kennedy, C., Ross, J., Profiled metal plate - cork mat loading systems on cellular FRP bridge decks to reproduce tyre-to-deck contact pressure distributions (2013). J. Constr. Bld. Mat., Vol. 49, pp. 1064-1082.

Tay, T.E., Williams, J.F., Jones, R., Characterisation of pure and mixed mode fracture in composite laminates (1987). Theor Appl Fracture Mechan., Vol. 7 (2), pp. 115-123.

Timoshenko, S.P, Gere J.M, Theory of elastic stability, 2nd Edition (1961). McGrawHill, New York.

Turvey, G.J., Structural analysis of CFRP-plated pultruded GRP beams (2006). Structures and Buildings, Vol, 159 (2), pp. 65-75.

Waimer, F., Knippers, J., New design strategy for CFRP and concrete freeform structures (2013). Advanced Composites in Construction 2013, ACIC 2013 - Conference Proceedings, pp. 335-344.

Vinson, J. R., Sandwich structures (2001). Applied Mechanics Reviews, Vol. 54 (3), pp. 201-214.

Zenkert D., An Introduction to Sandwich Construction (1995). Engineering Materials Advisory Services Limited.

Zureick, A., Scott D., Short-Term Behavior and Design of Fiber-Reinforced Polymeric Slender Members under Axial Compression (1997). J. Composites for Const. ASCE, Vol. 1 (4), pp.140-149.

Zureick, A., Steffen, R., Behavior and Design of Concentrically Loaded Pultruded Angle Struts. (2000). J. Struct. Eng. ASCE, Vol. 126 (3), pp. 406-416.

Zureick, A., Scott, D., Short term behavior and design of fiber reinforced polymeric slender members under axial compression (1997). J. Composites for Construction ASCE, Vol. 14, pp. 140-149.

Zureick, A., and Steffen, R. Behavior and Design of Concentrically Loaded Pultruded Angle Struts (2000). ASCE Journal of Structural Engineering, Vol. 126 (3), pp. 406-416.

7 SERVICEABILITY LIMIT STATES

7.1 General

(1) It should be demonstrated that the structure will fulfil the criteria for the serviceability limit states (SLS) throughout its service life, including:

- deformations which affect the outward appearance of the structure, the comfort of users and the functioning of the structure or cause damage to the finishing and non-structural elements (see § 7.2);
- vibrations which cause discomfort to users or affect the functionality of the structure (see § 7.3). This includes the transmission of loads within the structure (e.g. transmission of vibrations in a floor);
- damage that is likely to have an adverse effect on the outward appearance, durability or functioning of the structure (see § 7.4).

(2) When calculating deformation and vibration behaviour, the effects on the stiffness of the material due to aging should be considered. The effect of creep should also be considered. The least favourable situation for the design should be assumed. If a lower stiffness is unfavourable, a reduced elasticity modulus should be assumed in the design by using the suggested conversion factor (see § 2.3.6).

7.2 Deformations

(1) Deformation should be determined using representative mechanical models. Allowance should be made for the effects of anisotropy and shear deformation.

(2) In the case of slender structures, the second order effects should be taken into account, mainly regarding the consequences of initial imperfections (see § 5.2). They can induce unacceptable deformations even under service load levels.

(3) Deformation should not be greater than that which can be matched by other adjoining elements, such as partition walls, glazing, cladding, fittings or finishes. In some cases a limit may be required to ensure the proper functioning of machines or equipment on the structure or to prevent water accumulation on flat roofs.

(4) Deformations should be verified for all loading conditions

7.2.1 Deformation under frequent loads

(1) Deformation under frequent loads should not negate the required clear spaces.

7.2.2 Deformation under occasional loads

(1) Deformation under occasionally occurring loads should not produce a limitation in use or a risk.

(2) Greater deformations and vibrations might occur in FRP structures under accidental loads than is usual for structures made of steel, concrete or similar materials.

7.2.3 Response under quasi-permanent loads

(1) When verifying deformations occurring in the serviceability limit state, for permanent and quasi permanent loads allowance must be made for creep by taking the conversion factor for stiffness , $\eta^{E}_{cv,20}$ into account.

(2) Creep rupture must be prevented by limiting stresses under quasi-permanent load (qp). This goal can be reached by limiting the maximum stress in the composite member as follows,

$$f_{\mathrm{Ed,qp}} < f_{\mathrm{Rd,cr}} = \frac{\eta_{\mathrm{c}} f_{\mathrm{Rk,cr}}}{\gamma_{\mathrm{M}}}, \qquad (7.1)$$

where:
- $f_{\mathrm{Ed,qp}}$ is the maximum stress in the member under quasi-permanent load;
- $f_{\mathrm{Rd,cr}}$ is the design value of the creep rupture limit stress, i.e. the stress limit to ensure that the laminate does not enter the tertiary creep stage;
- $\eta_c = \eta_{ct}\, \eta_{cm}$;
- $f_{\mathrm{Rk,cr}}$ is the characteristic value of the creep rupture limit stress, i.e. the stress limit to ensure that the laminate does not enter the tertiary creep stage, determined at room temperature and dry conditions;
- γ_{M} the partial factor for the material as applicable for ULS strength verification.

(3) For laminates with predominantly unidirectional reinforcement, at room temperature and in dry conditions, the following limit values apply for axial tensile stresses (ACI Committee 440, 2008):
- for AFRP: $f_{\mathrm{Rk,cr}} = 0.5.\ f_{\mathrm{k,t}}$;
- for CFRP: $f_{\mathrm{Rk,cr}} = 0.9.\ f_{\mathrm{k,t}}$;
- for GFRP: $f_{\mathrm{Rk,cr}} = 0.3.\ f_{\mathrm{k,t}}$.

(4) For alternative situations, the characteristic value of the creep rupture limit stress must be derived from tests as listed in Table 3.1.

7.3 Vibration and comfort

(1) Specific reference to the applicable conversion factors provided in section 2.3.6 should be made.

7.3.1 Vibration

(1) Resonance should be taken into account in the design of FRP structures. The vibration behaviour should be verified in both the loaded and unloaded situation.

(2) The natural frequency and the vibration behaviour should be determined in situations with and without aging effects.

7.3.2 Comfort

(1) EN 1990, Annex A and the national annex apply with respect to the comfort criteria for pedestrians.

(2) Comfort should be determined in situations with and without aging effects.

(3) When determining the response, a material damping value of 0.5% and an average value of 1.0% can be assumed as a realistic conservative lower limit for calculations involving monolithic and sandwich structures. Higher damping values may be used if these have been substantiated by representative experimental data.

7.4 Damage

(1) Where the structure is expected to experience damage due to either proper or improper use, and the structure is required to remain functional after the damage has occurred, this damage should be taken into account in the verification.

(2) When repairing damage the possible redistribution of stresses in the structure should be taken into account.

7.5 References

ACI 440.2R-08 Guide for the Design and Construction of Externally Bonded FRP systems for strengthening Concrete structures, ACI Committee 440 (2008).

Allen, D.E., Murray, T.M., Design criterion for vibrations due to walking (1993). Engineering J. AISC, Vol. 30 (4), pp. 117-129.

Ascione, F., Influence of initial geometric imperfections in the lateral buckling problem of thin-walled GFRP I-profiles, Composite Structures (2014), Vol. 112, pp. 85-99.

Chalk, P., Corotis, R.B., A probability model for design live loads (1980). J. Struct. Div. ASCE, Vol. 106 (10), pp. 2017-2030.

Ellingwood, B.R., Structural serviceability (1989). Engineering J. AISC, Vol. 26 (1), pp. 1-8.

Engindinez, M., Zureick, A.H., Deflection response of glass fiber-reinforced pultruded components in hot weather climates (2008). J. Composites for Const. ASCE, Vol. 12 (3), pp. 355-363.

Turkstra, C., Madsen,H., Load Combinations in Codified Structural Design (1980). J. Struct. Div. ASCE, Vol. 106 (12), pp. 2527-2543.

8 CONNECTIONS

8.1 General

(1) Connection and joints between structural elements can be bolted, bonded or a hybrid combination of these two methods of connection.

(2) This guidance permits only bolted and adhesively bonded connections and joints. The connection method of mechanical interlocking should be demonstrated to be fit for purpose by design by testing in accordance with EN 1990 Annex D.

(3) Effect of actions and stresses acting on connections and joints should be determined by elastic analysis of the structure or appropriate sub-structure.`

(4) Connections and joints should have an adequate design resistance against the effect of actions that influence the structure over its intended service life.

(5) Joint resistance should be determined by taking into account the resistances of each single connection in that joint.

(6) Verification of the connection or joint resistance should be carried out by taking into account of all failure modes.

(7) Verification of connection or joint resistance should take into account the actual stress distribution and use the appropriate failure criterion or criteria.

(8) If connection or joint failure leads to disproportionate collapse in an FRP structure, design shall be done by assuring the existence for an alternative stress path.

(9) Environmental conditioning of an FRP component or structure must be considered in design as per Section 4.2 and during execution as per Section 9).

(10) The fire resistance of the joints in an FRP structure must be considered.

8.2 Design criteria

(1) Joints should be designed so that:
- the internal forces and moments are in static equilibrium with the design forces and design moments;
- each element of the joint should be capable of resisting the design forces and design moments.

(2) Configurations in bolted connections or joints should be defined so that the longitudinal axes (local x-direction) of the connected members converge to a single point.

(3) Eccentricity of the actions should be taken into account when determining the design forces and moments within the connection or joint.

8.3 Bolted joints

8.3.1 General

(1) Bolts and nuts of structural grade steels are to be in accordance with EN 1993-1-8 and of structural grade stainless steel are to be in accordance with EN 1993-1-4.

(2) Bolts made with FRP are not permitted.

(3) Connections between plate-to-plate elements subjected to shear action should have bolts with a constant diameter, *d*. When bolts of varying diameters are used in a bolt group the resistance should be determined by testing in accordance with the requirements of EN 1990 and Annex D.

(4) Diameter (*d*) of the bolts should not be less than the thickness of the thinnest connected element, t_{min}, and should be not greater than 1.5 times the thickness of the thinnest connected element.

(5) Hole should be drilled (or reamed, not punched) to have diameter d_0 that allows the bolt of diameter d to pass through without force. The clearance distance between d_0 and d should not exceed the limit specified in Table 8.1.

(6) Steel or stainless steel washers of diameter $d_r > 2d$, and conforming to ISO 7093 should be inserted under the bolt head as well as under the nut.

(7) Bolted connections should be designed on the assumption that the restraint from bolt torque is not beneficial to resistance and that connection force is transferred in bearing between connecting elements.

(8) Bolts should not be over-tightened to prevent compressive crushing failure of the FRP material in the through-thickness direction.

(9) Distances between the centres of the holes for p_1 (pitch spacing) and p_2 (gage spacing) should not be less than $4d$, as show in Figures 8.1 and 8.2. When bolts are staggered, the gage spacing, p_2, and the stagger distance, *L*, should be taken from Table 8.1.

(10) For connection configurations not defined by the geometry in Table 8.1 shall be required to be designed by testing in accordance with the requirements of EN 1990, Annex D.

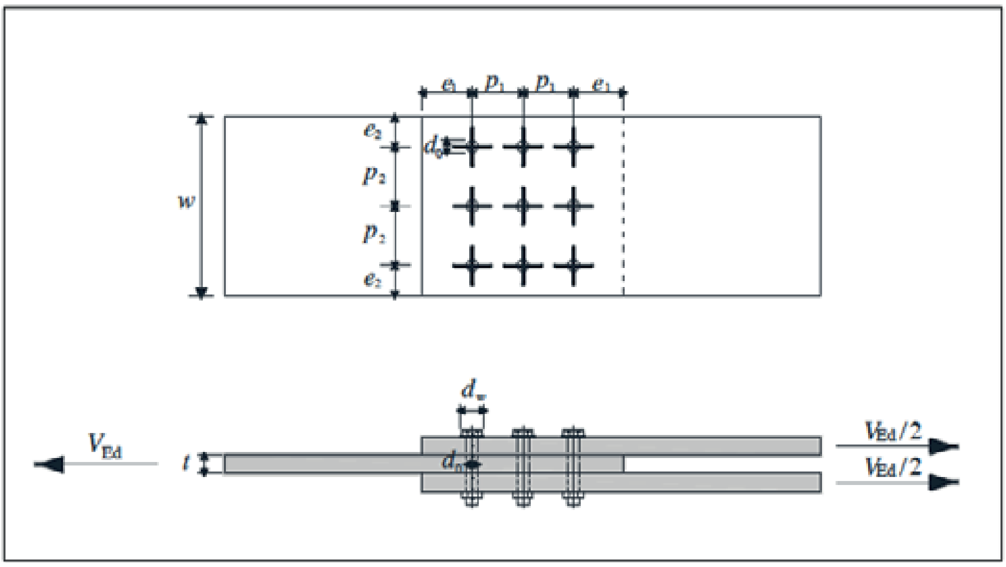

Figure 8.1 – Bolted lap shear joint with symbols for fasteners; not for staggered bolting.

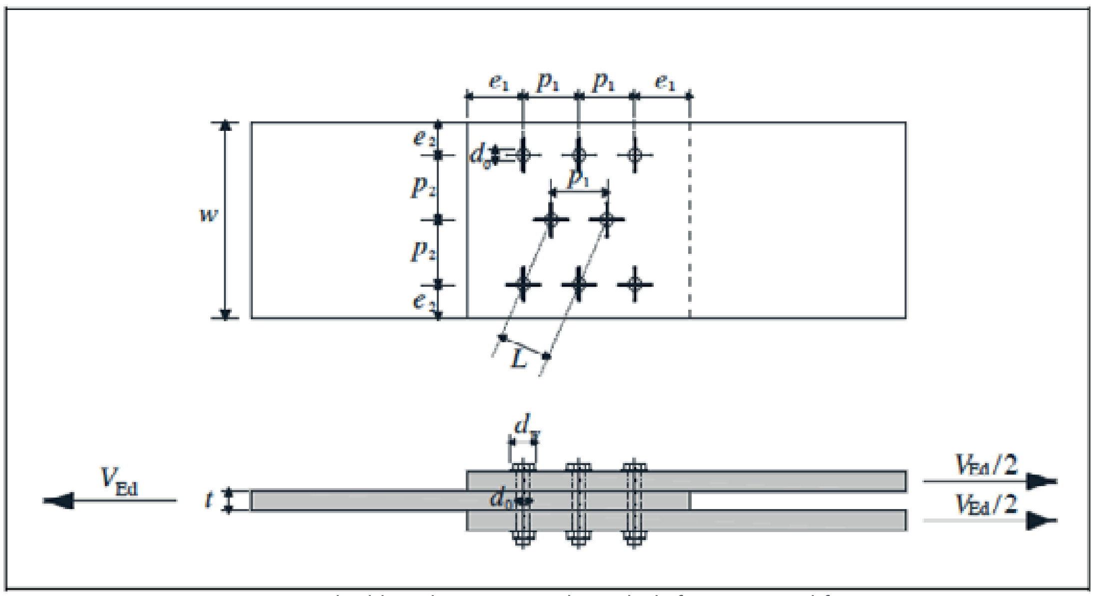

Figure 8.1 – Bolted lap shear joint with symbols for staggered fasteners.

Figure 8.3 shows that for elements, where $e_2 > e_1$ or $e_2 \geq p_2/2$, the effective width w^* and the effective edge distance e_2^* should correspond to the smallest distance in any direction from the hole centre to an adjacent edge and these distances replace width w and edge distance e_2 in the resistance formulae with distances w and e_2.

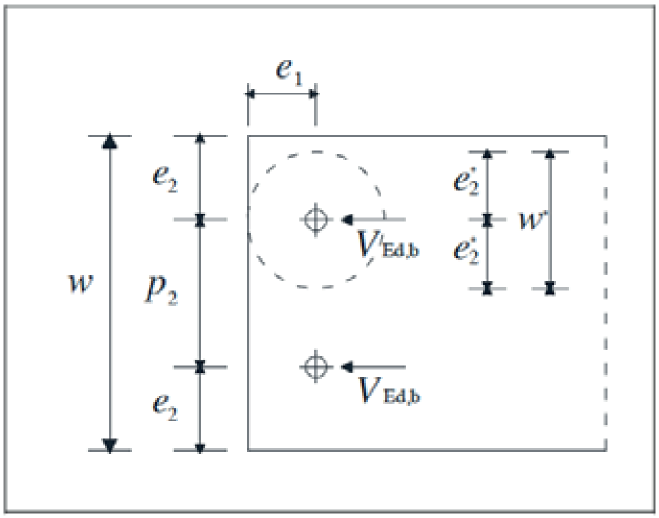

Figure 8.3 – Distances for bolted lap shear joint having a relative large width, *w*.

(11) Geometric limitations of bolted joints are given in Table 8.1.

Table 8.1. Minimum requirements for bolted connection geometries.

Bolt diameter (d) (recommended range)	$d \geq t_{min}$ ($t_{min} \leq d \leq 1.5\, t_{min}$)
Hole diameter (d_0)	$d_0 - d \leq 1$ mm
Distances between holes	$p_1 \geq 4d$ $p_2 \geq 4d$ $L \geq 2.8d$
Distances from edges single row multi-rows	side $e_2 \geq 2d$ end $e_1 \geq 4d$ end $e_1 \geq 2d$

(12) To avoid through-thickness crushing failure of the FRP the maximum bolt torque shall be controlled. Unless specified differently, a maximum average bearing stress of 20 MPa over the washer area can be permitted. For non-greased steel bolts having d_r/d = 2.2 the maximum tightening torque $T_{Rd}^{(tight)}$ is:

$$T_{Rd}^{(tight)} = \frac{d^3 \cdot f_{d,c}^{(th)}}{1.66}, \qquad (8.1)$$

where $f_{d,c}^{(th)}$ is the through-thickness compressive strength of the FRP material.

8.3.2 Design criteria

(1) Static equilibrium shall always be satisfied for the determination of the distribution of the:
- forces between the bolts in a connection;
- stresses in the FRP material adjacent to the holes;
- stress field distant from the influence of the holes.

(2) For bolted connections or joints subjected to in-plane actions, the following distinct failure modes should be taken into account:
- net-tension;
- pin-bearing;
- shear-out;
- bolt-shear.

Mode of failure may not be one of these four distinct modes when the number of bolt rows is two or higher or for a single row where bolt bearing force is not aligned to a principal axis of the laminate. Thus the resistance Equations (8.2) to (8.5) for the four distinct failure modes of double lap-shear joints might not predict a resistance that is lower than the resistance when failure is not one of them. Different failure modes like block shear failure for multi row-connections (8.3.3.4) may govern design.

(3) When the connection is for single lap shear the strength calculated shall be multiplied by a factor of 0.6.

(4) For bolted joints subjected to out-of-plane actions the failure modes that should be taken into account are:
- pull-out failure through the FRP element;
- bolt failure in tension.

8.3.3 Bolted joints subjected to in plane actions

(1) This clause should be used in the absence of a more rigorous procedure for the design of plate-to-plate lap shear joints. The rules apply to bolted connections, in which, at least, one component is of FRP material. Each bolt row has the same grade and size of steel bolts and number (n_b up to a maximum of four (see Figures 8.1 and 8.2)). Each bolt in a row transmits an equal part of the connection force, V_{Ed}, at that row.

(2) $V_{Ed,b}$ per bolt per row is given by:

$$V_{Ed,b} = \frac{V_{Ed}\, c_r}{n}, \tag{8.2}$$

$V_{Ed,b}$ is a design force acting through the cross-sectional area at the bolt row, and c_r is the bolt row load distribution coefficient in Table 8.2.

For joints connecting FRP and elements of structural grade steels, the steel joint should be designed in accordance with clauses in EN 1993-1-1 and EN 1993-1-8. Figure 8.4 shows that the first row of bolts for the FRP element on the left-side is Row 4, whereas for the FRP or steel element on the right-side it is Row 1.

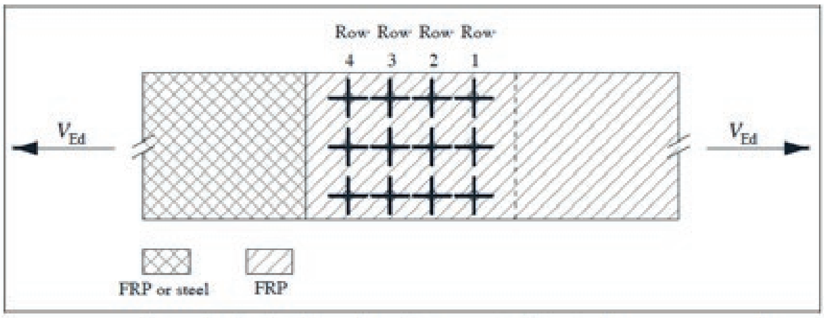

Figure 8.4 – layout of multi-bolted lap shear (connection) joint between two plate elements of which at least one is of FRP material.

Table 8.2. Load distribution coefficients, c_r, for the rows in a multi-bolted lap-shear joint.

Number of rows		Row 1	Row 2	Row 3	Row 4
1	FRP/FRP	1			
	FRP/steel	1			
2	FRP/FRP	0.5	0.5		
	FRP/steel	0.6	0.4		
3	FRP/FRP	0.4	0.2	0.4	
	FRP/steel	0.5	0.3	0.2	
4	FRP/FRP	0.3	0.2	0.2	0.3
	FRP/steel	0.4	0.3	0.2	0.1
> 4		Not permitted			

8.3.3.1 Net-tension failure

(1) For the situation where V_{Ed} is oriented with angle $0° \leq \theta \leq 5°$ to the major principal axis of an FRP pultruded laminate (1-axis in Figures 1.2 and 1.3 and illustrated in Figure 8.5) the net-tension resistance is:

$$V_{Ed} \leq \frac{1}{k_{tc}} \cdot f_{d,0,t} \cdot (w - n \cdot d_0) \cdot t \,, \qquad (8.3a)$$

where n is number of bolts across the first bolt row where there is net-tension failure mode, t is the FRP thickness, w the FRP width, $f_{d,0,t}$ is the design tensile strength of the FRP in the 1-direction and k_{tc} is a stress concentration factor. The coefficient k_{tc} should be assumed equal to 3.75.

(2) For the situation where V_{Ed} is oriented with angle $5° < \theta \leq 90°$ to the 1-direction of an FRP pultruded laminate the net-tension resistance is:

$$V_{Ed} \leq \frac{1}{k_{tc}} \cdot f_{d,90,t} \cdot (w - n \cdot d_0) \cdot t \,, \qquad (8.3b)$$

$f_{d,90,t}$ is the design tensile strength of the FRP material in the 2-direction (Figures 1.2 and 1.3) and k_{tc} is unchanged.

(3) In the case of a balanced symmetric cross-play laminate with continuous fibre layers arranged in the two orthogonal directions of 1 and 2, Equations (8.3a) and (8.3b) can be used by taking θ as the smallest angle between V_{Ed} and the principal directions 1 or 2 ($0° \leq \theta \leq 45°$). For $0° \leq \theta \leq 5°$ Equation (8.3a) should be used and for $5° < \theta \leq 45°$ Equation (8.3b) should be used.

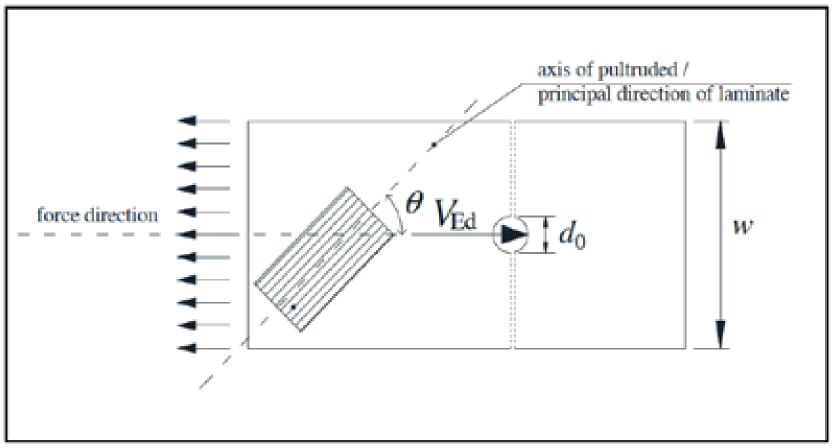

Figure 8.5 – Net tension failure mode illustrated with a single bolt.

8.3.3.2 Pin-bearing failure

(1) For the situation where $V_{Ed,b}$ is oriented with angle $0° \leq \theta \leq 5°$ to the major principal axis of an FRP pultruded laminate (1-axis in Figures 1.2 and 1.3 and illustrated in Figure 8.6),
the pin-bearing resistance is:

$$V_{Ed,b} \leq \frac{1}{k_{cc}} \cdot f_{d,0,br} \cdot d \cdot t \ . \qquad (8.4a)$$

For the situation where $V_{Ed,b}$ is oriented at an angle of $\theta > 5°$ to 90° to the 1-direction of an FRP pultruded laminate the pin-bearing resistance is:

$$V_{Ed,b} \leq \frac{1}{k_{cc}} \cdot f_{Rd,90,br} \cdot d \cdot t \ , \qquad (8.4b)$$

$V_{Ed,b}$ is the design value of bearing force transmitted per bolt, and $f_{d,0,br}$ and $f_{d,90,br}$ are the design values of pin-bearing strength in the 0° and 90° directions. k_{cc} is the reduction factor $(d_0/d)^2$ that accounts for the bearing compressive stress concentration in front of the bolt from having a clearance hole with limit of size given in Table 8.1.

(2) In the case of a balanced symmetric cross-play laminate with continuous fibre layers in the two orthogonal directions 1 and 2 Equations (8.4a) and (8.4b) can be used by taking q to be the smallest angle between $V_{Ed,b}$ and the principal directions 1 or 2 ($0° \leq \theta \leq 45°$). For $0° \leq \theta \leq 5°$ Equation (8.4a) should be used and for $5° < \theta \leq 45°$ Equation (8.4b) should be used.

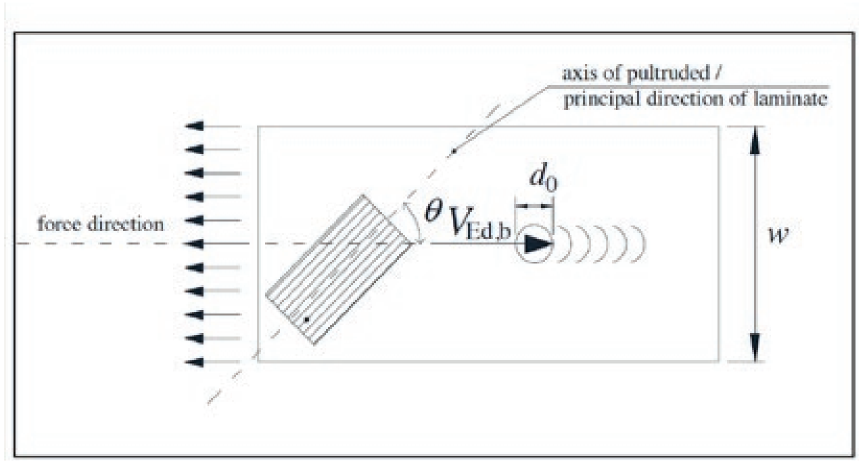

Figure 8.6 – Pin-bearing failure mode.

8.3.3.3 Shear-out failure

(1) For a connection having a single row of bolts the shear-out failure resistance per line of bolts is:

$$V_{Ed,b} \le f_{d,V} \cdot (2e_1 - d) \cdot t; \qquad (8.5a)$$

(2) For two rows of bolts (n = 2) separated by pitch spacing, p1, the shear-out resistance per line of bolts is:

$$V_{Ed,b} \le f_{d,V} \cdot 1.4(e_1 - 0.5 \cdot d_0 + p_1) \cdot t; \qquad (8.5b)$$

(3) For three or four rows of bolts separated by pitch spacing, p1, the shear-out resistance per line bolts is,

$$V_{Ed,b} \le f_{d,V} \cdot 2((n-1)p_1) \cdot t, \qquad (8.5c)$$

where $f_{d,V}$ is the design value of the in-plane shear strength of the FRP material, and $V_{Ed,b}$ is the design value of bearing force transmitted by a bolt or column line of bolts (Figure 8.7).

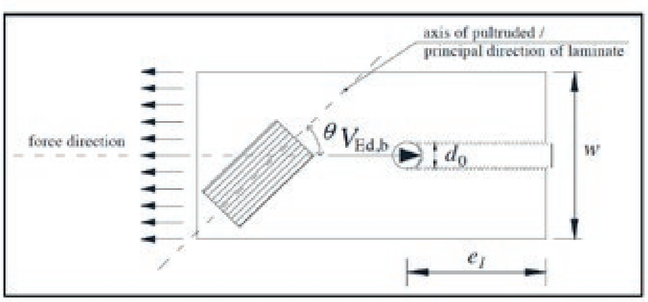

Figure 8.5 – Shear-out failure mode.

8.3.3.4 Block shear failure

(1) When the connection force is in tension, concentric to the group of bolts, and parallel to the direction of FRP material, the block shear strength for the multi-bolted connection shall be,

$$V_{Ed} \le 0.5 \cdot \left(A_{ns} f_{d,V} + A_{nt} f_{d,0,t} \right). \tag{8.6a}$$

(2) For a bolt group subject to eccentric in-plane loading, the block shear strength for the multi-bolted connection shall be,

$$V_{Ed} \le 0.5 \cdot \left(A_{ns} f_{d,V} + 0.5 \cdot A_{nt} f_{d,0,t} \right), \tag{8.6b}$$

where A_{ns} is the net area subjected to shear, A_{nt} is net area subjected to tension, which should be taken as its gross area less appropriate deductions for all holes, $f_{d,V}$ is the design value of the in-plane shear strength of the FRP material, and $f_{d,0,t}$ is design tensile strength of the FRP in the 1-direction.

8.3.3.5 Bolt-shear failure

(1) Shear resistance for a steel or stainless steel bolt should be designed in accordance with the clauses in EN 1993-1-8 or EN 1993-1-4.

8.3.4 Bolted joints subjected to out of plane actions

8.3.4.1 Pull-out failure

(1) To design for through-thickness shear failure (Figure 8.8) the pull-out resistance is:

$$N_{Ed,b} \le f_{d,V}^{(th)} \cdot \pi \cdot d_r \cdot t\,, \tag{8.7}$$

where d_r is the diameter of the washer and $f_{d,V}^{(th)}$ is the design value of the shear strength in the through thickness direction.

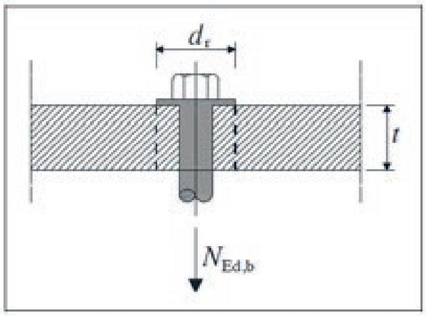

Figure 8.8 – Pull-out failure caused bu through-thickness tension action.

8.3.4.2 Bolt failure from tensile forces

(1) Steel bolts subjected to tensile forces (Figure 8.9) should be designed in accordance with the clauses in EN 1993-1-8 or EN 1993-1-4.

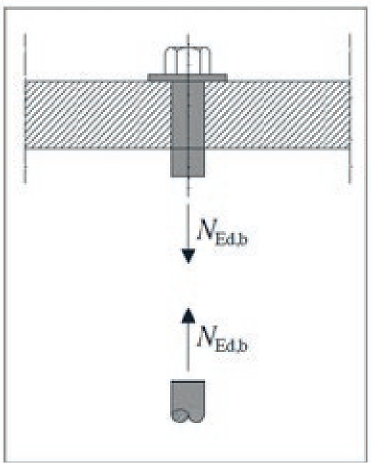

Figure 8.8 – Bolt failure due to tension forces.

8.3.5 Bolted joints subjected to in and out of plane actions

(1) For combined shear and tensile actions the resistance of an FRP laminate is given by the linear interaction failure criterion:

$$\frac{V_{Ed}}{R_{d,V}} + \frac{N_{Ed}}{R_{d,N}} \leq 1 \qquad (8.8)$$

In Equation (8.8) V_{Ed} and N_{Ed} are the design values of the shear and tensile actions, while $R_{d,V}$ and $R_{d,N}$ represent the corresponding design resistances of the FRP, after accounting for openings. $R_{d,V}$ and $R_{d,N}$ can be determined by using appropriate clauses in Chapter 6 for pultruded and laminate members.

(2) In presence of combined shear and tensile actions the resistance of steel bolts should be designed in accordance with the clauses in EN 1993-1-8 or EN 1993-1-4.

8.3.6 References

Ascione, F., Feo, L., Maceri, F., An experimental investigation on the bearing failure load of glass fibre/epoxy laminates (2009). Composites Part B: Engineering, Vol. 40, pp. 197-205.

Ascione, F., Feo, L. and Maceri, F., On the pin-bearing failure load of GFRP bolted laminates: An experimental analysis on the influence of bolt diameter (2010). Composites Part B: Engineering, Vol. 41, pp. 482-490.

Collings, T.A., The strength of bolted joints in multi-directional CFRP-laminates, Composites, January 1977, pp. 43-55

Feo, L., Marra, G. and Mosallam, A., Stress analysis of multi-bolted joints for FRP pultruded composite structures (2012). Composite Structures, Vol. 94 (7), pp. 3769-3780.

Evernden, M. and Pelly, R. J., Single bolt tension joints in pultruded PFRP legangle connections (2009), Proceedings Fourth International Conference on Advanced Composites in Construction (ACIC 2009), Net Composites Ltd., Chesterfield, UK, pp. 473-482.

McCarthy, M.A., McCarthy, C. T. and Padhi, G. S., A simple method for determining the effects of bolt-hole clearance on load distribution in single-column multi-bolt composite joints (2006), Composite Structures, Vol. 73 (1), pp. 78-81.

Mottram, J.T., Nominally pinned connections for pultruded frames,' in Clarke, J.L., (Ed.), Structural Design of Polymer Composites - EUROCOMP Design Code and Handbook, S. & F. N. Spon, London, (1996), 703-718.

Mottram, J. T. and Turvey, G. J., Physical test data for the appraisal of design procedures for bolted joints in pultruded FRP structural shapes and systems (2003). Progress in Structural Engineering and Materials, Vol. 5 (4), pp. 195-222.

Mottram, J. T., Determination of pin-bearing strength for the design of bolted connections with standard pultruded profiles (2009). Proceedings Fourth International Conference on Advanced Composites in Construction, Net Composites, Chesterfield, UK, pp. 483-495.

Mottram, J. T., Prediction of net–tension strength for multi-row bolted connections of pultruded material using the Hart-Smith semi-empirical modeling approach (2010). Journal of Composites for Construction, Vol. 14 (1), pp. 105-114.

Mottram J. T. and Zafari, B., Pin-bearing strengths for design of bolted connections in pultruded structures (2011). Structures and Buildings, Vol. 164 (5), pp. 291–305.

Mottram, J. T., Rationale for simplifying the strength formulae for the design of multi-row bolted connections failing in net tension (2013). Proceedings Sixth International Conference on Advanced Composites in Construction (ACIC 2013), NetComposites Ltd., Chesterfield, UK, 383-392.

Oppe, M., Zur Bemessung geschraubter Verbindungen von pultrudierten faserverstärkten Polymerprofilen (2009). Schriftenreihe Stahlbau, Heft 66, Shaker-Verlag Aachen, ISBN: 978-3-8322-8247-9

Oppe, M. and Knippers, J., Behaviour of bolted connections in GFRP subjected to tension loads (2009). Proceedings Fourth International Conference on Advanced Composites in Construction (ACIC2009), Net Composites, Chesterfield, UK, pp. 495-506.

Oppe, M. and Knippers J., A consistent design concept for bolted connections in standardized GFRP-profiles (2010). Proceedings of Fifth International Conference on FRP Composites in Civil Engineering – CICE2010, Beijing, China, Advances in FRP Composites in Civil Engineering – Vol. I FRP for Future Structures - ISBN: 978-3-642-17486-5

Prabhakaran, R., Razzaq, Z. and Devara, S. Load and Resistance Factor Design (LRFD) Approach for Bolted Joints in Pultruded Composites (1996), Composites - Part B: Engineering, Vol. 27(3-4), pp. 351-360.

Tajeuna, T. A. D., Legeron, F., Langlois, S., Labossiere, P. and Demers, M., Effect of geometric parameters on the behavior of bolted GFRP pultruded plates (2016). Journal of Composite Materials, Vol. 50(26), pp. 3731- 3749.

Turvey, G. J. and Wang, P., Thermal preconditioning study for bolted tension joints in pultruded GRP plate, (2007). Composite Structures, Vol. 77 (4), pp. 509-513.

Turvey, G. J. and Wang, P., Failure of pultruded GRP single-bolt tension joints under hot–wet conditions (2007). Composite Structures, Vol. 77 (4), pp. 514-520.

Turvey, G. J. and Wang, P., Failure of pultruded GRP angle leg junctions in tension (2009). Proceedings of Seventeenth International Conference on Composite Materials (ICCM-17), 27-31 July 2009, Paper A1:1. p. 11.

Wang, Y. J., Bearing behavior of joints in pultruded composites (2002). Journal of Composite Materials, Vol. 36 (18), pp. 2199-2216.

8.4 Adhesively bonded joints

8.4.1 General

(1) Bonded connections should not be allowed for primary load bearing components, where failure of the connection could lead to progressive collapse or unacceptable risks. In these situations, their use is only allowed in combination with bolted connections or an alternative backup solution.

(2) Bonded joints are formed with an FRP adherent subjected to axial force. The most common configurations are illustrated in Figure 8.10. Symmetry with respect to the plane orthogonal to the adhesive bondline is assumed. Similar joint configurations with tapering in adherent thickness to reduce stress concentrations are appropriate and the design will be conservative.

(3) The mechanical behaviour of joints c) and d) can be reduced to joints a) and b), respectively. On the basis of the large number of studies available in current literature, in the case a) the use of two adherends with the same thickness is recommended (simple-lap symmetrical joint).

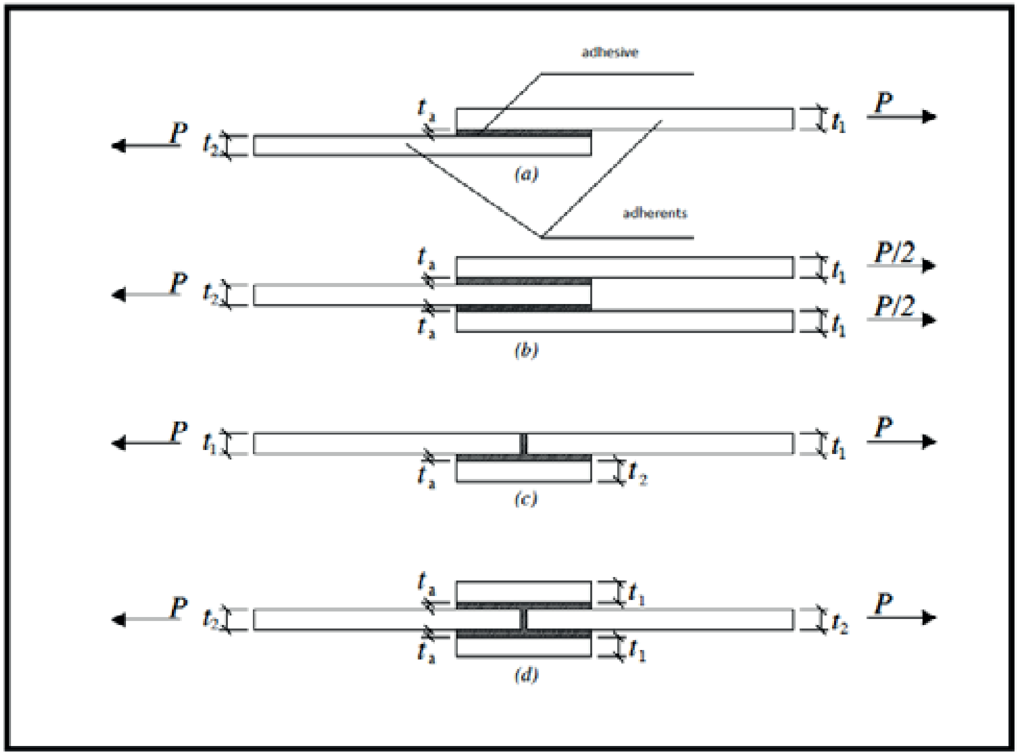

Figure 8.10 – Types of bonded joints: a) simple-lap; b) weighted double-lap;
c) simple covered-joint; d) double covered-joint.

8.4.2 Constitutive laws of the interface

(1) The layer of adhesive prevents the relative displacements between the bonded elements (Figure 8.11): the transversal displacements, δ, which induce an opening between the adherends, and those in the longitudinal direction, s, which induce sliding.

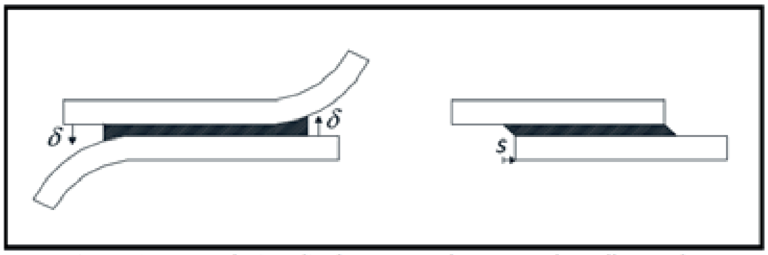

Figure 8.11 – Relative displacements between the adherends.

(2) The symbols σ and τ denote, respectively, the normal interfacial stress (orthogonal to plane of the joint) and the shear stress (parallel to the plane of the joint). Such quantities can be described by means of two uncoupled design cohesive laws, $\sigma(\delta)$ and $\tau(s)$ (Figure 8.12). The post-peak branches are generally schematized as linear segments. This assumption is made in the following.

The displacement at the end of the linear range in both diagrams is generally much less than at the end of the "*softening*" range.

The subtended areas of the two diagrams are equal to the fracture energies for mode I (diagram $\sigma(\delta)$) and mode II (diagram $\tau(s)$), respectively.

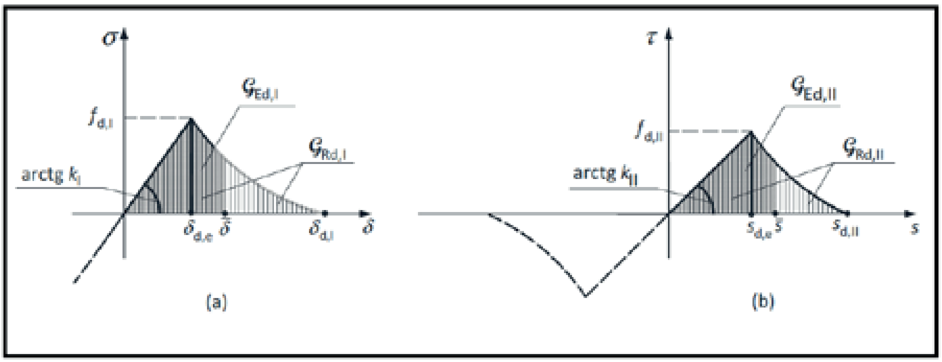

Figure 8.12 – Cohesive interfacial laws.

The symbols utilized in this Section have the following meaning:

- t_a thickness of the adhesive layer
- t_i thickness of the adherend i
- $f_{d,I}$ design value of the resistance of the adhesive for mode I
- $\delta_{d,I}$ design value of the ultimate opening exhibited by the adhesive
- $\delta_{d,e}$ design value of the opening exhibited by the adhesive at the end of the linear elastic range
- k_I actual stiffness of the adhesive in the linear elastic range of mode I
- $\mathcal{G}_{Rd,I}$ design value of fracture energy for mode I
- $\mathcal{G}_{Ed,I}$ design value of adhesion energy for mode I corresponding to the opening
- $f_{d,II}$ design value of the resistance of the adhesive for mode II
- $s_{d,II}$ design value of the ultimate sliding exhibited by the adhesive
- $s_{d,e}$ design value of the sliding exhibited by the adhesive at the end of the linear elastic range
- k_{II} shear stiffness of the adhesive in the linear elastic range of mode II
- $\mathcal{G}_{Rd,II}$ design value of fracture energy for mode II
- $\mathcal{G}_{Ed,II}$ design value of adhesion energy for mode I corresponding to the opening
- $\sigma_{Ed}^{(a)}$ design value of the normal stress orthogonal to the adhesive layer
- $\tau_{Ed}^{(a)}$ design value of the shear stress parallel to the adhesive layer

(3) Apart from more rigorous models, simplified constitutive interface laws could be used (Annex G).

(4) The simplest models consist of the only linear elastic branches until $f_{d,I}$ or $f_{d,II}$, respectively. In this case the assumptions $\delta_{d,e} = \delta_{d,I}$ and $s_{d,e}=s_{d,II}$ are made. The quantities $\delta_{d,e}/t_a$ and $s_{d,e}/t_a$ represent the dilatation and the shear strain of the adhesive layer (t_a is the thickness of the adhesive). Furthermore, k_I/t_a and k_{II}/t_a coincide with the modulus of elasticity and shear modulus of the adhesive, respectively.

(5) From the above it follows that the adhesive is characterized by the following quantities: $f_{d,I}$, $f_{d,II}$, $\delta_{d,I}$d, , $s_{d,II}$, k_I and k_{II} . The experimental evaluation of $f_{d,I}$, $f_{d,II}$, k_I and k_{II} can be performed by means of the standard ASTM D903. The evaluation of d $\delta_{d,I}$ $s_{d,II}$ requires the knowledge of the fracture energies for mode I (Double Cantilever Beam Test, ISO 15024:2001) and II (Calibrated End-Loaded Split Test, ISO 15114:2014). When adopting the linear elastic approach in (4), the evaluation of the fracture energies is not needed.

(6) If the post-peak branches are schematized as linear segments, it i $\delta_{d,I} = 2\mathcal{G}_{Rd,I} / f_{d,I}$; $s_{d,II} = 2\mathcal{G}_{Rd,II} / f_{d,II}$.

8.4.3 Interface failure

8.4.3.1 Failure due to sliding of the joint

(1) Joint strength prediction according to mode II failure (sliding) does not include the additional stress resultants from deformations caused by load eccentricity.

8.4.3.2 Failure due to sliding and opening of the joint

(1) If the joint is also subjected to shear and flexure, in the plane of symmetry, mixed mode I/II of failure occurs and the performance to transfer axial forces is penalized. The coupling between the normal and tangential stresses arising at the interface should be taken into account.

(2) The design value of axial resistance, N_{Rd}, could be calculated adopting a suitable mixed mode I/II of fracture, among those presented in current literature. These include the following relationship, which can be easily applied due to its additive character:

$$\frac{\mathcal{G}_{Ed,I}}{\mathcal{G}_{Rd,I}} + \frac{\mathcal{G}_{Ed,II}}{\mathcal{G}_{Rd,II}} \leq 1. \qquad (8.9a)$$

In (8.9a) the quantities $\mathcal{G}_I$ and $\mathcal{G}_{II}$ are, respectively, the areas subtended by the curves of Figure 8.12 over the ranges $[0,\bar{\delta}]$ and $[0,\bar{s}]$, where θ and s are, in that order, the design values of the opening and the sliding; $R_{d,I}$ G and $R_{d,II}$ G are, respectively, the design fracture energy for mode I: $\mathcal{G}_{Rd,I} = \mathcal{G}_I(\bar{\delta} = \delta_{d,I})$, and for mode II: $\mathcal{G}_{Rd,II} = \mathcal{G}_{II}(\bar{s} = s_{d,II})$

(3) When adopting the approach in 8.4.2 (4), the relationship (8.9a) becomes,

$$\frac{\sigma_{Ed}^{(a)}}{f_{d,I}} + \frac{\tau_{Ed}^{(a)}}{f_{d,II}} \leq 1 \qquad (8.9b)$$

where the numerators represent the design normal stress and the design shear stress on the adhesive, respectively.

8.4.4 Ultimate limit state of the joint

(1) The verification of the ULS of a bonded joint should require that the following conditions are satisfied:

- within the adherend: the prescriptions set for FRP elements (profiles or laminates) have to be satisfied;
- in the adhesive:

$$N_{Ed} \leq N_{Rd}\,, \tag{8.10}$$

where N_{Ed} is the design value of axial force to be transferred by the joint and N_{Rd} is the design value of axial resistance as evaluated in Section 8.4.3.2.

(2) The indication given in Sections 2.3.4 and 2.3.5 has to be taken into account.

(3) The resistance of a bonded joint can be verified through design by testing. This includes joint configurations not scoped by Figure 8.10. The design resistance can be determined in accordance to the procedure in EN 1990.

8.4.5 Pratical design regulations

(1) The thickness of the adhesive layer, t_a, should not be less than 0.1 mm.

(2) As a rule, the length of the bonding should not be less than:

$$L^* = \sqrt{\frac{\pi^2 \cdot t_{max} \cdot E_{fmax}}{k_{II}}}\,, \tag{8.11}$$

where t_{max} is the greatest thickness of the adherends (i.e. either t_1 or t_2 in Figure 8.10), and E_{fmax} is the modulus of elasticity of the FRP material in the direction of the axial force (P in Figure 8.10). When the design lap length is less than L* , evaluation of the interface resistance should be based on analysis with the cohesive interface laws presented in Figure 8.12. k_{II} can be established using the Annex G modelling approach.

8.4.6 Bonding control

(1) Quality control of the adhesively bond layer(s) should be carried out by using either destructive and/or non-destructive testing.

8.4.6.1 Destructive tests

(1) For joints made either in a factory or on site and a minimum of three samples of each joint type should be tested using an appropriate test method for their stiffness and resistance.

8.4.6.2 Nondestructive tests

(1) Non-destructive tests may be used to characterize the quality of the adhesively bonding by identifying fabrication defects due to adhesive or cohesive debonding failures, and from internal voiding.
Suitable test methods are sonic and/or ultra-sonic, acoustic and thermographic emissions.

(2) Internal strain or/and surface strain measurements may be used to verify that stresses are being transferred appropriately.

8.4.7 References

Abdelaziz A.T., Boukhili R., Achiou S., Gordon S., Boukehili, H., Bonded joints with composite adherends. Part I. Effect of specimen configuration, adhesive thickness, spew fillet and adherend stiffness on fracture (2006). Int J Adhes Adhes., Vol. 26, pp. 226–36.

Ascione, F., Mancusi, G., Curve adhesive joints (2012). Compos Struct. Vol. 94, pp. 2657–2664.

Ascione, F., Ultimate behaviour of adhesively bonded FRP lap joints (2009). Composites Part B: Engineering, Vol. 40, pp. 107-115.

Ascione, F., Mechanical behavior of FRP adhesive joints: A theoretical model (2009). Composites Part B: Engineering, Vol. 40, pp. 116-124.

CNR-DT 205/2007. Guide for the design and construction of structures made of pultruded FRP elements, Advisory Committee on Technical Recommendations for Construction, National Research of Italy, Rome, CNR, October 2008.

da Silva, LFM, Adams RD., Joint strength predictions for adhesive joints to be used over a wide temperature range (2007). Int J Adhes Adhes., Vol. 27, pp. 362–379.

Kafkalidis, MS., Thouless, MD., The effects of geometry and material properties on the fracture of single lap-shear joints (2002). Int J Solids Struct., Vol. 31, pp. 2537–2563.

Katnam, KB., Sargent, JP., Crocombe, AD., Khoramishad, H., Ashcroft, IA., Characterisation of moisturedependent cohesive zone properties for adhesively bonded joints (2010). Eng Fract Mech., Vol. 77, pp. 3105–3119.

Keller, T., Vallée, T., Adhesively bonded lap joints from pultruded GFRP profiles. Part I: Stress-strain analysis and failure modes (2005). Composites Part B: Engineering, Vol. 36 (4), pp. 331-340.
Sato C., Stress estimation of joints having adherends with different curvatures bonded with viscoelastic adhesives (2011). Int J Adhes Adhes, Vol. 31, pp. 315-321.

Shahverdi, M., Vassilopoulos, A.P., Keller, T., Mixed-mode quasi-static failure criteria for adhesively-bonded pultruded GFRP joints (2014). Composites Part A: Applied Science and Manufacturing, Vol. 59, pp. 45-56.

9 PRODUCTION, INSTALLATION AND MAINTENANCE

9.1 General

(1) The production and realization procedures of FRP structures should be described in an execution and quality plan.

(2) The production should be executed by producers and personnel with appropriate level of experience for the used FRP materials and production techniques.

(3) When determining the necessary level of experience, for all activities the complexity and consequence class of the structure should be taken into account.

(4) The procedures involved in the assembly and installation of the FRP structure should be described in the execution plan.

(5) The assembly and installation of an FRP structure should be executed under supervision of a professional with the required experience in working with FRP materials and FRP structures, in line with EN 1990. The executing personnel should be provided with clear instructions on working with FRP, before the start of the installation process.

(6) The general inspection of an FRP structure should be executed by a well instructed expert, described in accordance with an included inspection plan. A detailed inspection should be executed periodically, in accordance with a pattern described in advance, and in case of ascertained deviations.
Detailed inspections should be executed by an FRP expert.

(7) In addition to the above described guidelines it could be stipulated that for important structures (e.g. consequence class 3 structures) an independent check by an FRP expert is executed.

9.2 Quality plan

(1) A quality plan should be developed for production and installation.

(2) Before the start of the production, the following aspects should be prepared:
- A statement of the necessary characteristics and nominal properties of the FRP structure and materials.
- A test plan, describing the tests that should be executed and FRP material samples that should be prepared. The test plan involves the tests that are part of the quality control procedures as well as tests that are part of the proof of performance of the design.
- A quality plan of the production. This quality plan describes the materials, curing procedure, process control, end control.

(3) The manufacturer should have a quality system in place in accordance with current ISO standards in which the following are described:
- material control;
- process control;
- end control.

(4) The manufacturer should register the following information:
- materials used, including supplier data as well as health and safety information;
- estimated weight of the main parts, assembled parts included;
- report of the quality control;
- report of the executed design, product and process verifications and results;
- report of the executed tests and test results, in accordance with the provisions given in Section 3.

9.3 Materials

(1) The materials that are used should be traceable in accordance with EN16245.

(2) Fibre material and core materials should be free of dust and moisture.

(3) Fibres, resin, adhesives and other chemical materials should be processed in accordance with the technical specifications of producers and suppliers and may not be used beyond the expiry date.

9.4 Production

(1) Detailed working instructions should be provided describing the important steps in the production process that are critical to quality, such as handling of materials and equipment, checks, etc.

(2) As a minimum, the following parameters should be controlled and verified during the production of FRP parts:

- Temperature, moisture content and pressure during the process (impregnation and cure)
- Number of plies and ply thickness or weight
- Position of splices and overlap lengths
- Fibre orientation and fibre alignment
- Fibre tension (filament winding)
- Resin constitution, e.g. quantity of components, mixing time, viscosity, temperature.
- Fibre wetting
- Void content
- Fibre volume fraction
- Degree of cure, for example by glass transition temperature Tg or heat distortion temperature HDT. For sandwiches, complete adhesion between facings and core over the surface.
- Adhesion between fibre and resin, for example by Inter Laminar Shear Strength

(3) Presence of moisture and dust should be prevented during the production of FRP.

(4) FRP structural components should be cured in accordance with the specifications of the resin supplier. The cure temperature should be evaluated over the structure by measuring the temperature at predefined locations of the structure.

(5) FRP beams and shell structures should satisfy the quality requirements with respect to visual defects, equivalent to EN 13706-2, Table A.1.

9.4.1 Geometric tolerances, imperfections and deviations in fibre alignment

(1) In the final control of the FRP structure, the following should be verified as a minimum:
- geometrical dimensions and tolerances (deviations in dimensions, out-of-straightness and curvature);
- material quality (imperfections);
- coating (damage due to handling).

In case of deviations, the necessary measures should be defined with the designer or engineer.

(2) Effects of crimp and creep should be taken into account

(3) Profiles (whether or not pultruded) should meet the quality requirements with respect to geometrical imperfections equivalent to EN 13706-2, Table B.1.

(4) The orientation and straightness of the fibres of continuous, non-random, glass fibre or HS-carbon fibre reinforcement, should not deviate too much from the orientation of the material on which basis the strength properties are determined. The allowable deviation must be estimated beforehand.

(5) In case of the use of IM and HM carbon fibres, the handling and the placing of the fibres should be done very securely to prevent the breaking of the fibre and to obtain a good fibre alignment. For IM and HM carbon fibres, the influence of the misalignment should be taken into account in the determination of the strength.

9.4.2 Connections

(1) To obtain an appropriate and aligned structure composed of profiles and bolted connections, the use of oversized bolt holes can be necessary. The geometric limitations given in Table 8.1 should be satisfied.

(2) A narrower hole tolerance is favourable for the strength of the connection. The use of injection bolts or the realization of a bolt connection with bonded metals inserts could contribute to the realization of a slip free connection with a higher strength.

(3) All edges should be sealed with a coating (e.g. topcoat, kit, resin or lacquer), to prevent penetration of moisture. This coating should be compatible with the resin of the laminate.

(4) When drilling holes, FRP compatible tools should be used. During processing, FRP parts should be well supported to prevent cleaving, tearing and delamination.

(5) Bolts should not be tightened too hard. No damage on the laminate is allowed. The use of torque controlled tools should be recommended. The torque should be duly specified in the design.

(6) Overlap lengths and details of the adhesive connection including thickness should be specified in advance by the designer.

(7) Adhesive connections should be executed by sufficiently instructed personnel under supervision of a sufficiently knowledgeable and experienced supervisor.

(8) Adhesive connections should be achieved in climate controlled conditions in accordance with application instructions from the adhesive supplier. The T_g of the adhesive should be verified based on material tests.

(9) During surface preparation, mould release agents should be removed.

(10) The surface of the adherents should be clean and free of moisture, fat and dust. In case of bonding,crucial parameters are surface preparation, humidity, temperature, thickness of the adhesive, as well as pressure and temperature during the cure process.

9.5 Handling and storage

(1) During handling, concentrated loads should be avoided. Lifting of FRP parts is only allowed using prescribed methods and tool positions that are approved by the designer. In case of deviations, consequences should be assessed by the designer or an FRP expert.

(2) During transportation and handling, damage caused by handling FRP parts should be prevented.During storage and transportation, parts should be kept separated. When lifting FRP parts, the use of protective materials is preferred.

(3) Storage conditions – in order to preserve the properties and maintain safety in the storage of FRP materials, they should be stored in accordance with the manufacturer's recommendations.

9.6 Installation

(1) Before starting the work, a detailed execution plan should be established by all parties, in consultation with the designer or a sufficiently experienced FRP engineer.

(2) Installation of an FRP structure should be executed by sufficiently instructed personnel under supervision of a supervisor with the required level of experience and knowledge of FRP, in line with EN1990.

(3) If before or during the installation unanticipated loads and attachment points are introduced, this should be assessed and approved by the designer.

(4) After assembly and installation of a structure of components it should be verified whether the geometrical tolerances are met. In case of deviations, the necessary measures should be determined in communication with the designer.

9.7 Use

(1) If during the using period unanticipated loads and attachment points occur, this should be approved by the designer.

(2) The FRP structure should be inspected and maintained according to a predefined plan.

9.8 Maintenance, inspection and repair

(1) The FRP structure should preferably be provided with a maintenance and inspection plan. This plan should make it possible to:
- keep the structure in a functional state during its lifetime;
- achieve good and responsible inspection.

An appropriate plan contains:
- Locations where the structure should be inspected (i.e. position and damage criteria) and assessment criteria, determined by the designer. This can eventually be extended with a detailed inspection plan, including descriptions of the inspection intervals and inspection procedures and inspection report format.
- Restrictions during servicing, prepared by the engineer (for instance in cases when cleaning with high pressure is not allowed).
- Restrictions in use, prepared by the supplier.
- Complete overview of the realized structure with the used materials. This information should be provided, such that in case of damage of the structure, the repair can be done by a third party. This document is prepared by the supplier.
- If needed, repair instructions can be added with respect to important components.
- Instructions with respect to replacement of parts where relevant.

(2) To evaluate the quality of a structure over its lifetime, it is recommended to execute a so called 0-measurement of the behaviour of the structure directly after installation.

9.8.1 Maintenance

(1) The maintenance of the FRP structure parts could consist of:
- inspection (e.g. appearance and behaviour of the structure);
- cleaning of the surfaces;
- maintenance of connections (checking and tightening of bolts, maintenance of protective measures of adhesive connections);
- repair of superficial damage of coating, kit layers and laminates;
- repair of damage (for instance due to incidents, vandalism or fire);
- repair and replacement of secondary parts or accessories with a shorter lifetime than the structure's lifetime (for instance wear layers).

(2) It is advised to clean (coated) surfaces on a regular basis. This could be done by cleaning with water or special cleaners. For monolithic (non-sandwich) FRP structures, generally a high pressure washer could be used.

(3) In case of surface damage on coatings and kit layers, it is advised to repair these.

(4) Structural adhesive layers should be sealed from dirt and moisture.

(5) Bolted connections which are applied with a torque wrench should be tightened after completion at least once. After this, they should regularly be inspected for tightness.

9.8.2 Inspection

(1) Routine inspection is based on the following evaluations:
- examination of defects such as discolorations and eventual local damage;
- connections;
- possible differences of environment occurring during the use of the structure.

(2) More detailed inspection results from an evaluation of:
- permanent deformations;
- integrity of the structure;
- behaviour of the structure, for instance related to a 0-measurement at completion.

(3) Inspection that can be executed visually, whether or not supported by non-destructive techniques:
- surface condition, discolorations, crazing, tears, blistering;
- permanent deformations;
- visible damage caused by vandalism or incidents;
- tightness of connections;
- cracking, delamination, damage to adhesive layers;
- damage to insulation against galvanic corrosion.

(4) Visual inspections can be supported by non-destructive techniques like:
- (coin) tapping;
- acoustic measurements;
- infrared thermography;
- laser shearography;
- ultrasonic tests.
- strain measurements.

9.8.3 Repairs

(1) In case of damage and defects of the FRP structure, the necessary repairs should be determined in consultation with a qualified designer, FRP engineer and/or FRP supplier.

(2) In case of adhesive repairs, the same guidelines and conditions as prescribed for adhesive connections should apply.

(3) Possible repair methods:
- creation of a bypass through the application of plates (bonded or mechanically connected);
- filling with resin (in case of small superficial damages);
- removing of the damaged FRP material and laminating of replacement FRP material;
- laminating with FRP (strengthening).

(4) During the design and execution of the repair, the remaining lifetime of the structure should be taken into account. Any repair operation should be provided with appropriate inspection instructions.

(5) The repair should meet at least a level of confidence and reliability in conformity with adequate renovation standards.

10 ANNEX A (CONVERSION FACTOR $n_{cv,20}$)

(1) The conversion factors for creep given in this Annex are for glass-fibre reinforced laminates and have been derived under room-temperature conditions. As a conservative assumption these values may be used for carbon-fibre reinforced laminates.

(2) Table 10.1 provides examples of conversion factors $\eta_{cv}(t_v)$ for various load durations t_v, determined with equation (2.7) based on the conversion factor for a reference period of 20 years $\eta_{cv,20}$, which can be estimated using Tables 10.2 or 10.3 for strength and strain or stiffness, respectively, or to be derived via testing.

Table 10.1 – Examples of conversion factors $\eta_{cv}(t_v)$ to account for creep effects.

Level of proof	Loads to be considered	Conversion factors $\eta_{cv}(t_v)$ based on $\eta_{cv,20}$ estimated using Table 10.2 or 10.3 and the duration of exposure t_v					
$\eta_{cv,20}$ *(20 years)* *acc. to Table 10.2 or 10.3*	---	**0.67**	**0.50**	**0.40**	**0.33**	**0.29**	**0.25**
Permanent 50 years	permanent	0.65	0.48	0.38	0.31	0.27	0.23
Long-term 10 years	permanent, long	0.69	0.51	0.42	0.35	0.30	0.27
Medium-term 6 months	permanent, long, medium	0.74	0.59	0.49	0.43	0.38	0.34
Short-term 1 week	permanent, long, medium, short	0.80	0.67	0.59	0.53	0.49	0.45
Instantaneous 1 minute	permanent, long, medium, short, very short	1.00	1.00	1.00	1.00	1.00	1.00

(3) Table 10.2 provides conversion factors $\eta^f_{cv,20}$ for strength for a load duration of 20 years. The values given are to be used at ULS design stage (except for the verification of stability and fatigue).

Table 10.2 – Conversion facto $\eta^{f}_{cv,20}$ factor for strength (load duration of 20 years)
(Terms RLM, ML and FWL according to Table 10.4).

Type of material / Manufacturing process / Direction	$\eta^{f}_{cv,20}$ for strength					
Random laid laminate RLM	0.63					
Mixed laminate ML	$1/(2.0 - \delta)$					
Filament wound laminate FWL (properties parallel to the direction of winding)	$1/(1.8 - \delta)$					
Filament wound laminate FWL (properties normal to the direction of winding)	FWL 1	FWL 2	FWL 3	FWL 4	FWL 5	FWL 6
	0.56	0.47	0.36	0.59	0.5	0.42
with $\varepsilon_z > 0{,}2\%$	0.42	0.34	0.26	0.48	0.38	0.36
Pultruded profiles (properties in the direction parallel to the direction of pultrusion)	$1/(1.8 - \delta)$					
Pultruded profiles (properties normal to the direction of pultrusion)	0.53					
Pultruded profiles (properties in the direction parallel to the direction of Pultrusion with $\varepsilon_z > 0.2\%$)	0.50					
Pultruded profiles properties normal to the direction of pultrusion with $\varepsilon_z > 0.2\%$	0.33					

- Specific values must be considered for shear. In the absence of specific data for shear, the values for the direction normal to the direction of pultrusion may be considered;
- δ: accounts for the mass proportion of fibres in the direction of loading;
- ε_z: is the characteristic failure strain in tension normal to the winding direction/direction of pultrusion.

(4) Table 10.3 provides the conversion factor $\eta^{E}_{cv,20}$ for creep deformation for a load duration of 20 years. The values given are to be used to determine deformations under (quasi -) permanent loading conditions at SLS design verification and in stability verifications in the ULS design verification.

Table 10.3 - Conversion factors $\eta^{E}_{cv,20}$ for strain and stiffness (load duration 20 years) (Terms RLM, ML and FWL according to Table 10.4).

Type of material	$\eta^{E}_{cv,20}$ for strain and stiffness					
Random laid laminate RLM	Cured			Not Cured		
	1/(2.4-2δ)			1/(2.6-2δ)		
Mixed laminate ML	Cured			Not Cured		
	1/(2.3-2δ)			1/(2.5-2δ)		
Filament wound laminate FWL (properties parallel to the direction of winding)	Normal force			Bending		
	1/(1.75-δ)			1/(1.85-δ)		
Filament wound laminate FWL (properties normal to the direction of winding)	FWL 1	FWL 2	FWL 3	FWL 4	FWL 5	FWL 6
	1/(2.2-δ)	1/(2.45-δ)	1/(3.0-δ)	1/(2.15-δ)	1/(2.3-δ)	1/(3.2-2δ)
with $\varepsilon_z > 0.2\%$	1/(2.7-δ)	1/(3.1-δ)	1/(4.1-δ)	1/(2.6-δ)	1/(2.8-δ)	1/(4.0-2δ)
Pultruded profiles (properties in the direction parallel to the direction of pultrusion)	Normal force			Bending		
	1/(1.75-δ)			1/(1.85-δ)		
Pultruded profiles (properties normal to the direction of pultrusion)	Normal force			Bending		
	0.57			0,.54		
Pultruded profiles (properties normal to the direction of pultrusion with $\varepsilon_z > 0.2\%$)	Normal force			Bending		
	0.5			0.4		

- Specific values must be considered for shear. In the absence of specific data for shear, the values for the direction normal to the direction of pultrusion may be considered;
- δ: accounts for the mass proportion of fibres in the direction of loading;
- ε_z: is the characteristic failure strain in tension normal to the winding direction/direction of pultrusion.

(5) In the absence of specific values for shear, as a simplifying assumption, the conversion factor for creep applicable to the shear modulus of pultruded profiles can be taken as the value for bending creep in the normal direction (to winding / pultrusion). Shear creep factors for pultruded profiles are also given in the Italian *Guide for the Design and Construction of Structures made of FRP Pultruded Elements*.

Table 10.4 - Definition of fibre lay-up for GFRP laminates RLM, ML and FWL.

Type	360-630 g/m^2					
fibre mass proportion						
Mixed laminate ML						
Type	ML1			ML2		
Lay-up	fibre mass proportion g/m^2					
RF xxxxxxx	450			450		
T +=+=+= *n	580			690		
RF xxxxxxx *n	450			450		
Filament wound laminate FWL						
type	FWL1	FWL2	FWL3	FWL4	FWL5	FWL6
Lay-up	fibre mass proportion g/m^2					
RF xxxxxxx	450	450	450	450	450	450
R //////// *n	120	240	480	120	240	480
RF xxxxxxx *n	300	300	300	450	450	450
R ////////	120	240	480	120	240	480
RF xxxxxxx	450	450	450	450	450	450
comments						
Random Fibres (RF)	xxxxxxx					
Roving (R)	////////					
Textile (T)	+=+=+=					

** For detailed specification of RLM, ML and FWL 1-6 see DIN 18820 .

10.1 References

BÜV — Tragende Kunststoff Bauteile im Bauwesen [TKB] – Richtlinie für Entwurf, Bemessung und Konstruktion (2014).

CNR-DT — Advisory Committee on Technical Recommendations for Construction (CNR). Guide for the Design and Construction of Structures made of FRP Pultruded Elements. CNR-DT 205/2007. National Research Council of Italy, Rome, 2008.

11 ANNEX B (INDICATIVE VALUES OF FIBRES, RESINS, PLY AND LAMINATE PROPERTIES)

11.1 General

(1) While characteristic values should be used in design calculations, indicative values can be used as reference or for an initial assessment of the feasibility of a specific design.

(2) This Annex provides indicative values of fibres, resins, ply and laminate properties which are useful for preliminary design.

(3) In the following the symbol V_f denotes the fibre volume fraction (or content), the subscripts "1" and "2" refer to the material principal directions of the ply (Figure 1.2), the subscripts "f" and "R" refer to fibre and resin, respectively.

11.2 Fibres

11.2.1 General

(1) Generally speaking, suppliers use different surface treatments on the fibres, so called 'sizings'. The sizing used affects the fibre-resin adhesion and is adapted to the specific resin type (for instance polyester resin or epoxy resin). Not every fibre available on the market is compatible with every type of resin. Glass fibres are supplied with a sizing suitable for polyester, vinyl ester or epoxy resins. In general, carbon fibre is produced with a sizing that is suitable for epoxy or vinyl ester resins. The use of fibres with a different resin than that for which the sizing is intended may result in significantly lower values of the main mechanical properties of a resulting ply or laminate. Table 11.1 shows indicative values of fibre properties. A wide range of fibre types exist for IM and HM carbon fibre. The values listed are within the range of material properties reported in literature.

(2) In contrast to glass fibre, carbon fibre is orthotropic. The compression strength of carbon fibre is significantly lower than its tensile strength. Carbon fibres are more sensitive to loads from the axis of the fibre that can for instance occur due to deviations in the fibre orientation, in connection to the production of FRP parts.

(3) Aramid fibres are extremely well suited for resisting tensile forces and for energy absorption, but less well suited to absorbing compression loads.

Table 11.1 – Typical values of fibre properties (indicative values).

		Glass		Carbon		
		E-glass	R-glass	HS	IM	HM
		Indicative values	Indicative values	Indicative values	Indicative values	Indicative values
Density (kg/m^3)		2570	2520	1790	1750	1880
Tension in fibre direction	Poisson's ratio ν_f	0.238	0.2	0.3	0.32	0.35
	Young's modulus E_{f1} (MPa)	73100	86000	238000	350000	410000
	Strain limit ε_{f1} (%)	3.8	4	1.5	1.3	0.6
	Strength σ_{f1} (MPa)	2750	3450	3600	4500	4700
Tension perpendicular to fibre direction	Poisson's ratio ν_f	0.238	0.26	0.02	0.01	0.01
	Young's modulus E_{f2} (MPa)	73100	86000	15000	10000	13800
	Strain limit ε_{f2} (%)	2.4	2.4	0.9	0.7	0.45
	Strength σ_{f2} (MPa)	1750	2000	135	70	60
Compression in fibre direction	Strain limit ε_{f1} (%)	2.4	2.4	0.9	0.6	0.45
	Strength σ_{f1} (MPa)	1750	2000	2140	2100	1850
Shear	Modulus G_f (MPa)	30000	34600	50000	35000	27000
	Strain limit γ_{f12} (%)	5.6	5.6	2.4	3	3.8
	Strength τ_{f12} (MPa)	1700	1950	1200	1100	1000
Thermal expansion	α (10^{-6} K^{-1})	5.0	3.0	-0.4	-0.6	-0.5

11.3 Resin

11.3.1 General

(1) The resin used should be appropriate to the surface treatment ('sizing') of the fibre.

(2) The choice of resin should be appropriate to the required properties, such as glass transition temperature, chemical resistance, fire reaction properties (e.g., flammability, heat release, smoke production) and electrical conductivity.

(3) Additives and fillers may be added to the resin to give it specific properties. The effect of additives and fillers on the mechanical properties should be taken into account. Examples include modifications in fire reaction properties, electrical conductivity and UV resistance. If the concentration of fillers is too high, this can have a negative effect on the resin properties, such as strength, stiffness, viscosity, glass transition temperature and durability. It is recommended to discuss the quantity and effect of additives and fillers with the resin supplier.

11.3.2 Thermoset resins

Indicative values of thermoset resins properties are given in Table 11.2.

Table 11.2 – Indicative values of thermoset resins properties.

	Polyester	Vinyl ester	Epoxy
Density	1.2	1.1	1.25
Poisson's ratio ($\nu_{12,resin}$)	0.38	0.26	0.39
T_g (°C)	approx. 60 [(1)]	approx. 100 [(1)]	80 - 150 [(1)]
Tensile or compression strength (MPa)	55 [(2)]	75 [(2)]	75 [(2)]
Young's modulus in tension (MPa)	3550	3350	3100
Strain limit in tension or compression (%)	1.8	2.2	2.5
In-plane shear modulus (MPa)	1350	1400	1500
Shear strength (MPa)	approx. 50	approx. 65	approx. 80
Shear strain limit (%)	3.8	3.7	5
Expansion coefficient (10^{-6} K^{-1}) [(3)]	50 - 120	50 - 75	45 - 65

(1) The actual value of T_g depends on the polymerisation process applied and in particular on the temperature applied during post-curing.

(2) There is a large variation in strength properties within every resin type. It should be verified during the production phase whether the resin used has the above properties as a minimum. The influence of the resin on fibre-dominated properties is limited. Resin properties mainly affect resin-dominated properties such as ILSS, compression strength, shear strength, curing shrinkage and delamination.

(3) The thermal properties of resin may vary widely depending on a precise composition. If thermal expansion is key to the design it is recommended that the analysis be based on test values.

11.4 Fillers and additives

(1) The influence of fillers and additives on the material properties should be characterised.

(2) Additives are added for various reasons, such as in order to influence the processing properties, to improve specific material properties (such as fire reaction properties), or to reduce costs.

(3) It is recommended that the minimum required or maximum recommended quantity of fillers or additive is established in consultation with the supplier.

11.5 Core materials

(1) For core materials, design data based on tests as detailed in Section 3.1.3 should be used in the design.

(2) Natural core materials, such as balsa wood, have a higher scatter in the material properties owing to variations in material density, when compared to foam core materials or honeycomb cores.

(3) Frequently used core materials include rigid foam (PUR, PS, PVC, PET, and PMI), balsa wood and various types of honeycomb cores (aluminium, aramid paper, PP, PET), syntactic foam and bulking materials.

(4) Indicative values for the typical properties of a number of core materials are given in Table 11.3.

Table 11.3 - Indicative values for the typical values of foam core material properties.

	Density [kg/m^3]	Compression strength [N/mm^2]	Shear strength [N/mm^2]	Elasticity modulus [N/mm^2]	In-plane shear modulus [N/mm^2]
	Indicative values	Indicative values	Indicative values	Indicative values	Indicative values
PUR	50	0.3 - 0.5	approx. 0.2	6 - 10	4 - 5
	100	0.6 - 1.0	0.3 - 0.5	approx. 30	approx. 10
PVC	40	0.5 - 0.8	0.3 - 0.4	20 - 30	approx. 10
Cross linked	80	1.2 - 2.0	0.7 - 1.0	60 - 90	20 - 30
Linear	80	approx. 0.9	0.5 – 1.0	approx. 50	20
PMI	30	approx. 0.5	approx. 0.3	approx. 30	approx. 15
	70	approx. 1.5	approx. 1.0	approx. 90	approx. 30

(5) Climatic influences and long-term effects should be taken into account in the design. The conversion factors for fibre-reinforced polymers do not apply to core materials. Climatic influences and long-term effects should be defined on the basis of the core material behaviour.

(6) The document BÜV-Empfelung, Tragende Kunststoffbauteile im Bauwesen [TKB], 2010, shows indicative values for the influence of temperature and aging on PUR foam. The anticipated aging effects of core materials are limited if there is a proper seal, and provided that the laminate quality of the sandwich facings is good. The influence of temperature on foam cores depends to a large extent on the type of polymer and may be significant. Generally speaking, the influence of temperature at service temperatures of < 40 °C is limited (in the order of 10 %).

(7) When lightweight foam core materials are used, their low strength and robustness means there is a significant risk at the bonding interface between the sandwich facings and the core. In situations where PUR foam is to play a long-term structural role, it is recommended that a material with a density of at least 50 kg/m^3 is used, due to the brittleness of the material and its low strength.

11.6 PLY Properties

11.6.1 General

(1) Plies should be classified on the basis of the orientation of the fibre reinforcement. A distinction is made between:

- unidirectional plies (UD roving, UD tapes, UD non-crimp fabric);
- bi-directional plies (woven roving WR, woven fabric, woven cloth, stitched fabric);
- mat plies (discontinuous or chopped strand mat (CSM), continuous fibre mat and spray roving).

(2) Characteristic ply properties with a 5 % risk of being exceeded or underestimated should be used in the calculations. This in accordance with EN 1990, Appendix D.

(3) Ply properties should be defined in conformity with the procedures described in Table 3.1. In the case of laminates that fulfil the following conditions:

- a fibre volume fraction of at least 15 %
- a thermoset matrix of unsaturated polyester, vinyl ester or epoxy resins.

(4) Halpin-Tsai formulas (UD ply and bi-directional plies) or Manera's formulas (mat plies) are used in the procedures described.

(5) Fibre-dominated properties of FRP are generally easy to predict. Resin-dominated strength properties are more susceptible to imperfections and processing conditions. The purpose of the minimum specified amount of fibre reinforcement in the material principal directions is to make the in-plane material behaviour of the laminate sufficiently fibre-dominated. Resin-dominated mechanical strength properties include compression strength, compression and tensile strength transverse to the fibre, in plane shear strength and ILSS..

11.6.2 Indicative values for ply stiffness properties

11.6.2.1 Ud plies

(1) The (mean) stiffness properties of UD plies can be calculated from:

$$E_1 = \left[E_R + (E_{f1} - E_R) \cdot V_f\right] \cdot \varphi_{UD} \tag{11.1}$$

$$E_2 = \left[\frac{(1+\xi_2 \eta_2 V_f)}{(1-\eta_2 V_f)} \cdot E_R\right] \cdot \varphi_{UD} \tag{11.2}$$

$$G_{12} = \left[\frac{(1+\xi_G \eta_G V_f)}{(1-\eta_G V_f)} \cdot G_R\right] \cdot \varphi_{UD} \tag{11.3}$$

$$\nu_{12} = \nu_R - (\nu_R - \nu_f) \cdot V_f \tag{11.4}$$

where:

with E_2: $\eta_2 = \dfrac{\left(\dfrac{E_{f2}}{E_R} - 1\right)}{\left(\dfrac{E_{f2}}{E_R} + \xi_2\right)}$, $\xi_2 = 2$; with G_{12}: $\eta_G = \dfrac{\left(\dfrac{G_f}{G_R} - 1\right)}{\left(\dfrac{G_f}{G_R} + \xi_G\right)}$, $\xi_G = 1$.

In which:

E_1, E_2	is the in plane Young's modulus of the ply in the 1 or 2-direction;
G_{12}	is the in ply shear modulus of the ply;
ν_{12}	is the Poisson's ratio of the fibre reinforced ply;
ν_R	is the Poisson's ratio of the resin;
ν_F	is the Poisson's ratio of the fibre;
ϕ_{UD}	is an empirical reduction factor;
E_R	is the Young's modulus of the resin;
E_{F1}, E_{F2}	is the Young's modulus of the fibre in the 1 or 2-direction;
G_R	is the shear modulus of the resin;
V_f	is the fibre volume ratio of the ply.

The formulas are derived from the semi-empirical Halpin and Tsai equations, where an additional empirical reduction factor φ_{UD} = 0.97 has been applied.

(2) For a UD ply on a base of E-glass with unsaturated polyester, the typical values given in Table 11.4 can be used.

Table 11.4 - Indicative UD ply E-glass stiffness values

V_f	E_1 [GPa]	E_2 [GPa]	G_{12} [GPa]	ν_{12}
40 %	30.4	8.9	2.7	0.30
45 %	33.8	10.1	3.0	0.29
50 %	37.2	11.4	3.4	0.29
55 %	40.5	12.9	3.8	0.28
60 %	43.9	14.6	4.3	0.27
65 %	47.3	16.8	5.0	0.27
70 %	50.7	19.4	5.8	0.26

11.6.2.2 Bi-directional plies

(1) The (mean) stiffness properties of balanced bi-directional plies (0/90 orientation) can be calculated from:

$$E_1 = E_2 = \frac{1}{2} \cdot \left[E_R + \left(E_{F1} - E_R\right) \cdot V_f + E_R \cdot \frac{\left(1+\xi_1 \eta_1 V_f\right)}{\left(1-\eta_1 V_f\right)} \right] \cdot \varphi_{0/90} \qquad (11.5)$$

$$G_{12} = \left[\frac{\left(1+\xi_G \eta_G V_f\right)}{\left(1-\eta_G V_f\right)} \cdot G_R \right] \cdot \varphi_{0/90} \qquad (11.6)$$

$$\nu_{12} = \left[\nu_R - \left(\nu_R - \nu_F\right) \cdot V_f\right] \cdot \frac{1}{2} \cdot \left[1 + E_R \cdot \frac{\frac{\left(1+\xi_1 \eta_1 V_f\right)}{\left(1-\eta_1 V_f\right)}}{E_R + \left(E_{F1} - E_R\right) \cdot V_f} \right] \cdot \varphi_{0/90} \qquad (11.7)$$

where:

with E_1, E_2 and V_{12}: $\eta_1 = \dfrac{\left(\frac{E_{f1}}{E_R} - 1\right)}{\left(\frac{E_{f1}}{E_R} + \xi_1\right)}$, $\xi_1 = 2$; with G_{12}: $\eta_G = \dfrac{\left(\frac{G_f}{G_R} - 1\right)}{\left(\frac{G_f}{G_R} + \xi_G\right)}$, $\xi_G = 1$.

The formulas are derived from the semi-empirical Halpin and Tsai equations, where an additional empirical reduction factor $\varphi_{0/90}$ = 0.93 has been applied due to the influence of imperfections.

(2) For a balanced bi-directional ply based on E-glass with polyester resin, the typical values given in Table 11.5 can be used.

Table 11.5 – Indicative balanced bi-directional ply E-glass stiffness values.

V_f	E_1 [GPa]	E_2 [GPa]	G_{12} [GPa]	ν_{12}
25 %	12.8	12.8	1.9	0.21
30 %	14.7	14.7	2.1	0.20
35 %	16.8	16.8	2.4	0.20
40 %	18.9	18.9	2.6	0.19
45 %	21.0	21.0	2.9	0.19
50 %	23.3	23.3	3.3	0.19
55 %	25.6	25.6	3.7	0.18

11.6.2.3 Mat ply

(1) Using UD ply properties in conformity with 11.6.2.1, the (mean) stiffness properties of mat plies can be calculated from:

$$E_1 = E_2 = \left[\frac{(U_1 + U_4)\cdot(U_1 - U_4)}{U_1}\right]\cdot\varphi_{mat} \qquad (11.8)$$

$$G_{12} = \left[\frac{(U_1 - U_4)}{2}\right]\cdot\varphi_{mat} \qquad (11.9)$$

$$\nu_{12} = \frac{U_4}{U_1} \qquad (11.10)$$

with

$$U_1 = \frac{3C_{11} + 3C_{22} + 2C_{12} + 4C_{66}}{8}$$

$$U_4 = \frac{C_{11} + C_{22} + 6C_{12} - 4C_{66}}{8}$$

$$C_{11} = \frac{E_{1UD}}{1 - \nu_{12UD}^2 \cdot \dfrac{E_{2UD}}{E_{1UD}}}$$

$$C_{22} = \frac{E_{2UD}}{1 - \nu_{12UD}^2 \cdot \dfrac{E_{2UD}}{E_{1UD}}}$$

$$C_{12} = \frac{\nu_{12UD} \cdot E_{1UD}}{1 - \nu_{12UD}^2 \cdot \frac{E_{2UD}}{E_{1UD}}}$$

$$C_{66} = G_{21UD}$$

The formulas are derived from Manera's equations and φ mat an empirically defined reduction factor of value 0.91.
(2) For a mat ply on a base of E-glass with polyester resin, the typical values given in Table 11.6 can be used.

Table 11.6 - Indicative mat ply E-glass stiffness values.

V_f	E_1 [GPa]	E_1 [GPa]	G_{12} [GPa]	ν_{12}
15 %	7.1	7.1	2.6	0.34
17.5 %	7.7	7.7	2.9	0.34
20 %	8.4	8.4	3.2	0.34
25 %	9.8	9.8	3.7	0.34
30 %	11.3	11.3	4.2	0.34

11.6.3 Indicative values for ply strength properties

(1) In case of thermoset fibre reinforced polymers with a fibre volume fraction of at least 15%, the following can be applied for ply strength:

- for UD plies the values stated in Table 11.7;
- for bi-directional plies the values stated in Table 11.8;
- for mat plies the values stated in Table 11.9.

Table 11.7 - Indicative UD ply strain limits.

Strains		FRP type				
		E-glass Polyester	R-glass epoxy	HS carbon Epoxy	IM carbon epoxy	HM carbon Epoxy
		Indicative values [%]	Indicative values [%]	Indicative values [%]	Indicative values [%]	Indicative values [%]
Tension	$\varepsilon_{1t,k}$	2.2	3.1	1.1	1.15	0.7
	$\varepsilon_{2t,k}$	0.34	0.35	0.76	0.65	0.4
Compression	$\varepsilon_{1c,k}$	1.44	1.8	0.76	0.65	0.45
	$\varepsilon_{2c,k}$	1.24	0.88	2.0	2.3	2.1
Shear	$\gamma_{12,k}$	1.44	1.5	1.6	1.7	1.8
	$\gamma_{13,k}$	1.44	1.5	1.6	1.7	1.8
	$\gamma_{23,k}$	2.0	1.8	1.9	1.85	1.8

Table 11.8 - Indicative strain limits for balanced bi-directional plies.

Strains		FRP type				
		E-glass Polyester	R-glass epoxy	HS carbon Epoxy	IM carbon epoxy	HM carbon Epoxy
		Indicative values [%]	Indicative values [%]	Indicative values [%]	Indicative values [%]	Indicative values [%]
Tension	$\varepsilon_{1t,k}$	1.44	2.3	1.0	0.8	0.45
	$\varepsilon_{2t,k}$	1.44	2.3	1.0	0.8	0.45
Compression	$\varepsilon_{1c,k}$	1.44	2.5	0.76	0.8	0.5
	$\varepsilon_{2c,k}$	1.44	2.5	0.76	0.8	0.5
Shear	$\gamma_{12,k}$	1.2	1.5	1.55	1.6	1.85
	$\gamma_{13,k}$	1.44	1.8	1.55	1.6	1.85
	$\gamma_{23,k}$	1.44	1.8	1.55	1.6	1.85

Table 11.9 - Indicative strain limits for mat plies.

Strains		FRP type
		E-glass polyester
		Indicative values [%]
Tension	$\varepsilon_{1t,k}$	1.24
	$\varepsilon_{2t,k}$	1.24
Compression	$\varepsilon_{1c,k}$	1.24
	$\varepsilon_{2c,k}$	1.24
Shear	$\gamma_{12,k}$	1.6
	$\gamma_{13,k}$	1.72
	$\gamma_{23,k}$	1.72

(2) Unreinforced resin should have a failure strain of at least 1.8%, as determined by EN-ISO 527.

(3) The above assumes that the fibre properties are in conformity with Table 11.1 and that the resin properties are in conformity with Table 11.2.

(4) In the case of FRP, strength is expressed as a strain limit (failure strain).

11.6.4 Linear coefficient of expansion for plies

(1) The linear thermal expansion coefficient of UD plies, bi-directional plies or mat plies is calculated from:

$$\alpha_1 = \frac{V_f \alpha_{f1} E_{f1} + V_R \alpha_R E_R}{E_1} \tag{11.11}$$

$$\alpha_2 = \alpha_3 = \alpha_{f2}\sqrt{V_f} + \left(1-\sqrt{V_f}\right)\cdot\left(1+V_f \nu_R E_{f1}/E_1\right)\cdot \alpha_R \tag{11.12}$$

The equations specified are derived from Chamis formulas. The linear coefficients of thermal expansion of an FRP material are dependent on the fibre direction, the fibre volume percentage and the linear coefficient of thermal expansion of the fibre and matrix.

(2) For a ply made of E-glass with polyester, typical values can be used as given in:

- for a UD ply: Table 11.10;
- for a bi-directional ply: Table 11.11;
- for a mat ply: Table 11.12.

Table 11.10 - Indicative values for UD plies with E-glass, in the plane.

	UD plies			
V_f	$\alpha_R = 50 \cdot 10^{-6}\ K^{-1}$		$\alpha_R = 120 \cdot 10^{-6}\ K^{-1}$	
	$\alpha_1\ [\cdot 10^{-6}\ K^{-1}]$	$\alpha_2\ [\cdot 10^{-6}\ K^{-1}]$	$\alpha_1\ [\cdot 10^{-6}\ K^{-1}]$	$\alpha_2\ [\cdot 10^{-6}\ K^{-1}]$
40 %	8.2	27.7	13.0	62.1
45 %	7.7	25.4	1.6	56.3
50 %	7.2	23.2	10.5	50.8
55 %	6.9	21.1	9.6	45.5
60 %	6.6	19.1	8.8	40.4
65 %	6.3	17.1	8.1	35.5
70 %	6.1	15.2	7.5	30.7

Table 11.11 - Indicative values for bi-directional plies with E-glass and polyester, in the plane.

	Bi-directional plies			
V_f	$\alpha_R = 50 \cdot 10^{-6}\ K^{-1}$		$\alpha_R = 120 \cdot 10^{-6}\ K^{-1}$	
	$\alpha_1\ [\cdot 10^{-6}\ K^{-1}]$	$\alpha_2\ [\cdot 10^{-6}\ K^{-1}]$	$\alpha_1\ [\cdot 10^{-6}\ K^{-1}]$	$\alpha_2\ [\cdot 10^{-6}\ K^{-1}]$
25 %	17.9	17.9	37.2	37.2
30 %	16.1	16.1	32.7	32.7
35 %	14.7	14.7	29.1	29.1
40 %	13.6	13.6	26.2	26.2
45 %	12.6	12.6	23.6	23.6
50 %	11.7	11.7	21.6	21.6
55 %	11.0	11.0	19.6	19.6

Table 11.12 - Indicative values for mat plies with E-glass and polyester, in the plane.

	Mat plies			
V_f	$\alpha_R = 50 \cdot 10^{-6}\ K^{-1}$		$\alpha_R = 120 \cdot 10^{-6}\ K^{-1}$	
	$\alpha_1\ [\cdot 10^{-6}\ K^{-1}]$	$\alpha_2\ [\cdot 10^{-6}\ K^{-1}]$	$\alpha_1\ [\cdot 10^{-6}\ K^{-1}]$	$\alpha_2\ [\cdot 10^{-6}\ K^{-1}]$
10 %	28.5	28.5	64.1	64.1
15 %	23.7	23.7	51.9	51.9
20 %	20.5	20.5	43.7	43.7
25 %	18.0	18.0	37.5	37.5
30 %	16.3	16.3	33.1	33.1

11.6.5 Coefficient of thermal conductivity for plies

(1) The linear coefficient of thermal conductivity of UD plies, bi-directional plies or mat plies can be calculated from: $\lambda_1 = V_f \lambda_{f1} + V_R \lambda_R$

$$\lambda_1 = V_f \lambda_{f1} + V_R \lambda_R \qquad (11.13)$$

$$\lambda_2 = \lambda_3 = \left(1 - \sqrt{V_f}\right) \cdot \lambda_R + \frac{\lambda_R \sqrt{V_f}}{1 - \sqrt{V_f} \cdot \left(1 - \lambda_R / \lambda_{f2}\right)} \qquad (11.14)$$

The formulas specified are derived from Chamis. The coefficients of thermal conductivity (λ_1 and in the plane and λ_1 perpendicular to the plane) of a composite FRP are dependent on the type of resin and fibre, fibre direction and the fibre volume percentage.

(2) For a ply on a base of E-glass with polyester, typical values can be used as given in:
- for UD plies in Table 11.13;
- for bi-directional plies Table 11.14;
- for mat plies Table 11.15.

Table 11.13 - Indicative values for UD plies of E-glass and polyester.

V_f	λ_1 [W/m·K]	λ_2 [W/m·K]
40 %	0.55	0.31
45 %	0.59	0.33
50 %	0.64	0.36
55 %	0.69	0.40
60 %	0.73	0.44
65 %	0.78	0.48
70 %	0.82	0.53

Table 11.14 - Indicative values for bi-directional plies of E-glass and polyester.

V_f	λ_1 [W/m·K]	λ_2 [W/m·K]
25 %	0.33	0.33
30 %	0.36	0.36
35 %	0.39	0.39
40 %	0.43	0.43
45 %	0.46	0.46
50 %	0.50	0.50
55 %	0.54	0.54

Table 11.15 - Indicative values for mat plies of E-glass and polyester.

V_f	λ_1 [W/m·K]	λ_2 [W/m·K]
10 %	0.24	0.24
15 %	0.27	0.27
20 %	0.30	0.30
25 %	0.33	0.33
30 %	0.36	0.36

11.6.6 Swelling of plies

(1) If swelling can occur, this should be calculated using the same calculation method as for the thermal expansion. The following applies to the coefficients β_1 and β_2 in the plane and β_3 perpendicular to the plane:

$$\beta_1 = \frac{V_f \beta_{f1} E_{f1} + V_R \beta_R E_R}{E_1} \tag{11.15}$$

$$\beta_2 = \beta_3 = \beta_{f2}\sqrt{V_f} + \left(1-\sqrt{V_f}\right)\cdot\left(1+V_f \nu_R E_{f1}/E_1\right)\cdot\beta_R \tag{11.16}$$

11.7 Laminate properties

11.7.1 General

(1) Characteristic values for laminate properties can be determined in a number of ways:
- from classical laminate theory using the properties of the layers obtained from tests, as per Table 3.1;
- from tests to determine the characteristic laminate properties in terms of stress resultants.

(2) It is recommended to apply a symmetrical and balanced laminate structure in the design. A nonsymmetrical laminate structure would result in torsion deformation under a purely symmetrical tensile load.

11.7.2 Stiffness and strength

(1) Assuming the UD ply stiffness stated in §11.6.2 and that classical laminate theory is applied, results in stiffness properties as per Table 11.16. In the following, the subscript "1" refers to 0°-direction, while the subscript "2" refers to 90° direction.

Table 11.16 - Calculated stiffness values for two different GFRP laminates (V_f = 50 %).

Stiffness properties	Quasi-isotropic GFRP laminate Proportions 25%/25%/25%/25% in orientations [0°/ 90°/ +45°/-45°], symmetrical, balanced lay up	Anisotropic GFRP laminate Proportions 55%/15%/15%/15% in orientations [0°/ 90°/ +45°/-45°], symmetrical, balanced lay up
E_1 [GPa]	18.6	25.8
E_2 [GPa]	18.6	15.9
G_{12} [GPa]	7.0	5.6
ν_{12}	0.33	0.32

(2) The application of the 1.2 % strain limit and 1.6 % shear strain limit results in the following typical strengths for these laminates as shown in Table 11.17.

Table 11.17 - Calculated strength values for two laminates (V_f = 50 %).

Strength properties	Quasi-isotropic GFRP laminate Proportions 25%/25%/25%/25% in orientations [0°/ 90°/ +45°/-45°], symmetrical, balanced lay up	Anisotropic GFRP laminate Proportions 55%/15%/15%/15% in orientations [0°/ 90°/ +45°/-45°], symmetrical, balanced lay up
σ_{1t} [MPa]	223	310
σ_{1c} [MPa]	223	310
σ_{2t} [MPa]	223	191
σ_{2c} [MPa]	223	191
τ_{12} [MPa]	112	90

11.7.2.1 Interlaminar shear strength of laminates (ILSS)

(1) Typical values can be used as given in Table 11.18 for the interlaminar shear strength (ILSS). Higher values may only be used if these values are based on test results.

Table 11.18 - Typical values for interlaminar shear strength ILSS in glass fibre reinforced laminates.

Resin type for the GRP laminate	Interlaminar shear strength ILSS [MPa]
Polyester resin	20
Vinyl ester resin	25
Epoxy resin	30

(2) The values stated in Table 11.18 may also be used as assumed values for carbon laminates.

(3) A relatively low ILSS value may indicate incompatibility between the resin and fibre or poor conditions during production.

11.7.3 Coefficients of thermal expansion for laminates

(1) The linear coefficients of thermal expansion a1 and a2 for a laminate that consists of several plies with different fibre directions can be calculated using classical laminate theory.

(2) For a laminate that consists of different plies (n) with different fibre directions, the linear coefficients of thermal expansion along two directions 1 and 2, α_1 and α_2, can be calculated using the classical laminate theory.

$$\alpha_{1,\text{Laminate}} = \frac{\alpha_{1,1}t_1 + \alpha_{1,2}t_2 + \ldots + \alpha_{1,n}t_n}{t_1 + t_2 + \ldots + t_n}$$

$$\alpha_{2,\text{Laminate}} = \frac{\alpha_{2,1}t_1 + \alpha_{2,2}t_2 + \ldots + \alpha_{2,n}t_n}{t_1 + t_2 + \ldots + t_n}$$

where tj is the layer thickness and $\alpha_{i,j}$ is the value of the thermal expansion coefficient of the j-th ply along the assigned direction i (= 1, 2).

11.7.4 Material properties for fatigue analysis

(1) In preliminary design for laminates with 35 % ≤ V_f ≤ 65 %, the values from Table 11.19 may be used for the fatigue regression parameters when determining the S-N line at ply level in the fibre direction. This only applies to material directions with more than 12.5 % of fibre reinforcement.

(2) As an assumption of the first estimate for the B-value of the tensile-tensile fatigue the static tensile strength can be taken. For all other fatigue loads, the compressive strength of the laminate can be taken.

(3) For V_f equal to 55 % the *S-N* curves are shown in Figure 11.1. For other values of V_f a correction should be made as specified in Table 11.19.

Table 11.19 - Reference values for regression parameters a and *B* for UD laminate.

UD non-crimp fabric	Glass/epoxy UD non-crimp fabric	Glass/polyester UD non-crimp fabric	Carbon/epoxy UD non-crimp fabric
	a, B	a, B	a, B
R = -1	-10, 600*(V_f/0.55)	-9, 700*(V_f/0.55)	-15,900*(V_f/0.55)
R = 0.1	-10, 1100*(V_f/0.55)	-7, 1300*(V_f/0.55)	-30, 1200*(V_f/0.55)
R = 10	-18, 750*(V_f/0.55)	-	-

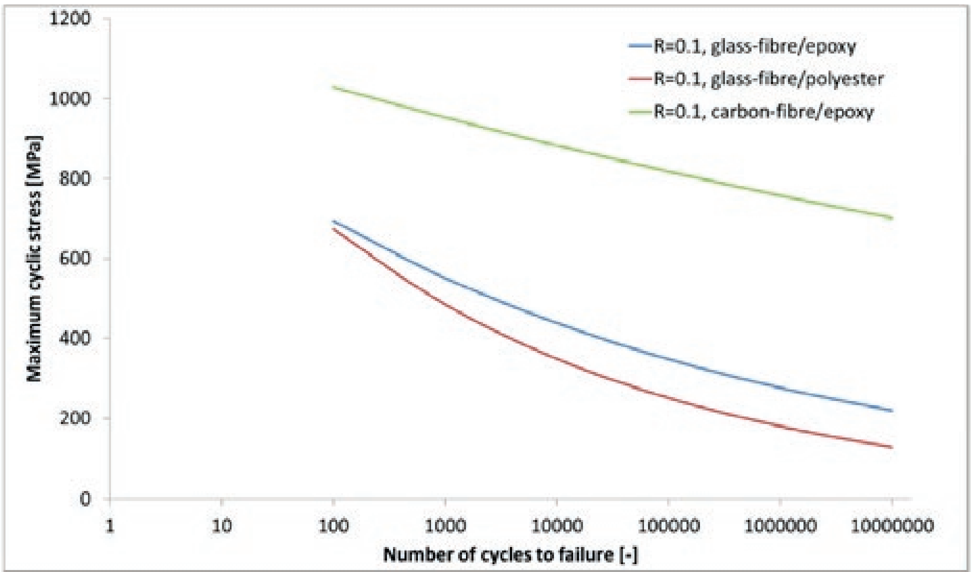

Figure 11.1 - *S*-*N* curves for a number of materials, V_f 55%, *R*= 0.1.

For the meaning of the symbols R, a, and B, reference is made to Section 6.5.

11.8 References

CUR 96 Fibre Reinforced Polymers in Civil Load Bearing Structures (Dutch Recommendation, 2003).

12 ANNEX C (VALUES OF $N_{RD2,C}$ FOR DOUBLE SYMMETRIC PROFILES AND ANGLE, CRUCIFORM AND T PROFILES)

(1) This Annex provides the design formulas to estimate the local buckling force, $N_{Rd2,loc}$, of columns (members under compression) with double symmetric profiles (I-section and tubular section), as well as the reduction coefficient that takes into account the interaction between local and global buckling, χ. The formulas given in this Annex do not consider the effect of rotational restraint between different elements (flange and web) of the cross-section. Annex E provides formulas that consider such effect.

(2) This Annex also provides formulas to estimate of the torsional buckling load, $N_{Rd,T}$, of pultruded profiles having all section walls converging into a single point (shear centre), such as angle, cruciform and T sections.

12.1 Double symmetric profiles

(1) In the case of pultruded profiles with double symmetric section, the value of $N_{Rd,loc}$ can be obtained from the following relation,

$$N_{Rd,loc} = A \cdot f_{d,loc}^{axial}, \tag{12.1}$$

where $f_{d,loc}^{axial}$ is the design value of the local critical stress.

(2) The design value of the local critical stress, $f_{d,loc}^{axial}$, can be calculated from,

$$f_{d,loc}^{axial} = \frac{\eta_c}{\gamma_M} \cdot \min\{(f_{k,loc}^{axial})_f, (f_{k,loc}^{axial})_w\}, \tag{12.2}$$

where $(f_{k,loc}^{axial})_f$, and $(f_{k,loc}^{axial})_w$ are the critical stresses of the uniformly compressed flanges and web respectively, determined through the expressions reported in Annex E. The partial factors for the FRP material, different for local and global stability, are defined in Table 2.1.

(3) The value of the critical stress of the compressed flange, assumed simply supported at the connection with the web, $(f_{k,loc}^{axial})_f^{SS}$, can be conservatively calculated based on the following formula,

$$\left(f_{k,loc}^{axial}\right)_f = \left(f_{k,loc}^{axial}\right)_f^{SS} = 4 \cdot G_{LT} \cdot \left(\frac{t_f}{b_f}\right)^2, \tag{12.3}$$

where the symbols are defined in Figure 12.1(a) and the subscripts *"L"* and *"T"* mean longitudinal and transversal, respectively.

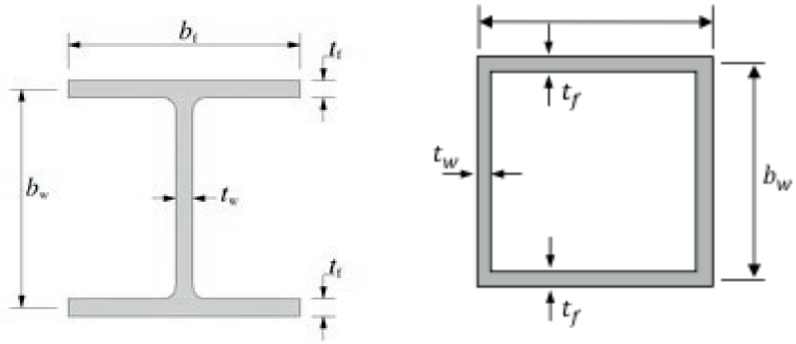

Figure 12.1 – Symbols used for the geometric dimensions of double symmetric sections:
(a) I-section and (b) tubular section

(4) In the case of pultruded I-section columns, the value of the critical stress of the compressed web, assumed simply supported at the connection with the flanges, , can b$\left(f_{k,loc}^{axial}\right)_w$servatively calculated based on the following formula,

$$\left(f_{k,loc}^{axial}\right)_w = \left(f_{k,loc}^{axial}\right)_w^{SS} = k_c \cdot \frac{\pi E_{Tc}}{12\left(1-\nu_{LT}\nu_{TL}\right)} \cdot \left(\frac{t_w}{b_w}\right)^2, \qquad (12.4)$$

where k_c is the plate buckling coefficient and the subscripts "*T*" and "*c*" mean transversal and compressive, respectively.

(5) The coefficient k_c in (12.4) is obtained from the relation:

$$k_c = 2\sqrt{\frac{E_{Lc}}{E_{Tc}}} + 4\frac{G_{LT}}{E_{Tc}} \cdot \left(1-\nu_{LT}\nu_{TL}\right) + 2\nu_{LT} \qquad (12.5)$$

(6) For the pultruded profiles classified by EN 13706-3 the ratio E_{Lc}/E_{Tc} equals approximately 3.33. For pultruded profiles currently available in the market, the following conditions apply:

- $0.40 \leq G_{LT}/E_{Tc} \leq 0.57$;
- $0.23 \leq \nu_{LT} \leq 0.35$.

For these value intervals, equation (12.5) gives the minimum value $k_c = 5.66$.

(7) In the case of pultruded tubular columns, the value of the critical stress of the compressed flange, assumed simply supported at the connection with the webs, $\left(f_{k,loc}^{axial}\right)_f^{SS}$, can be conservatively calculated based on the following formula,

$$\left(f_{k,loc}^{axial}\right)_f = \left(f_{k,loc}^{axial}\right)_f^{SS} = \frac{\pi^2}{t_f b_f^2} \cdot \left[2\sqrt{(D_{11})_f (D_{22})_f} + 2(D_{12})_f + 4(D_{66})_f\right], \quad (12.6)$$

where the symbols are defined in Figure 12.1(b), the subscript "f" refers to the flanges, and the values of the flexural stiffness of the flanges (D_{11}, D_{12}, D_{22} and D_{66}) are given by the following relations (assuming characteristic values of the elasticity moduli),

$$D_{11} = \frac{E_{Lc} \cdot t^3}{12 \cdot (1 - \nu_{LT} \cdot \nu_{TL})}, \quad (12.7)$$

$$D_{12} = \nu_{LT} \cdot D_{22}, \quad (12.8)$$

$$D_{22} = \frac{E_{Tc} \cdot t^3}{12 \cdot (1 - \nu_{LT} \cdot \nu_{TL})}, \quad (12.9)$$

$$D_{66} = \frac{G_{LT} \cdot t^3}{12}, \quad (12.10)$$

where the subscripts "L" and "T" mean longitudinal and transversal, respectively, and "c" means compressive.

(8) In the case of pultruded tubular columns, the value of the critical stress of the compressed web, assumed simply supported at the connection with the flanges, , can be conservatively calculated based on the following formula:

$$\left(f_{k,loc}^{axial}\right)_w = \left(f_{k,loc}^{axial}\right)_w^{SS} = \frac{\pi^2}{t_w b_w^2} \cdot \left[2\sqrt{\left(D_{11}\right)_w \left(D_{22}\right)_w} + 2\left(D_{12}\right)_w + 4\left(D_{66}\right)_w\right], \quad (12.11)$$

(9) The reduction factor χ to take into account the interaction between local and global buckling can be obtained through the expression,

$$\chi = \frac{1}{c \cdot \lambda^2} \cdot \left(\Phi - \sqrt{\Phi^2 - c \cdot \lambda^2}\right), \quad (12.12)$$

where c is a coefficient that, in the absence of test results, can be assumed equal to 0.65 and Φ is an auxiliary coefficient given by,

$$\Phi = \frac{1 + \lambda^2}{2}. \quad (12.13)$$

In (12.7) and (12.8), the parameter λ represents the member's slenderness and is given by,

$$\lambda = \sqrt{\frac{N_{\mathrm{Rd,loc}}}{N_{\mathrm{Rd,E}}}}\,, \qquad \text{(12.14}$$

where $N_{\mathrm{Rd,loc}}$ is the local buckling load (§ 14(1)) and $N_{\mathrm{Rd,E}}$ is the design value of the global (flexural or Euler) buckling load, given by,

$$N_{\mathrm{Rd,E}} = \frac{\eta_c}{\gamma_M} \times \frac{\pi^2 E_{\mathrm{Lc}} I}{(kL)^2} \times \left(1 + \frac{\pi^2 E_{\mathrm{Lc}} I}{(kL)^2 G_{\mathrm{LT}} A_{\mathrm{v}}}\right)^{-1}, \qquad (12.15)$$

where k is the buckling coefficient that takes into account the restraining effects of supports to flexural buckling of the column about the relevant axis (L_0 = k × L is the effective length), I is the moment of inertia about the relevant axis, and A_v is the area of the cross-section resistant to shear (shear area). k may be different for y-axis (major-axis) and z-axis (minor-axis), depending on the restrain to rotation provided by the supports. k is equal to 1.0 for simply supported columns, 0.5 for fully clamped columns and 0.7 for clamped-simply supported columns. A_v depends on the cross-section shape and shear force orientation (see Table 6.1).
The value χ , which depends on λ , is plotted in Figure 12.2. In the presence of constraints that prevent global buckling the coefficient χ in (12.1) assumes a unit value.

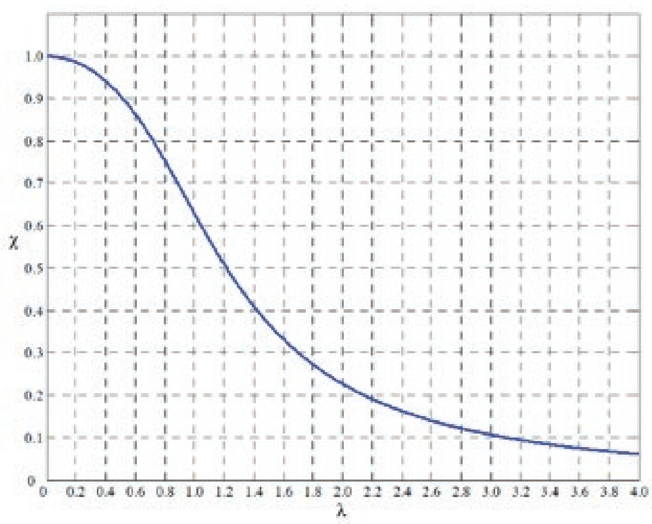

Figure 12.2 – Interaction curve between local and global modes of instability due to axial compression.

12.2 Angle, cruciform and t profiles

(1) For pultruded profiles having all section walls converging into a single point (shear centre), such as angle, cruciform and T sections, the design value of the torsional buckling load, $N_{Rd,T}$, is given by,

$$N_{Rd,T} = \frac{A}{I_0}\left[\frac{\pi^2 E_{L,c} I_\omega}{(k_\omega L)^2} + G_{LT} I_t\right], \qquad (12.16)$$

where A is the cross-section area of the profile, I_0 is the polar second moment of area, I_t and I_ω are the torsional and warping constants of the section, respectively, k_ω is an end restraint coefficient for torsional buckling (conservatively can be considered as unit) and L is the member length.

(2) In case of members with angle section where the connection to other members is located in one of the legs, the compression force is eccentric with respect to the centroid. Therefore, since the member is under compression and bending, it shall comply with clause 6.2.2.3 (combination of bending and axial compression force).

12.3 References

CNR-DT 205/2007 Guide for the Design and Construction of Structures made of Pultruded FRP elements, Italian National Research Council (2008).

Barbero E, Tomblin J. A phenomenological design equation for FRP columns with interaction between local and global buckling (1994). Thin-Walled Structures, Vol. 18(2), pp. 117-131.

Zureick A, Scott D. Short-term behavior and design of fiber-reinforced polymeric slender members under axial compression (1997). Journal of Composites for Construction, Vol. 1, pp. 140-149.

13 ANNEX D (ELASTIC BUCKLING FORMULAS FOR BEAMS WITH DOUBLE SYMMETRIC PROFILES UNDER MAJOR-AXIS BENDING)

(1) This Annex provides the design formulas to estimate the local buckling moment, $M_{Rd,loc}$, of beams (members under major-axis bending) with double symmetric profiles (I-section and tubular section), as well as the reduction coefficient that takes into account the interaction between local and global buckling , χ_{FT}. The formulas given in this Annex do not consider the effect of rotational restraint between different elements (flange and web) of the cross-section. Annex E provides formulas that consider such effect.

(2) The design value of the bending moment associated to the local buckling of the pultruded profile is given by,

$$M_{Rd,loc} = W \cdot f_{d,loc}^{flex} \tag{13.1}$$

with *w* being the major-axis flexural modulus of gross cross-section and $f_{d,loc}^{flex}$ denoting the design value of the flexural stress associated to local buckling of the beam profile. The design value of $f_{d,loc}^{flex}$ may be estimated using the formulae provided next.

(3) The design value of the flexural stress associated to local buckling of the beam profile under major-axis bending should be calculated from,

$$f_{d,loc}^{flex} = \frac{\eta_c}{\gamma_M} \cdot f_{k,loc}^{flex}, \tag{13.2}$$

where $f_{k,loc}^{flex}$ is the characteristic value of the flexural stress associated to local buckling, given by

$$f_{k,loc}^{flex} = min\left\{\left(f_{k,loc}^{axial}\right)_f ; \left(f_{k,loc}^{flex}\right)_w\right\}. \tag{13.3}$$

In these equations, $\left(f_{k,loc}^{axial}\right)_f$ is the critical stress value of the compressed flange assuming a uniform stress distribution along the flange width and $\left(f_{k,loc}^{flex}\right)_w$ is the critical stress value of the web assuming a linear stress distribution along the web height. The value of $f_{k,loc}^{flex}$ may be obtained from numerical modelling (§ 5.2(4)).

(4) In the case of pultruded I-section beams under major-axis bending, the value of $\left(f_{k,loc}^{flex}\right)_f$ is given by

$$\left(f_{k,loc}^{flex}\right)_f = \left(f_{k,loc}^{flex}\right)_f^{SS} = 4 \cdot G_{LT} \cdot \left(\frac{t_f}{b_f}\right)^2, \tag{13.4}$$

which neglects the elastic restraint provided by the web to the twist of compressed flange. The value of $\left(f_{k,loc}^{flex}\right)_f$ may also be calculated using the formulas reported in Annex E, which consider not only this rotational restraint but also the influence of web compressive stresses on the rotational stiffness.

(5) In the case of pultruded I-section beams under major-axis bending, the value of may be determined through the following formula,

$$\left(f_{k,loc}^{flex}\right)_w = k_f \frac{\pi^2 E_{T,c}}{12\left(1-\nu_{LT}\nu_{TL}\right)}\left(\frac{t_w}{b_w}\right)^2, \tag{13.5}$$

where the plate buckling coefficient k_{flex} is given by,

$$k_f = 13.9\sqrt{\frac{E_{L,c}}{E_{T,c}}} + 22.2\frac{G_{LT}}{E_{T,c}}\left(1-\nu_{LT}\nu_{TL}\right) + 11.1\nu_{LT}. \tag{13.6}$$

Equation (13.5) is conservative because it considers the web simply supported at the connection with the flanges, neglecting the rotational restraint provided by the flanges.

(6) For pultruded profiles classified by EN 13706-3 (see Appendix C of this standard), the ratio $E_{L,c}/E_{T,c}$ equals approximately 3.33, whereas for pultruded profiles currently available in the market it gives the minimum value of k_f = 36.6, for the following intervals of values:

- $0.40 \leq G_{LT}/E_{T,c} \leq 0.57$
- $0.23 \leq \nu_{LT} \leq 0.35$

(7) In the case of pultruded tubular beams under major-axis bending, the value of $\left(f_{k,loc}^{flex}\right)_f$ is given by

$$\left(f_{k,loc}^{flex}\right)_f = \left(f_{k,loc}^{flex}\right)_f^{SS} = \frac{\pi^2}{t_f b_f^2}\cdot\left[2\sqrt{\left(D_{11}\right)_f\left(D_{22}\right)_f} + 2\left(D_{12}\right)_f + 4\left(D_{66}\right)_f\right], \tag{13.7}$$

where the values of the flexural stiffness of the webs (D_{11}, D_{12}, D_{22} and D_{66}) are given by the following relations (assuming characteristic values of the elasticity moduli),

$$D_{11} = \frac{E_{Lc} \cdot t^3}{12 \cdot (1 - \nu_{LT} \cdot \nu_{TL})}, \tag{13.8}$$

$$D_{12} = \nu_{LT} \cdot D_{22}, \tag{13.9}$$

$$D_{22} = \frac{E_{Tc} \cdot t^3}{12 \cdot (1 - \nu_{LT} \cdot \nu_{TL})}, \tag{13.10}$$

$$D_{66} = \frac{G_{LT} \cdot t^3}{12}, \tag{13.11}$$

where the subscripts "*L*" and "*T*" mean longitudinal and transversal, respectively, and "c" means compressive. Note that Eq. (13.7) neglects the elastic restraint provided by the webs to the transverse bending of the compressed flanges. The value of $^{T}/_{c}$ may also be calculated using the formulas reported in Annex E, which consider not only this rotational restraint but also the influence of webs' compressive stresses on this rotational stiffness.

(8) In the case of pultruded tubular beams under major-axis bending, the value of $\left(f_{k,loc}^{flex}\right)_w$ is given by,

$$\left(f_{k,loc}^{flex}\right)_w = \left(f_{k,loc}^{flex}\right)_w^{SS} = \frac{\pi^2}{t_w b_w^2} \cdot \left[13.9\sqrt{(D_{11})_w (D_{22})_w} + 11.1(D_{12})_w + 22.2(D_{66})_w\right], \tag{13.12}$$

(9) The reduction coefficient for local-global buckling interaction is given by

$$\chi_{FT} = \frac{1}{c \cdot \lambda_{FT}^2}\left(\Phi_{FT} - \sqrt{\Phi_{FT}^2 - c \cdot \lambda_{FT}^2}\right) \tag{13.13}$$

where c = 0.7 is an interaction coefficient, $\Phi_{FT} = (1 + \lambda_{FT}^2)/2$ is an auxiliary parameter and χ_{FT} is the beam slenderness for local-global buckling interaction, which is given by,

$$\lambda_{FT} = \sqrt{\frac{M_{Rd,loc}}{M_{Rd,FT}}} \tag{13.14}$$

with $M_{Rd,FT}$ being the design value of the bending moment associated to local buckling of the pultruded profile and $M_{Rd,FT}$ denotes the design value of the bending moment associated to global (flexural-torsional) buckling of the beam, which can be computed according to clause 13(12).

(10) If sufficient restraints, i.e., lateral bracings, are provided to the beam to avoid any possibility of global (flexural-torsional) buckling, the reduction coefficient for local-global buckling interaction should be $\chi_{FT} = 1.0$.

(11) In case of beams under minor-axis bending, global (flexural-torsional) buckling does not occur in practice and, thus, $\chi_{FT} = 1.0$.

(12) The design value of the moment associated to global (flexural-torsional) buckling of the beam under major-axis (i.e. strong-axis) bending should be calculated from the following formula,

$$M_{Rd,FT} = \frac{\eta_c}{\gamma_M} \cdot M_{Rk,FT}, \qquad (13.15)$$

where $M_{Rk,FT}$ is the characteristic value of the moment associated to global (flexural-torsional) buckling, given by

$$M_{Rk,FT} = \frac{\pi^2 E_{L,c} I_{min}}{(kL)^2} \left[\sqrt{(C_2 z_q)^2 + k^2 \frac{I_\omega}{I_{min}} + \frac{(kL)^2 G_{LT} I_t}{\pi^2 E_{L,c} I_{min}}} - C_2 z_q \right], \qquad (13.16)$$

In these equations, is the beam length, I_{min} is the minor-axis second moment of area of the section, ar I_ω I_t are the torsional and warping constants of the section, respectively, z_q is the minor-axis coordinate of transversal load application point, k is the effective length coefficient allowing for the effect of minor-axis rotation at beam supports, C_1 is the equivalent moment factor that depends on the variation of M_{ed} along the beam length and C_2 is a factor that takes into account the transverse load application point. The value of $M_{Rk,FT}$ may be obtained from numerical modelling (§ 5.2(4)).

(13) The effective length coefficient allowing for the effect of minor-axis rotation at beam supports is k = 1.0 if the sections at both supports are free to rotate about the minor-axis (simple support for out-ofplane rotation) and k = 0.5 if the sections at both supports cannot rotate about the minor-axis (fixed support for out-of-plane rotation). Conservatively, it may be assumed k = 1.0 .

(14) The minor-axis coordinate of transversal load application point z_q is positive if the load is applied on the compressed part of the section (load at top flange, z_q = + h/2), null if the load is applied at the shear centre (z_q = 0), and negative if the load is applied at the tensioned part of the section (load at bottom flange, z_q = - $h/2$).

(15) The equivalent moment factor C_1 depends on variation of M_{Ed} along the beam length, through the ratio $\psi = M_{min}$ M_{max} (for beams loaded by moments at supports) or the shape of bending moment diagram (beams under transverse loads) and also on the out-of-plane support conditions, through the effective length coefficient k. Tables 13.1 and 13.2 present values of C_1 for several loading configurations.

(16) The values of factor C_2 for the transverse load application point are given in Tables 13.1 and 13.2 for some loading configurations. In case of beams loaded by moments at supports, $C_2 = 0$ because there are no transverse loads applied.

(17) For other loading configurations, it is possible either to obtain the values of factors C_1 and C_2 from literature or determine $M_{Rd,FT}$ from numerical methods (linear buckling analysis of the beam without imperfections – bifurcation analysis). For sections without double symmetry, the value of $M_{Rd,FT}$ may also be determined from numerical analysis.

Table 13.1 – Values of factors C_1 and C_2 for beams loaded by moments at supports.

Loading and support conditions	Bending moment diagram	*k*	C_1	C_2
	ψ=+1 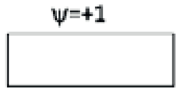	1.0	1.00	0
		0.5	1.00	0
	ψ=+3/4 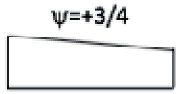	1.0	1.14	0
		0.5	1.19	0
	ψ=+1/2 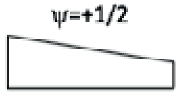	1.0	1.31	0
		0.5	1.37	0
	ψ=+1/4 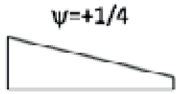	1.0	1.52	0
		0.5	1.60	0
	ψ= 0 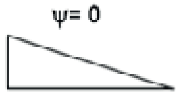	1.0	1.77	0
		0.5	1.86	0
	ψ=-1/4 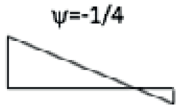	1.0	2.06	0
		0.5	2.15	0
	ψ=-1/2 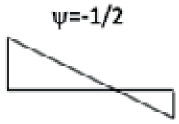	1.0	2.35	0
		0.5	2.42	0
	ψ=-3/4 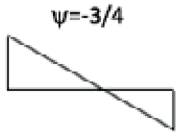	1.0	2.60	0
		0.5	2.45	0
	ψ=-1 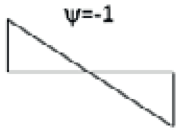	1.0	2.60	0
		0.5	2.45	0

Table 13.2 – Values of coefficients C_1 and C_2 for beams under transverse loads

Loading and support conditions	Bending moment diagram	k	C_1	C_2
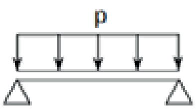		1.0 0.5	1.12 0.97	0.45 0.36
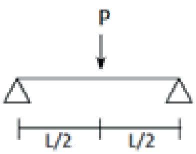	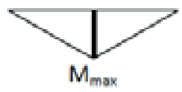	1.0 0.5	1.35 1.05	0.59 0.48
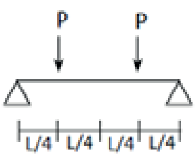	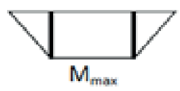	1.0 0.5	1.04 0.95	0.42 0.31

14 ANNEX E (LOCAL INSTABILIY OF DOUBLE SYMMETRIC PROFILES)

(1) This Annex provides the design formulas to estimate the local buckling stresses for profiles with doubly symmetric section (I-section and tubular section) under either compression (columns) or major-axis bending (beams). These formulas consider the rotational restriction provided by the cross-section walls (interaction between the web and flange) while those formulas given in Sections 12 (Annex C, for columns) and 13 (Annex D, for beams) do not consider this effect.

(2) The element (web or flange) in the cross-section that first triggers local buckling of the profile is identified through the calculation of the following coefficient

$$R=\frac{\left(f_{\text{loc,k}}^{\text{axial}}\right)_{f}^{SS}\cdot\left(E_{Lc}\right)_{w}}{\left(f_{\text{loc,k}}^{\text{axial}}\right)_{w}^{SS}\cdot\left(E_{Lc}\right)_{f}}, \tag{14.1}$$

where $\left(f_{\text{loc,k}}^{\text{axial}}\right)_{f}^{SS}$ and $\left(f_{\text{loc,k}}^{\text{axial}}\right)_{w}^{SS}$ are the characteristic values of the critical stresses of the flange and web, respectively, corresponding to no interaction between flange and web (flange simply supported in the web and web simply supported in the flange)

14.1 Members under compression (columns)

(1) In the case of pultruded I-section columns, the values of $\left(f_{\text{loc,k}}^{\text{axial}}\right)_{f}^{SS}$ and $\left(f_{\text{loc,k}}^{\text{axial}}\right)_{w}^{SS}$ to calculate R can be evaluated using equations (12.3) and (12.4), respectively. Alternatively, the following expressions may be applied,

$$\left(f_{\text{k,loc}}^{\text{axial}}\right)_{f}^{SS}=\frac{12\cdot\left(D_{66}\right)_{f}}{t_{f}\cdot\left(\frac{b_{f}}{2}\right)^{2}}, \tag{14.2}$$

$$\left(f_{\text{k,loc}}^{\text{axial}}\right)_{w}^{SS}=\frac{\pi^{2}}{t_{w}\cdot b_{w}^{2}}\cdot\left\{2\cdot\sqrt{\left(D_{11}\right)_{w}\cdot\left(D_{22}\right)_{w}}+2\cdot\left[\left(D_{12}\right)_{w}+2\cdot\left(D_{66}\right)_{w}\right]\right\}, \tag{14.3}$$

(1) This Annex provides the design formulas to estimate the local buckling stresses for profiles with doubly symmetric section (I-section and tubular section) under either compression (columns) or major-axis bending (beams). These formulas consider the rotational restriction provided by the cross-section walls (interaction between the web and flange) while those formulas given in Sections 12 (Annex C, for columns) and 13 (Annex D, for beams) do not consider this effect.

(2) The element (web or flange) in the cross-section that first triggers local buckling of the profile is identified through the calculation of the following coefficient

$$D_{11}=\frac{E_{Lc}\cdot t^{3}}{12\cdot\left(1-\nu_{LT}\cdot\nu_{TL}\right)}, \tag{14.4}$$

$$D_{12}=\nu_{LT}\cdot D_{22}, \tag{14.5}$$

$$D_{22}=\frac{E_{Tc}\cdot t^{3}}{12\cdot\left(1-\nu_{LT}\cdot\nu_{TL}\right)}, \tag{14.6}$$

$$D_{66}=\frac{G_{LT}\cdot t^{3}}{12}, \tag{14.7}$$

where the subscripts "*L*" and "*T*" mean longitudinal and transversal, respectively, and "c" means compressive.

(2) In the case of pultruded I-section columns, if R<1 the flanges buckle first than the web and the characteristic value of the critical stress of the flanges, $\left(f_{k,loc}^{axial}\right)_f$, taking into account the rotational constraint provided by the web to the flanges, is given by

$$\left(f_{k,loc}^{axial}\right)_f = \frac{\sqrt{(D_{11})_f \cdot (D_{22})_f}}{t_f \left(\frac{b_f}{2}\right)^2} \left\{K \cdot \left[15.1 \cdot \eta \cdot \sqrt{1-\rho} + 6 \cdot (1-\rho) \cdot (1-\eta)\right] + \frac{7 \cdot (1-K)}{\sqrt{1+4.12 \cdot \zeta}}\right\}, \text{ if } K \leq 1 \qquad (14.8)$$

$$\left(f_{k,loc}^{axial}\right)_f = \frac{\sqrt{(D_{11})_f \cdot (D_{22})_f}}{t_f \cdot \left(\frac{b_f}{2}\right)^2} \cdot \left[15.1 \cdot \eta \cdot \sqrt{1-\rho} + 6 \cdot (1-\rho) \cdot (K-\eta)\right], \text{ if } K > 1, \qquad (14.9)$$

where the parameters K, ρ, ζ and η in (14.8) and (14.9) are given by:

$$K = \frac{2 \cdot (D_{66})_f + (D_{12})_f}{\sqrt{(D_{11})_f \cdot (D_{22})_f}}, \qquad (14.10)$$

$$\rho = \frac{(D_{12})_f}{2 \cdot (D_{66})_f + (D_{12})_f}, \qquad (14.11)$$

$$\zeta = \frac{2}{1-R} \cdot \frac{(D_{22})_f b_w}{(D_{22})_w b_f}, \qquad (14.12)$$

$$\eta = \frac{1}{\sqrt{1+(7.22-3.55 \cdot \rho) \cdot \zeta}}. \qquad (14.13)$$

(3) In the case of pultruded I-section columns, if R > 1 the web buckles first than the flanges and the characteristic value of the critical stress of the web, $(f_{k,loc}^{axial})_w$, taking into account the rotational constraint provided by the flanges to the web, is given by

$$\left(f_{k,loc}^{axial}\right)_w = \frac{\pi^2}{t_w \cdot b_w^2} \cdot \left\{2 \cdot \sqrt{1+4.14\xi} \cdot \sqrt{(D_{11})_w \cdot (D_{22})_w} + \left(2+0.62 \cdot \xi^2\right) \cdot \left[(D_{12})_w + 2 \cdot (D_{66})_w\right]\right\}. \qquad (14.14)$$

where:

$$\xi = \left[1+0.61 \cdot \left(\frac{R}{4(R-1)} \cdot \frac{(D_{22})_w b_w}{(D_{66})_f b_f}\right)^{1.2}\right]^{-1}. \qquad (14.15)$$

(4) In the case of pultruded tubular columns, the values of $\left(f_{loc,k}^{axial}\right)_f^{SS}$ and $\left(f_{loc,k}^{axial}\right)_w^{SS}$ to calculate R can be evaluated using equations (12.6) and (12.11), respectively.

(5) In the case of pultruded tubular columns, if R < 1 the flanges buckle first than the webs and the characteristic value of the critical stress of the flanges, $\left(f_{k,loc}^{axial}\right)_w$, taking into account the rotational constraint provided by the webs to the flanges, is given by,

$$\left(f_{k,loc}^{axial}\right)_f = \frac{\pi^2}{b_f^2 t_f}\left[2\sqrt{(1+4.139\xi)(D_{11})_f (D_{22})_f} + \left(2+0.62\xi^2\right)\left((D_{12})_f + 2(D_{66})_f\right)\right] \qquad (14.16)$$

where:

$$\xi = \left(1 + \frac{5}{1-R}\cdot\frac{(D_{22})_f b_w}{(D_{22})_w b_f}\right)^{-1}. \qquad (14.17)$$

(6) In the case of pultruded tubular columns, if R > 1 the webs buckle first than the flanges and the characteristic value of the critical stress of the webs, $(f_{k,loc}^{axial})_w$, taking into account the rotational restraint provided by the flanges to the webs, is given by,

$$\left(f_{k,loc}^{axial}\right)_w = \frac{\pi^2}{b_w^2 t_w}\left[2\sqrt{(1+4.139\xi)(D_{11})_w (D_{22})_w} + \left(2+0.62\xi^2\right)\left((D_{12})_w + 2(D_{66})_w\right)\right], \qquad 14.18)$$

where:

$$\xi = \left(1 + \frac{5R}{R-1}\cdot\frac{(D_{22})_w b_f}{(D_{22})_f b_w}\right)^{-1}. \qquad (14.19)$$

14.2 Members under major-axis bending (beams)

(1) In the case of pultruded I-section beams under major-axis bending, the values of $(f_{loc,k}^{axial})_f^{SS}$ and $(f_{loc,k}^{axial})_w^{SS}$ to calculate R can be evaluated using equations (13.4) and (13.5), respectively. Alternatively, the following expressions may be applied,

$$\left(f_{k,loc}^{flex}\right)_f^{SS} = \frac{12\cdot(D_{66})_f}{t_f\cdot\left(\frac{b_f}{2}\right)^2}, \qquad (14.20)$$

$$\left(f_{k,loc}^{flex}\right)_w^{SS} = \frac{\pi^2}{t_w\cdot b_w^2}\cdot\left\{13.9\sqrt{(D_{11})_w (D_{22})_w} + 11.1(D_{12})_w + 22.2(D_{66})_w\right\}. \qquad (14.21)$$

(2) In the case of pultruded I-section beams under major-axis bending, if R < 1 the flanges buckle first than the web and the characteristic value of the critical stress of the flanges,   , taking into account the rotational constraint provided by the web to the flanges, is given by,

$$\left(f_{k,loc}^{flex}\right)_f = \frac{\sqrt{(D_{11})_f\cdot(D_{22})_f}}{t_f\left(\frac{b_f}{2}\right)^2}\left\{K\cdot\left[15.1\cdot\eta\cdot\sqrt{1-\rho}+6\cdot(1-\rho)\cdot(1-\eta)\right] + \frac{7\cdot(1-K)}{\sqrt{1+4.12\cdot\zeta}}\right\}, \text{ if } K \le 1 \qquad (14.22)$$

$$\left(f_{k,loc}^{flex}\right)_f = \frac{\sqrt{(D_{11})_f\cdot(D_{22})_f}}{t_f\cdot\left(\frac{b_f}{2}\right)^2}\cdot\left[15.1\cdot\eta\cdot\sqrt{1-\rho}+6\cdot(1-\rho)\cdot(K-\eta)\right], \text{ if } K > 1, \qquad (14.23)$$

where the parameters K, ρ, ζ and η in (14.22) and (14.23) are given by:

$$K = \frac{2 \cdot (D_{66})_f + (D_{12})_f}{\sqrt{(D_{11})_f \cdot (D_{22})_f}}, \qquad (14.24)$$

$$\rho = \frac{(D_{12})_f}{2 \cdot (D_{66})_f + (D_{12})_f}, \qquad (14.25)$$

$$\zeta = \frac{4}{1-R} \cdot \frac{(D_{22})_f b_w}{(D_{22})_w b_f}, \qquad (14.26)$$

$$\eta = \frac{1}{\sqrt{1+(7.22-3.55 \cdot \rho) \cdot \zeta}}. \qquad (14.27)$$

(3) In the case of pultruded I-section beams under major-axis bending, if R > 1 the web buckles first than the flanges; in this case, there is yet no explicit solution available for the critical stress of the web (plate with rotationally restrained edges and under linearly varying stress diagram). The value of $(f_{k,loc}^{flex})_w$ may conservatively be determined using Eq. (13.5) or Eq. (14.21), considering the edges simply supported.

(4) In the case of pultruded tubular beams under major-axis bending, the values of $\left(f_{loc,k}^{axial}\right)_f^{SS}$ and $\left(f_{loc,k}^{axial}\right)_w^{SS}$ to calculate R can be evaluated using equations (13.7) and (13.12), respectively.

(5) In case of pultruded tubular beams under major-axis bending, if R < 1 the flanges buckle first than the webs and the characteristic value of the critical stress of the flanges, $(f_{k,loc}^{flex})_f$, taking into account the rotational constraint provided by the webs to the flanges, is given by

$$\left(f_{k,loc}^{flex}\right)_f = \frac{\pi^2}{b_f^2 t_f}\left[2\sqrt{(1+4.139\xi)(D_{11})_f (D_{22})_f} + \left(2+0.62\xi^2\right)\left((D_{12})_f + 2(D_{66})_f\right)\right] \qquad (14.28)$$

where:

$$\xi = \left(1 + \frac{2.5}{1-R} \cdot \frac{(D_{22})_f b_w}{(D_{22})_w b_f}\right)^{-1}. \qquad (14.29)$$

(6) In the case of pultruded tubular beams under major-axis bending, if R > 1 the webs buckle first than the flanges; in this case, there is yet no explicit solution available for the critical stress of the web (plate with rotationally restrained edges and under linearly varying stress diagram). The value of $(f_{k,loc}^{flex})_w$ may conservatively be determined using Eq. (13.12), considering the edges simply supported.

14.1 References

CNR-DT 205/2007. Guide for the Design and Construction of Structures made of Pultruded FRP elements, Italian National Research Council (2008).

Kollár, L.P., Local Buckling of Fiber Reinforced Plastic Composite Structural Members with Open and Closed Cross Sections (2003). Journal of Structural Engineering, Vol. 129 (11), pp. 1503-1513.

15 ANNEX F (INSTABILITY OF ORTHOTROPIC SYMMETRICAL PLATES)

(1) This Annex presents provisions to estimate the buckling stresses of orthotropic symmetrical plates and shells.

15.1 General provisions

(1) The stability of plates and shells should be checked at the laminate level.

(2) The stability of plates and shells may be checked using experimental tests (see § 5.5(1)) or numerical modelling (§ 5.2(4)). In the latter approach, when conducting geometrically non-linear FEM analysis, an initial imperfection should be considered with the critical buckling mode shape determined from linear buckling analysis.

(3) For non-symmetrical laminates, the buckling load may be estimated using the classical laminate theory.

15.2 FORMULAE FOR ORTHOTROPIC SYMMETRICAL PLATES

15.2.1 Pure compression

(1) The stability of a plate under uniform compressive stresses should be verified from:

$$\frac{f_{Ed,c}}{f_{Rd,c}} \leq 1, \tag{15.1}$$

where:

$f_{d,c\,N}$ is the design value for an evenly distributed compression load occurring for each width unit (aligned in the longitudinal direction of the plate);

$f_{d,c\,N}$ is the design value for buckling resistance obtained by factorizing the theoretical critical value, $f_{x,cr}$, as indicated below.

(2) For a plate width L_y the values of $f_{x,cr}$ are as follows:

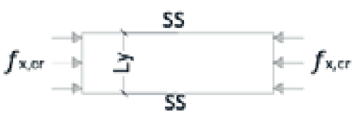	$f_{x,cr} = \frac{\pi^2}{t \times L_y^2}\left[2\sqrt{D_{11}D_{22}} + 2(D_{12} + 2D_{66})\right]$
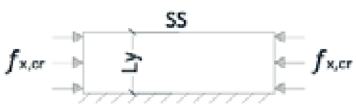	$f_{x,cr} = \frac{\pi^2}{t \times L_y^2}\left[3.125\sqrt{D_{11}D_{22}} + 2.33(D_{12} + 2D_{66})\right]$
	$f_{x,cr} = \frac{\pi^2}{t \times L_y^2}\left[4.53\sqrt{D_{11}D_{22}} + 2.44(D_{12} + 2D_{66})\right]$
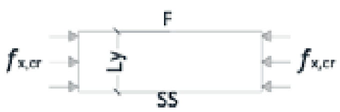	$f_{x,cr} = 12\frac{D_{66}}{t \times L_y^2}$
	$f_{x,cr} = \frac{1}{t \times L_y^2}\sqrt{D_{11}D_{22}}\left[15.1K\sqrt{1-\nu} + 7(1-K)\right]$ when $k \le 1$ $f_{x,cr} = \frac{1}{t \times L_y^2}\sqrt{D_{11}D_{22}}\left[15.1K\sqrt{1-\nu} + 6(K-1)(1-\nu)\right]$ when $k > 1$

where:

- $\nu = D_{12} / (2D_{66} + D_{12})$
- $K = (2D_{66} + D_{12}) / \sqrt{D_{11}D_{22}}$.

The support conditions for the non-supported edges are either simply supported (SS), free (F) or clamped (C).

The meaning of quantities D_{11}, D_{22}, D_{12}, D_{66} has been introduced in Annex E, with the symbol "L" referring to the direction of L_y and the symbol "T" to the orthogonal direction.

15.2.2 Pure shear

(3) The stability of a plate under shear force should be verified from:

$$\frac{f_{Ed,s}}{f_{Rd,s}} \leq 1 \tag{15.2}$$

where:

$f_{Ed,s}$ is the design value for shear force for each width unit;
$f_{Rd,s}$ is the design value for buckling resistance obtained by factorizing the theoretical critical stress $f_{xy,cr,}$ as indicated below.

(2) For a plate width L_y the values of $f_{xy,cr}$ are as follows:

	$f_{xy,cr} = \frac{4}{t \times L_y^2} \sqrt[4]{D_{11} D_{22}^3}\,(8.125 + 5.045k)$ when $k \leq 1$ $f_{xy,cr} = \frac{4}{t \times L_y^2} \sqrt{D_{22}(D_{12} + 2D_{66})}(11.7 + \frac{1.46}{k^2})$ when $k > 1$
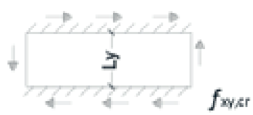	$f_{xy,cr} = \frac{4}{t \times L_y^2} \sqrt[4]{D_{11} D_{22}^3}\,(15.07 + 7.08k)$ when $k \leq 1$ $f_{xy,cr} = \frac{4}{t \times L_y^2} \sqrt{D_{22}(D_{12} + 2D_{66})}(18.59 + \frac{3.56}{k^2})$ when $k > 1$

15.2.4 Pure bending

(1) The stability of a plate under pure bending should be verified from:

$$\frac{f_{Ed,b}}{f_{Rd,b}} \leq 1 \tag{15.3}$$

where:

$f_{Ed,b}$ is the design value for peak load for each width unit;
$f_{Rd,b}$ is the design value for buckling resistance obtained by factorizing the theoretical critical stress, $f_{b,cr}$ as indicated below.

(2) For a plate with with thickness t and length L_y the values of $f_{b,cr}$ are obtained as follows:

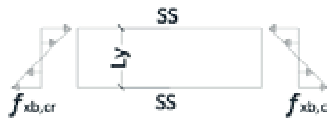	$f_{b,cr} = \frac{\pi^2}{t \times L_y^2}\left[13.4\sqrt{D_{11}D_{22}} + 10.4(D_{12} + 2D_{66})\right]$
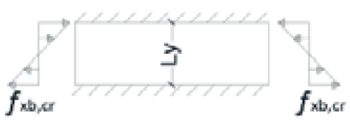	$f_{b,cr} = \frac{\pi^2}{t \times L_y^2}\left[13.4\sqrt{D_{11}D_{22}} + 10.4(D_{12} + 2D_{66})\right]$ when $k \leq 3$ $f_{b,cr} = \frac{4}{t \times L_y^2}\sqrt{D_{22}(D_{12} + 2D_{66})}(18.59 + \frac{3.56}{k^2})$ when $k > 3$

15.2.4 Combined stresses

(1) For a combination of uniform compression, shear or bending stresses, the following interaction formulae may be used. These apply to long orthotropic symmetrical plates with clamped or hinge-supported plate edges.

- For compression with shear:

$$\left(\frac{N_{Ed,c}}{N_{Rd,c}}\right) + \left(\frac{V_{Ed,s}}{V_{Rd,s}}\right)^{1.9+0.1\cdot K} \leq 1; \tag{15.4}$$

- For compression with bending:

$$\left(\frac{f_{Ed,c}}{f_{Rd,c}}\right) + \left(\frac{f_{Ed,b}}{f_{Rd,b}}\right)^{2} \leq 1 \tag{15.5}$$

- For bending with shear:

$$\left(\frac{f_{Ed,b}}{f_{Rd,b}}\right)^{(13.8+K)/6} + \left(\frac{f_{Ed,s}}{f_{Rd,s}}\right)^{(12+K)/6} \leq 1 \tag{15.6}$$

15.3 References

CUR 96 Fibre Reinforced Polymers in Civil Load Bearing Structures (Dutch Recommendation, 2003).

Clarke, J.L., Structural Design of Polymer Composites, Eurocomp Design Code and Handbook (1996). The European Structural Polymeric Composites Group, E & FN Spon, Chapman & Hall.

Fokker Technical Handbook TH 3.370, TH 3.372-3.374, 1992.

Lubin, G., Handbook of composites (1982). Van Nostrand Reinhold Company.

Phillips, L.N., Design with Advanced Composite Materials, The Design Council (1989). Springer Verlag.

ESA, Structural Materials Handbook (1994). Vol. 2.

Tarján, G., Sapkás A. Kollár,L.P. Local Buckling of Composite Beams, 2009. Proceeding of ICCM 17.

Bank, L. C., Composites for construction (2006). J. Wiley & Sons.

Bleich, F., Buckling of metal structures (1952). McGraw-Hill, New York.

Qiao, P., Davalos, J. F., Wang, J., Local buckling of composite FRP shapes by discrete plate analysis (2001) J. Struct. Eng., Vol. 127 (3), pp. 245-255.

Timoshenko, S. P., Gere, J. M., Theory of elastic stability (1961). McGraw-Hill, New York.

Mottram, J. T., Discussion of Local Buckling of FRP Composite Structural Members with Open and Closed Cross Sections (2004). J. of Structural Engineering.

Mottram, J. T., Determination of critical load for flange buckling in concentrically loaded pultruded columns (2004). Composites Part B: Engineering, Vol. 35 (1), pp. 35-47.

Shan, L. and Qiao, P., Explicit Local Buckling Analysis of Rotationally Restrained Plates under Uniaxial Compression (2008). Engineering Structures, Vol. 30, pp. 136-140.

Veres, I. A., Kollár, L. P., Buckling of orthotropic Plates with different edge supports (2001). Journal of Composite Materials, Vol. 35, pp. 625-635.

Barbero, E. J., Introduction to composite materials design (1999). Taylor &Francis, Philadelphia.

16 ANNEX G (SIMPLIFIED CONSTITUTIVE INTERFACE LAWS)

(1) The mechanical behaviour of an adhesive is generally schematized by means of two continual series of independent springs (Figure 16.1), with the first one preventing the opening δ and the other the sliding s (Figure 8.11)

(2) More simplified interface laws, respect to that depicted in Figure 8.12, are presented in Figure 16.2. These diagrams subtend areas equal to those subtended by the diagrams in Figure 8.12.

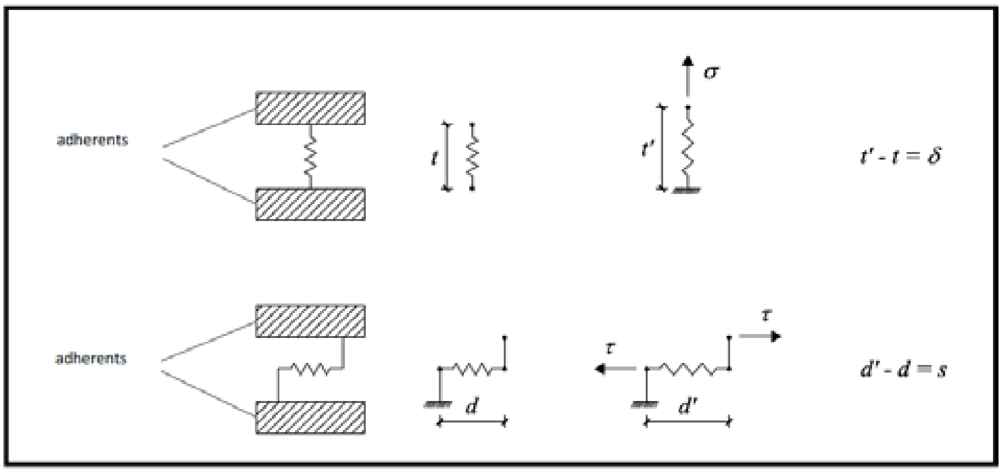

Figure 16.1 – Transversal and longitudinal springs.

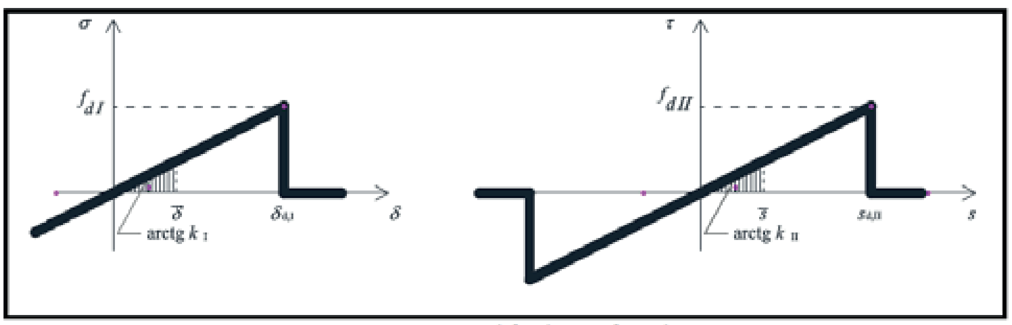

Figure 16.2 – Simplified interface laws.

The first set of springs exercises a normal stress on the interface, which referred to the unit of the surface is:

$$\sigma = K_I \cdot \delta \quad \text{if } \delta \leq \delta_{d,I}, \tag{16.1a}$$

$$\sigma = 0 \quad \text{if } \delta > \delta_{d,I}, \tag{16.1b}$$

in which:

$$K_{\mathrm{I}} = \frac{f_{\mathrm{d,I}}}{\delta_{\mathrm{d,I}}}. \tag{16.1c}$$

Analogously, the second set of springs exercises a tangential stress, along the axis of the joint, which referred to the unit of the surface is:

$$\tau = K_{\mathrm{II}} \cdot s \qquad \text{if } |s| \leq s_{\mathrm{d,II}}, \tag{16.2a}$$

$$\tau = 0 \qquad \text{if } |s| > s_{\mathrm{d,II}}, \tag{16.2b}$$

in which:

$$K_{\mathrm{II}} = \frac{f_{\mathrm{d,II}}}{s_{\mathrm{d,II}}}. \tag{16.2c}$$

(3) Because of the linearization of the constitutive laws of the adhesive interfaces, the ULS verification can be carried out by means of the relationship (8.10 b).

(4) A full linear elastic approach has already been presented in Section 8.4.2 (4).

16.1 References

CNR-DT 205/2007 Guide for the Design and Construction of Structures made of Pultruded FRP elements, Italian National Research Council (2008).

17 ANNEX H (FATIGUE TESTING)

17.1 Defining an s-n diagram by testing

(1) Fatigue tests should be carried out on test specimen of a material that is representative of the structural problem under exam, i.e. with the same type of resin and fibres, with equal fibre volume fraction, and produced according to the same process with identical process parameters.
Test pieces for an application that are produced with a one-sided mould may also be produced with a twosided mould in order to obtain test pieces with the same surface quality on both sides.

(2) For the choice of R value, see the typical values mentioned in Table 17.1.

(3) Static test data may not be used when determining the regression line.

(4) The test piece geometry should be implemented in accordance with Figure 17.1. The thickness should be determined based on the laminate type to prevent buckling.

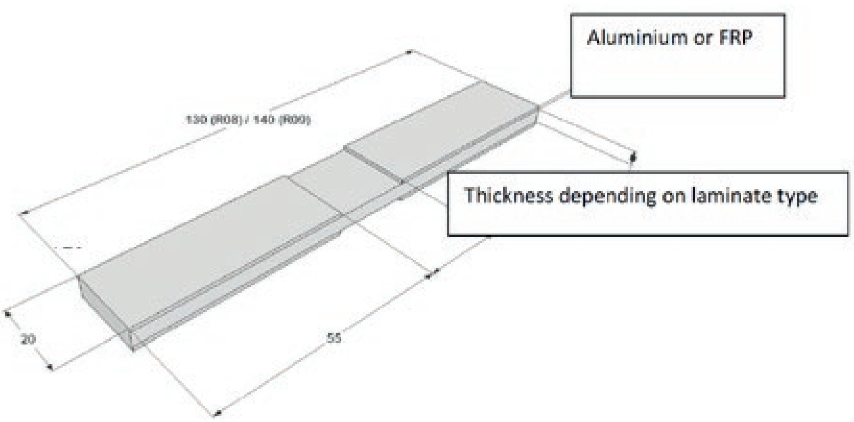

Figure 17.1 - Recommended geometry for fatigue tests (dimensions in mm).

Table 17.1 - Recommended test piece geometry for fatigue tests.

R value	UD, quasi-isotropic
0.1	R08, ISO 527-4
-1	R08, R09
10	R08, R09
Note: the geometry is suitable for laminate thickness up to approx. 5 mm. Glued tabs approx. 1 mm thick are recommended to protect the ends of the test pieces on both sides against the clamping device and to introduce the test load evenly into the test piece	

(5) As a rule the temperature increase, measured at the least favourable location on the surface, may not exceed 5°C.

(6) The load frequencies depend on the laminate structure and are based in particular on the avoidance of (internal) overheating of the test piece due to viscoelastic effects. Refer to Table 17.2 for guidance on typical frequencies.

Table 17.2 - Recommended test frequencies [Hz].

R value	Nominal life	
	1000	1000000
0.1	2	7
-1	1	3
10	2	7

(7) The data in an *S-N* (S = amplitude of cycle versus N = number of cycles) diagram should satisfy the following requirements:

- the data has been collected over at least 3 different load levels, the mean life per level differing by a factor of 5 - 10;
- the highest level corresponds to approx. 1000 cycles;
- the lowest level corresponds to approx. $5 \cdot 10^5$ cycles;
- if the operational number of cycles is greater than 10^5, the lowest load level should be at least one order of magnitude below the number of load cycles expected in operation.
- the distribution over the stress range may be spread uniformly or at discrete levels (at least 3 levels in the latter case), but at the highest and lowest level there should be at least 3 and 2 data points respectively in order to determine the gradient of the *S-N* curve satisfactorily.

(8) To define an *S-N* curve from fatigue data, reference is made to 17.1, and for a statistical evaluation to EN1990 Appendix D8.

17.2 CLD diagrams

(1) If no *S-N* line is available for the relevant R value, the mean service life should be determined using a constant life diagram. A constant life diagram (CLD) is a diagram in which the permissible number of cycles is shown as a function of the type of load.

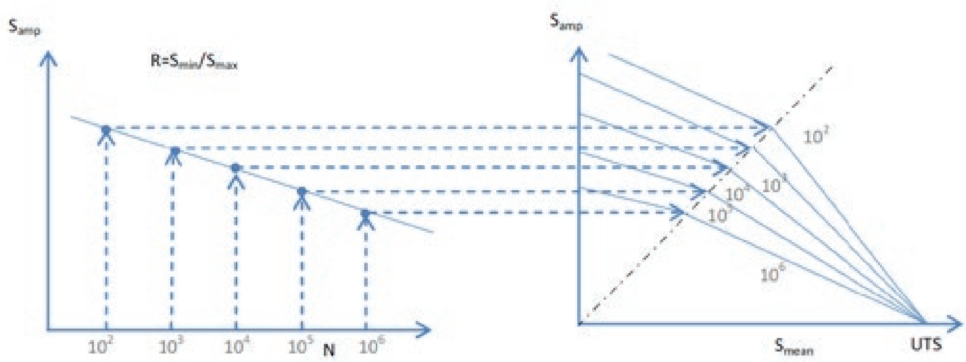

Figure 17.2 - Creating CLD from *S-N* lines.

The CLD is created by plotting, on a graph with mean stress on the horizontal axis and stress amplitude on the vertical axis, points corresponding to previously chosen lives, differing from each other by a maximum of 1 decade, e.g. 10, 100, 1000, etc. cycles. These points are derived from the available *S-N* lines.

(2) The characteristic *S-N* lines should be used for the CLD. The CLD should be constructed by connecting points of the same life to one another. These lines of constant life converge at the tensile strength and the compressive strength.

(3) If only the *S-N* line at *R*=-1 is known, the linear Goodman diagram may be used as a special case of the CLD. Therefore the linear Goodman diagram is also determined by plotting the stresses corresponding to e.g. 10, 100, 1000 cycles on the vertical axis and connecting these points with the tensile or compressive strength on the horizontal axis.

17.3 References

CUR 96, Fibre Reinforced Polymers in Civil Load Bearing Structures (Dutch Recommendation, 2003).

van Delft, D., Joosse, P.A., de Winkel, G.D., Fatigue behaviour of fibreglass wind turbine blade material under variable amplitude loading, paper nr. AIAA-97-0951, 1997.

Dutch Prestandard NVN 11400-0 Wind turbines part 0: Criteria for type-certification-Technical criteria,
Dutch Normalisation Institute, 1st ed., April 1999.

Authors

Luigi Ascione, Jean-François Caron, João Ramôa Correia,
Wouter De Corte, Patrice Godonou, Jean Knippers,
Eric Moussiaux, Toby Mottram, Matthias Oppe,
Nuno Silvestre, Peter Thorning, Liesbeth Trom

EuCIA
European Composites
Industry Association